



This is to certify that the

thesis entitled

PHYSICAL CHEMICAL STUDIES
OF THE ANTIBIOTIC IONOPHORE MONENSIN
AND ITS COMPLEXES

presented by

John Garret Hoogerheide

has been accepted towards fulfillment of the requirements for

Ph.D. degree in Chemistry

Major professor

Date R June 1978

O-7639

enir o

PHYSICAL CHEMICAL STUDIES OF THE ANTIBIOTIC IONOPHORE MONENSIN AND ITS COMPLEXES

Ву

John Garret Hoogerheide

A DISSERTATION

Submitted to

Michigan State University
in partial fulfillment of the requirements

for the degree of

DOCTOR OF PHILOSOPHY

Department of Chemistry

Clians

ABSTRACT

PHYSICAL CHEMICAL STUDIES OF THE ANTIBIOTIC IONOPHORE MONENSIN AND ITS COMPLEXES

Бу

John Garret Hoogerheide

Sclution and solid-state studies have been carried out on the antibiotic monensin and its complexes with the alkali metal ions as well as with H⁺, Tl⁺, and Ag⁺. Complexes of metal ions with the monensin anion (Mon⁻) and with the free acid form have been studied.

Potentiometric, cyclo-voltammetric, and fluorimetric studies have been carried out on Mon complexes with univalent metal ions and the proton in absolute methanol. Stoichiometry of the MonTl complex was determined by cyclic voltammetry. Formation constants for the complexes were corrected for activity effects. Of all the metal ions, silver forms the most stable complex with Mon, while among the alkali ions the most stable complex is MonNa.

Conductimetric titration, Tl⁺ fluorescence, and ²³Na nuclear magnetic resonance were used in methanol solutions to confirm the existence of complexes of the type MonHMX,

where MX is a metal salt. Potentiometric determination of formation constants in methanol indicated that MonHMX complexes are much weaker than the corresponding MonM complexes. The most stable metal ion complex formed with MonH was MonHAgClO $_{\mbox{$\downarrow$}}$, while MonHNaClO $_{\mbox{$\downarrow$}}$ was the strongest alkali metal ion complex.

Solid MonHNaX complexes were characterized by infrared spectroscopy to investigate the effects of varying the anion of the salt. An X-ray crystallographic determination of the structure of MonHNaBr showed the complex to be very similar to MonNa.

The study of MonHMX complexes in methanol solution is complicated by slow decomposition. The decomposition reaction has been studied as a function of time, of temperature, and of concentration.

Thermodynamics of complexation for the formation of MonH, MonNa, and MonHNaClO $_{\downarrow \downarrow}$ in methanol was studied by the temperature dependence of the formation constants. Experimental values of ΔH° , ΔG° , and ΔS° indicate that both MonH and MonNa are enthalpy and entropy stabilized, while MonHNaClO $_{\downarrow \downarrow}$ is enthalpy stabilized and entropy destabilized.

Pop

7::-

are

W.T.

Ste Her

War

\$;; \$ ·

Com

i

Four

Stat

te:

Whos

לאַינ^{ָל}:

cr ti

ACKNOWLEDGMENTS

The author wishes to thank Professor Alexander I.

Popov for his constant guidance into the areas of chemical research and scientific writing.

The special contributions of Professor Alexander
Tulinsky as second reader are appreciated. Also, thanks
are extended to Professor Andrew Timnick for his constant
willingness to discuss technical problems.

The friendship, criticism, and encouragement of Pierre-Henri C. Heubel supported the entire research project.

Special appreciation is likewise extended to Dr. Donald L. Ward for his expert tutelage in computer programming and system usage.

Generous gifts of monensin received from the Eli Lilly Company were indispensable and are gratefully acknowledged.

Financial support was provided by the National Science Foundation and by the Chemistry Department of Michigan State University.

The author owes a debt to his parents which can never be fully repaid, for their interest and diligence in providing a full and sound education.

Finally, deep appreciation is extended to my wife, whose patience, consideration, and encouragement contributed in large measure to the successful completion of this research project.

TABLE OF CONTENTS

Chapt	er																		Page
LIST	OF	TABLES	•		•	•	•	•	•	•		•	•	•	•	•	•	•	vi
LIST	OF	FIGURES	•		•	•	•	•	•	•	•	•	•	•	•	•	•	•	vii
1	HIS	TORICAL	RE'	VIE	W.	•	•	•	•	•	•		•	•	•	•		•	1
	1.1	Intro	duc	tio:	n.	•	•	•	•	•	•	•	•	•	•	•	•		2
	1.2	Disco Biolo								ar	nd •	it	•	•	•	•	•	•	3
	1.3	Assay	s o	f M	one	ens	ir	١.	•	•	•	•		•	•	•	•	•	15
	1.4	Physi Monen			ica	al •	Pr	op	er •	ti	les •	•	of •	•	•	•	•	•	16
	1.5	Concl	usi	ons	•	•	•	•	•	•	•	•	•		•		•	•	22
2	EXP	ERIMENT	AL 1	MAT:	ER:	IAI	٦S	ΑN	1D	ME	ETH	OI	s	•	•	•	•	•	23
	2.1	Mater	ial	s.	•	•	•	•	•	•		•	•	•	•	•	•	•	24
		2.1.1	R	eag	en'	ts	•	•		•	•	•	•	•	•		•	•	24
		2.1.2	S	olv	ent	ts	•	•	•	•	•	•	•	•	•	•	•	•	28
	2.2	Metho	ds																
		2.2.1	E	lec	tr	och	en	nis	str	у	•	•	•	•	•	•	•	•	28
			2	.2.	1.	1	C2	7c]	lic	,	Jo]	ta	mn	net	rj	7.			28
			2	.2.	1.	2	Po	ola	arc	gr	rap	h	7.	•	•	•	•	•	32
			2	.2.	1.	3					lme								32
			2	.2.	l.	4					ome								32
			2	.2.	1.	5	Cc	u]	Lor	net	try	7.	•	•	•	•	•	•	36
		2.2.2	S	pec	tr	osc	op	у	•	•	•	•	•	•	•	•	•	•	42
			2	.2.	2.	1	Ir	ıfr	aı	rec	ı.	•	•	•	•	•	•	•	42
			2	.2.	2.	2	U]	Ltr	av	/ic	016	et-	-v:	ls:	lb:	le	•	•	42
			2	.2.	2.	3	F]	Luc	ore	esc	cer	nc e	.	•					42

(
!
3
+ + +
!

Chapt	ter							Page
			2.2.2.4	Nuclear Resonan				43
		2.2.3	Other Ana	alyses .				43
			2.2.3.1	Gas Chr	omatog	raphy.		43
			2.2.3.2	Water A	nalysi	s		44
			2.2.3.3	X-Ray A	nalysi	s		44
			2.2.3.4	Flame A	nalysi	s		45
			2.2.3.5	Mass Sp	ectrome	etry .		46
			2.2.3.6	Melting	Point	Analy	sis.	46
			2.2.3.7	Data Re	duction	n		46
3			OMPLEXES V			SIN	• •	. 47
	3.1	Introdu	action					. 48
	3.2	Polaro	graphy and	d Cyclic	Volta	mmetry	•	. 48
	3.3	Potent	iometry .				•	. 59
	3.4	Fluores	scence				•	. 69
	3.5	Metal :	Ion NMR .					. 79
	3.6	Format	ion Consta	ants			•	. 83
	3.7	Conclus	sions				• •	. 88
4			TH THE AC					. 91
	4.1	Introdu	uction				•	. 92
	4.2	Determ	ination of	f the pk	a of M	onensi	.n.	• 93
	4.3	Evidence MonHM ⁺	ce for the Complexes	e Existe	ence of		•	• 99
	4.4	Charact Involv	terization ing MonH a	n of the	Compl	ex • • •	•	. 112
	4.5		ination on the compi					. 141
	4.6	Conclus	sions				•	. 149

Chapt	ter														Page
5	THE	RMODY	NAMICS	OF M	IONEN	ISIN	CC	MPI	LEX.	AT:	[0]	J.	•	•	150
	5.1	Int	roducti	on.			•	•		•	•	•	•	•	151
	5.2		rmodyna plexati		of	Mon	ens	in.		•	•	•	•	•	151
	5.3	Con	clusior	ıs .							•		•		159
_							•	•		•	•	•	•	•	- , ,
6	APPI	ENDIC	ES												
	Α.		icatior IT4 to									2			
		Sele	ctive E	Clect	rode	es .	•	•	• •	•	•	•	•	•	160
		A.l	Electr Ions.	odes	Ser	nsit	ive •	· to	M c	eta •	al •	•	•	•	161
			A.1.1	Pro	gran	ı Fu	nct	ior	ı .	•		•	•	•	161
			A.1.2	SUE	ROUI	TINE	EG	N.		•	•		•	•	162
			A.1.3	Dat	a Li	lsti	ng	•		•	•	•	•	•	162
		A.2	Electr	odes	Ser	nsit	ive	e to	э Н	ydı		ger	ו		260
			Ions.	• •	• •	• •	•	•	• •	•	•	•	•	•	163
			A.2.1	Pro	gran	n Fu	nct	io	n .	•	•	•	•	•	163
			A.2.2	SUE	ROUI	TINE	EG	N		•	•	•	•	•	164
			A.2.3	Dat	a Li	lsti	ng	•		•	•	•	•	•	164
	в.	MINI	icatior QUAD76 <i>A</i> librium	to	the	Det	ern	nina	ati	on	of		_		
			c Data											•	165
		B.1	Progra	ım Fu	ıncti	lon.	•	•		•	•	•	•	•	166
		B.2	Data I	nput	Ins	stru	cti	lon	s.	•	•	•	•	•	169
		B.3	Data I	isti	ng.		•	•		•	•	•	•	•	173
ਹਵਾਵਤ	PENC	70													ול די ר

LIST OF TABLES

Table		Page
I	Formation Constants of Monensin Complexes	
	with Univalent Cations in Anhydrous	
	Methanol, $\log K_f (K_f \text{ in } l \cdot mole^{-1}) \dots$	21
II	Experimental Conditions for Metal	
	Ion NMR	44
III	Selectivity Order for MonM	
	Complexes	85
IV	Melting Points for Several	
	Monensin Complexes	113
v	Comparison of Cell Parameters of	
	Structures of Monensin (184).	
	(Reproduced with the permission of	
	the copyright holder.)	122
VI	Crystal Data on the Sodium and Bromide	
	Ion Coordination in MonHNaBr. The	
	oxygen atoms are numbered as in Figure	
	1	128
VII	Formation Constants for MonHM+ Com-	
	plexes in Anhydrous Methanol	147
VIII	Thermodynamic Parameters for	
	Monensin Complexes	156

LIST OF FIGURES

Figure		Pa	.ge
1	The molecular structure of monensin		
	free acid, MonH (184). (Reproduced		
	with the permission of the copyright		
	holder.)		5
2	The crystalline structure of monensin		
	free acid (5). (Reproduced with the		
	permission of the copyright holder.)	•	7
3	The crystalline structure of the		
	silver salt of monensin (167). (Re-		
	produced with the permission of the		
	copyright holder.)		18
4	Loss of methanol from the titration		
	cell at room temperature (23°C) with		
	nitrogen gas bubbling through the		
	solvent at a rate of 40 $ml \cdot min^{-1}$.		
	*, no gas flow; ●, dry gas; □, gas		
	passed through a single fritted bubbler		
	in methanol before reaching cell; o,		
	gas passed through two bubblers before		
	cell		31
5	Block diagram of the constant-current		
	aoulometem		28

Figure		Page
6	Waveforms typical of a single coulometric	
	titration step	41
7	Reversibility plot for a polarogram of	
	a solution of 5.0 x 10^{-4} \underline{M} TlClO ₄ and	
	$5.95 \times 10^{-3} \underline{\text{M}} \text{Mon}^{-} \text{in anhydrous methanol.}$	51
	The points are measured values and the	
	line is a least-squares fit	
8	Representative polarograms in anhydrous	
	methanol solution. I, the supporting	
	electrolyte, 0.1 \underline{M} tetra-n-butylammonium	
	perchlorate; II, 2 x 10^{-4} M TlClO ₄ in	
	supporting electrolyte; III, 2 x 10^{-4} M	
	T1C10 ₄ , 4.9 x 10^{-3} M Mon ⁻ in supporting	
	electrolyte	54
9	Lingane plot of $\Delta E_{1/2}$ as a function of	
	log [Mon] for the MonTl system in	
	absolute methanol. The line is a least-	
	squares fit through the observed points	
	(218). (Reproduced with the permission	
	of the copyright holder.)	56
10	Calibration curve for the ion-selective	
	electrode in absolute methanol. The	
	solid curve is the calculated calibra-	
	tion curve and the solid circles are	

Figure		Page
	experimental points (218). (Reproduced	
	with the permission of the copyright	
	holder.)	63
11	Temperature dependence of the slope $\underline{\mathtt{m}}$	
	in the Nernstian equation $E = E^{\circ} + \underline{m} \log$	
	[Na ⁺]. Solid line is the calculated tem-	
	perature dependence (218). (Reproduced	
	with the permission of the copyright	
	holder.)	65
12	Potentiometric titration curve for	
	the MonNa system in absolute methan-	
	cl. \square , calculated points; \bullet , observed	
	points (218). (Reproduced with the	
	permission of the copyright holder.)	68
13	Quenching of the fluorescence of a 1.15	
	x 10^{-4} $\underline{\text{M}}$ TlClO ₄ solution in methanol by	
	Mon The ligand to metal mole ratios are	
	as follows: curve 1, 0.00; 2, 0.0627; 3,	
	0.1402; 4, 0.1733; 5, 0.3098; 6, 0.4758;	
	7, 0.5680; 8, 0.7376; 9, 0.8446; 10,	
	0.9147; 11, 1.062; 12, 1.346; 13, 1.579;	
	14, 2.290; 15, baseline	73
14	Fluorescence intensity at 360 nm as a	
	function of the ligand to metal mole	
	ratio in the titration of 3.000 ml of	

Figure		Page
	1.15 x 10^{-4} M TlClO ₄ with	
	$1.268 \times 10^{-3} M Mon^{-1}$ in absolute	
	methanol. The data have been cor-	
	rected for dilution and background	
	fluorescence and normalized to 100	
	for the fluorescence of Tl ⁺ in the	
	absence of Mon	73
15	Fluorescence spectra of (1) 1.047	
	\times 10 ⁻⁴ \underline{M} T1C10 ₄ and (2) 3.594	
	$x 10^{-3} M Mon^-$ solutions in methanol	76
16	Relative fluorescence intensity at	
	343 nm as a function of the Mon con-	
	centration. The data have been cor-	
	rected for dilution and background	
	fluorescence	78
17	Changes in the linewidth of the $^{23}\mathrm{Na}$	
	resonance with the addition of monensin	82
18	Selectivity of the Mon complexa-	
	tion reaction for the alkali, Tl ⁺ , and	
	Ag tions (218). (Reproduced with the	
	permission of the copyright holders.)	87
19	Structures of representative cryptands	90
20	Endpoint errors in the coulometric	
	titration of benzoic acid in anhydrous	

methanol solutions. \Box , titration

Figure		Page
	data from bromide medium; •, titra-	
	tion data from perchlorate medium.	
	The arrow indicates the calculated	
	endpoint	96
21	Conductimetric titrations of methanol	
	solutions with 5.684 x 10^{-3} M NaClO ₄	
	solution. • represents NaClO4 addition	
	to 50.00 ml of methanol; x, represents	
	NaClO_{4} addition to 50.00 ml of 2.360	
	$x 10^{-3} M MonH solution in methanol$	103
22	Fluorescence intensity at 360 nm as	
	a function of the ligand to metal mole	
	ratio in the titration of 3.000 ml of	
	1.120 x 10^{-4} M T1C10 ₄ with 1.991 x 10^{-3}	
	$\underline{\mathtt{M}}$ MonH in absolute methanol. The data	
	have been corrected for dilution and	
	background fluorescence and normalized	
	to 100 for the fluorescence of Tl + in	
	the absence of MonH	107
23	Chemical shift of 0.100 \underline{M} CsSCN in	
	anhydrous methanol as a function of	
	the MonH-metal mole ratio	109
24	Chemical shift of 1.13 x 10^{-2} M T1C10 ₄	
	in anhydrous methanol as a function of the	
	MonH-metal mole ratio	111

Figure		Page
25	Infrared spectra of Nujol mulls of	
	several monensin species	116
26	Comparison of the O-H stretching	
	regions in the infrared spectra of	
	Nujol mulls of three monensin species.	
	, Nujol;, MonH;, MonHNaBr;	
	, MonNa	118
27	Comparison of the O-H stretching	
	regions in the infrared spectra of	
	Nujol mulls of MonHNaX complexes.	
	, $X = Br;$, $X = C1;$, $X = I;$	
	\dots , $X = Clo_{4}$. \dots	120
28	Two stereo views of the crystal struc-	
	ture of MonHNaBr (184). (Reproduced	
	with the permission of the copyright	
	holder.)	124
29	Schematic representation and bond	
	lengths (A) of Na $^+$ coordination in the	
	crystal structure of MonHNaBr. The	
	oxygen atoms are numbered as in	
	Figure 1	127
30	Schematic representation of the	
	crystalline hydrogen-bonding in three	
	monensin species (5). (Reproduced in	
	part with the permission of the copy-	
	right holder.)	. 130

Figure		Page
31	Titrations of monensin free acid with	
	tetra-n-butylammonium hydroxide in	
	anhydrous methanol solution with	
	various supporting electrolytes	133
32	Titrations of 20.00 ml of 2.012	
	\times 10 ⁻³ \underline{M} MonH, 6.115 \times 10 ⁻³ \underline{M} NaClO ₄	
	with $5.07 \times 10^{-2} \underline{\text{M}}$ TBAH in absolute	
	methanol at 22°C. The titrations were	
	begun 0.0 (\bullet), 3.0 (x), and 21.0 (+)	
	hours after mixing the MonH and $NaClO_4$	
	solutions	136
33	Temperature dependence of the decomposi-	
	tion in methanolic solutions of MonH	
	and $NaClO_{4}$. The inset defines the two	
	observed endpoints, EP1 and EP2.	
	•, 1°C; +, 22°C; x, 35°C	. 138
34	Concentration dependence of the de-	
	composition in methanolic solutions	
	of MonH and NaClO4 at 22°C. The inset	
	defines the two observed endpoints, EP1	
	and EP2. x, $C_{MonH} = 0.17 \text{ M}, C_{Na+} = 0.50$	
	\underline{M} ; *, $C_{MonH} = 0.15 \underline{M}$, $C_{Na+} = 0.15 \underline{M}$; o,	
	$C_{MonH} = 2 \times 10^{-3} \underline{M}, C_{Na}^{+} = 6 \times 10^{-2} \underline{M}; +$	
	$c_{MonH} = 2 \times 10^{-3} \underline{M}, c_{Na+} = 1 \times 10^{-3} \underline{M}$. 140

Figure		Page
35	Quenching of the fluorescence of a	
	1.120 x 10^{-4} M T1C10 ₄ solution in	
	methanol by MonH. The ligand to metal	
	mole ratios are as follows: curve 1,	
	0.00; 2, 0.060; 3, 0.118; 4, 0.178;	
	5, 0.237; 6, 0.296; 7, 0.415; 8,	
	0.533; 9, 0.652; 10, 0.770; 11, 0.948;	
	12, 1.245; 13, 1.541; 14, 1.985; 15,	
	2.578; 16, 3.763; 17, 5.541; 18,	
	7.319; 19, 23.71	144
36	Temperature dependence of $\ln K_{\hat{\mathbf{f}}}$ for	
	three monensin complexes in methanol	
	solutions. Curve 1, MonH; 2, MonNa;	
	3, MonHNaClO $_4$	155

CHAPTER 1

HISTORICAL REVIEW

1.1. INTRODUCTION

Metal ion complexes have been a subject of considerable interest for many years, but it has been only in the last decade that a significant number of ligands for alkali metal ions have been discovered. These new ligands attracted the attention of chemists since in the past alkali metal complexes have been practically unknown. In addition, alkali metal complexes are of considerable importance to the life scientists since the new ligands have demonstrated the ability to mediate ion transport across biological membranes. Thus, at the present time both groups of scientists are actively investigating the properties of these ligands and their complexes.

The determination of the physical and chemical characteristics of the alkali metal ion ligands are well-suited to the techniques of the analytical chemist, who is equipped with a variety of sensitive and precise measurement probes. In the following account we shall describe the application of several analytical techniques to the study of the antibiotic ionophore monensin, its alkali metal complexes, and its solution chemistry.

Mon

(1) in

the sil

had the

lation

and ant

Ecehn (

icam ci

D, Whia

Other e

Vielis

ut3 raplear

Paphy (

formatt.

and pol

tility

trity

lkC lab

propion derivat

(8), ar.

1.2. DISCOVERY OF MONENSIN AND ITS BIOLOGICAL ACTIVITY

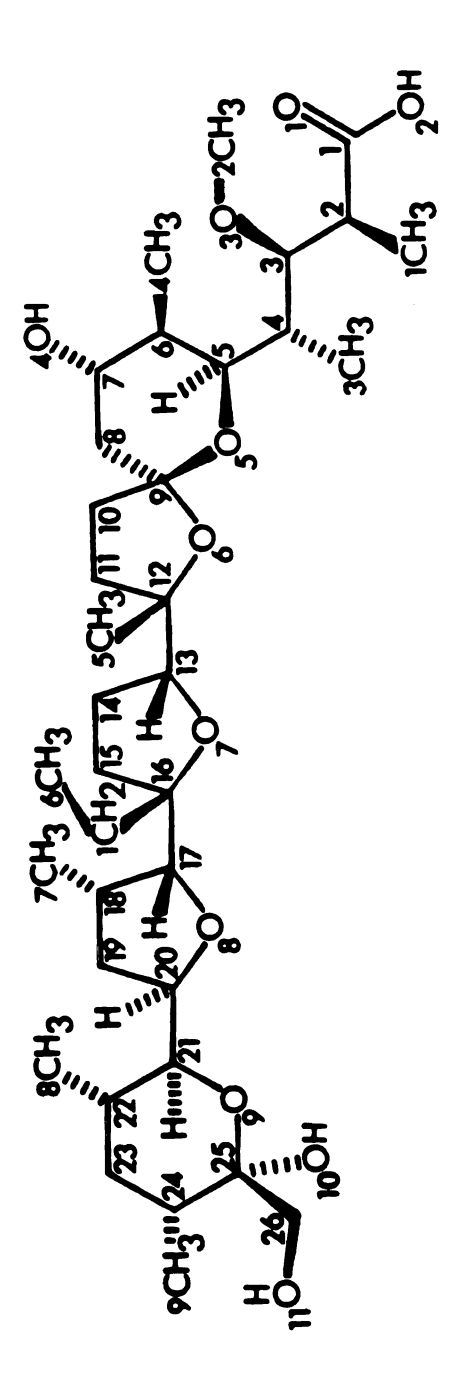
Monensin, a polycyclic, polyether, monocarboxylic acid antibiotic, was first isolated from the culture filtrates of <u>Streptomyces cinnamonensis</u> by Agtarap <u>et al</u>. (1) in 1967. On the basis of the crystal structure of the silver salt, they showed that the monensin molecule had the structure shown in Figure 1. Details of the isolation of monensin and studies on its physical, chemical, and antibiotic properties were presented by Haney and Hoehn (2). These workers found that monensin exists as four closely related factors referred to as A, B, C, and D, which differ by no more than a single -CH₂- group. Other early papers described the optimization of monensin yields by varying the fermentation media (3,4).

Studies which employed mass spectrometry and proton nuclear magnetic resonance (5) as well as x-ray crystallog-raphy (1,6) showed that monensin exists in a cyclic conformation as shown in Figure 2. The hydrophobic exterior and polar interior apparently account for the low solubility of monensin in water and for its appreciable solubility in most organic solvents.

The biosynthesis of monensin was studied by using ^{14}C labelled nutrients, including glucose, acetate, propionate, butyrate, and methionine (7). A glucopyranosyl derivative was produced by the fermentation of monensin (8), and synthetic lactone (9) and dehydroxymethyl (10)

Figure 1. The molecular structure of monensin free acid,

MonH (184). (Reproduced with the permission of
the copyright holder.)



igure 1

Figure 2. The crystalline structure of monensin free acid (5).

(Reproduced with the permission of the copyright holder.)

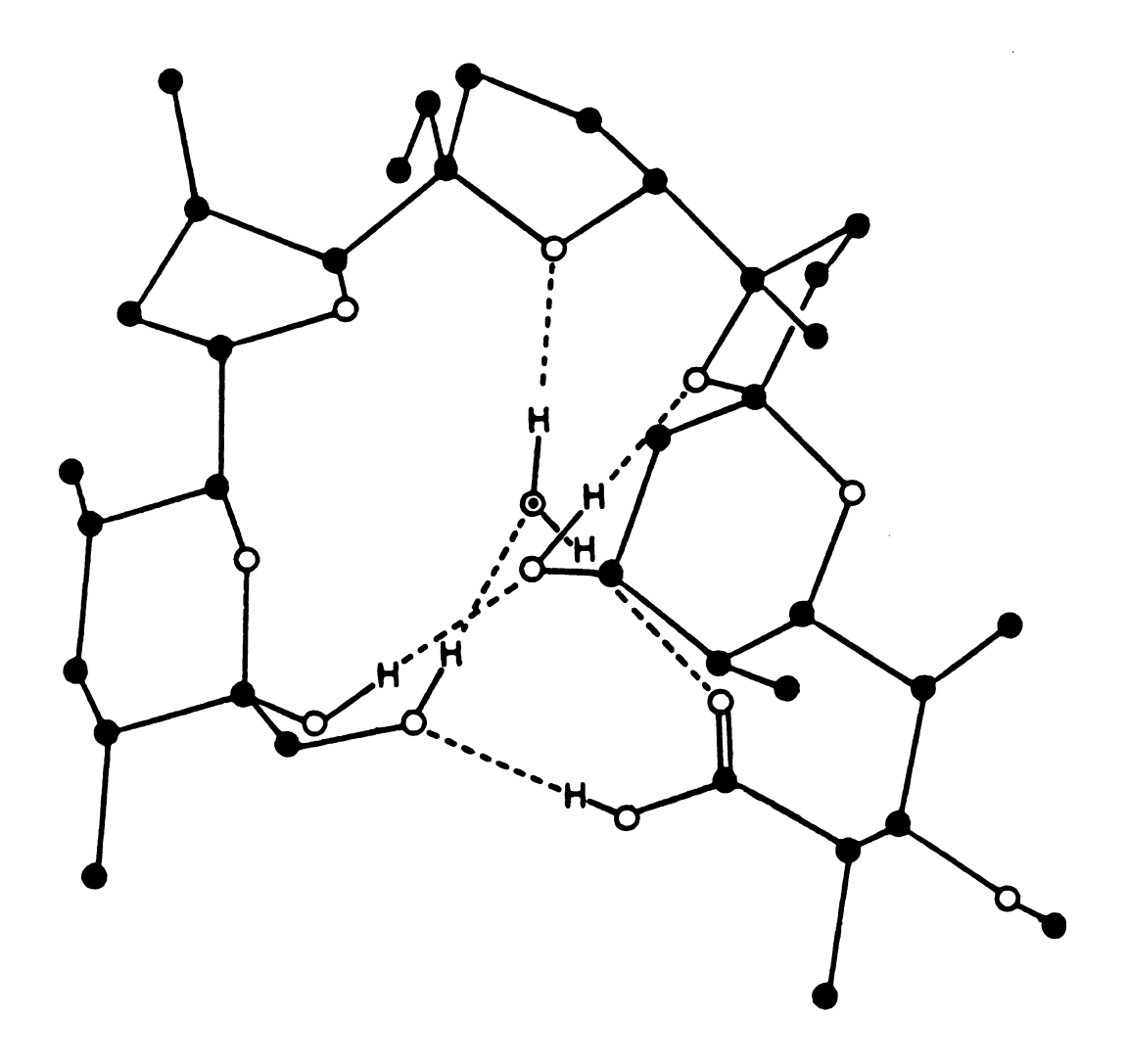


Figure 2

derivati:

ensin pla

The p

Inis grow

(11), as

X-537A (1

(16), %-2

ioid (20)

lonomyoir

£23187 (2

Much

by the bi

scientis:

on in wi

tural us

number a

The

News tin

anue int

mitochor

tron tre

Phate 1:

discuss; ionopho:

the memi

the dec

derivatives have also been prepared.

The polycyclic and polyether characteristics of monensin place the drug in the nigericin class of antibiotics. This growing group includes the title compound nigericin (11), as well as dianemycin (12), lasalocid A, also called X-537A (13), salinomycin (14), septamycin (15), grisorixin (16), X-206 (17), Ro 21-6150 (18), lysocellin (19), emericid (20), alborixin (21), carriomycin (22), A-204A (23), lonomycin (24), narasin (25), and the related compound A23187 (26).

Much of the interest in monensin has been generated by the biological activity of the antibiotic. Life scientists have been intrigued by the effects of monensin on in vivo and in vitro membrane phenomena, while agricultural uses of the drug have rapidly increased both in number and in scope.

The effects of monensin on mitochondrial membranes were first recorded by Estrada-O et al. who found that the drug inhibited uptake of alkali metal ions into rat liver mitochondria (27,28). Monensin also stimulated an electron transport-dependent accumulation of calcium and phosphate in those mitochondria (29). Pressman (30,31) has discussed the ion transport properties of nigericin-group ionophores in terms of alkali metal-proton exchange across the membrane. The role of nigericin-group antibiotics in the decoupling of oxidative phosphorylation in mitochondria

has been Philip an cell memb growth of ion trans chromator salt of m and decre cells cou of the so have show the erri external exchar.ge Inter Phenomena was found total oca The mean investig eτ εζ. μ and magn

> Ther ty Ashto

lets and

⁽⁴⁵⁾.

has been considered by Wipf and Simon (32) as well as by Philip and Allan (33). Monensin was said to alter the cell membrane structure in such a way as to alter the growth of fungi (34). The antibiotic drastically affected ion transport and photophosphorylation in bacterial chromatophores (35,36). In isolated frog skin, the sodium salt of monensin increases the diffusion of the K⁺ ion and decreases Na⁺ transport (37). Respiration in bacterial cells could be stimulated by monensin only in the presence of the sodium ion (38). Studies on barnacle muscle fibers have shown that monensin injected into the fibers increased the efflux of Na⁺ (39,40) and, as acidification of the external medium enhanced the efflux, a metal ion-proton exchange was postulated.

Interest in the effects of monensin on cardiovascular phenomena has resulted in several papers. The antibiotic was found to produce increased cardiac contractility, total coronary flow, and cardiac output in dogs (41,42). The mechanisms involved in such coronary action were investigated in several other papers (43,44). Feinstein, et al. have found that monensin reduces both the rate and magnitude of serotonin uptake by human blood platelets and they proposed a Na⁺ dependent carrier process (45).

Thermodynamics of ion transport have been considered by Ashton and Steinrauf (46), while Huang developed a

(47,48). ions inc ent which concept momensin in solut Rese Flicatio the drug ness of terella for a di The discove: ed the chicken proved were ca or more end adu

found t

(61).

did not

on the

for met

non-equi

non-equilibrium kinetic theory of antibiotic ion carrier (47,48). Cussler suggested that membranes could pump ions from low to high concentrations if a solute is present which provides the energy for the pump (49). The concept was successfully applied to a membrane containing monensin (50,51). Cussler has also described the increase in solute diffusion rates by the use of antibiotics (52).

Research into the use of monensin in agricultural applications has increased steadily since the discovery of the drug. <u>In vitro</u> experiments have shown the effectiveness of monensin in controlling coccidia such as <u>Fimeria</u> tenella (53,54), which is the microorganism responsible for a digestive tract disease known as coccidiosis.

The anticoccidial activity of monensin in poultry was discovered in the routine biological testing which followed the discovery of the drug (2,55). Feeding monensin to chickens reduced lesions in the digestive tract and improved weight gain and feed conversion (56,57). Studies were carried out to determine the optimum feeding levels of monensin (58) and results were reported for both chicks and adults (59,60). Environmental temperature was not found to influence the efficacy of monensin treatments (61). Nutrition experiments showed that monensin intake did not affect the daily sodium chloride requirement (62); on the other hand, monensin treatment eliminated the need for methionine supplements for infected birds (63). The

ef ha

> (6 ct

te

£ã

of em

to

K.e

1: 1:

TO ha

:e s:

e;

05

t);

efficacy of monensin in combatting chicken coccidiosis has been compared to that of several other coccidiostats (64). Monensin has also been used in conjunction with other drugs (65-68), and to combat a combination of diseases in chickens (69).

Several researchers have shown interest in the longterm effects of monensin on poultry. The drug was found to have no effect on the production, quality, or fertility of eggs (70). Drug resistance studies began with chick embryos (71) and progressed to adult birds (72) and entire flocks (73). No monensin-resistant pathogenic species were found in a large number of experiments (74).

Food and Drug Administration clearance was given to monensin sodium for use in broiler chicken feeds and premixes (75,76) and the regulations were later republished (77). Approval was also granted for the use of monensin in combinations with several other drugs (78-80), although in one case the medicated feed was required to be withdrawn 72 hours prior to slaughter (80). The tolerance for monensin in the edible tissues of cattle and chickens has been set at 0.05 ppm (81). Withdrawal of medicated feeds from chickens five days before slaughter did not significantly affect the rate of weight gain and feed efficiency in the final days without medication (82). Other studies on the effects of monensin on chickens showed that the drug does not affect the flavor of the meat (83),

but feed a mentation or not mon chickens (Preatm resently t differ fro of eccedad The ef feed effic teem obser tegan as to include Papers de (93-98) h diets (95 drug in m have been and calve Monen Junetion intake en tional mo (117-119) effects c

The r

but feed additives can be used to improve the meat pigmentation (84). There is some disagreement as to whether or not monensin influences the feather development of chickens (85,86).

Treatment of turkey coccidiosis with monensin has recently been studied. Although the pathogenic species differ from those afflicting chickens, monensin control of coccidiosis has been observed in turkey poults (87,88).

The effects of monensin in increasing weight gain and feed efficiency are not limited to poultry, but have also been observed in cattle. The cattle-feeding experiments began as feedlot experiments (89-92) but have expanded to include a variety of feeds and experimental conditions. Papers dealing with monensin given to cattle on pastures (93-98) have been complemented by others considering corn diets (99), monensin in liquid supplements (100), and the drug in molasses blocks (101,102). The animals considered have been heifers (103,104), steers (105-109), bulls (110), and calves (111).

Monensin in cattle feed has also been used in conjunction with other additives such as urea (112-114), feed-intake enhancers (115), and biuret (116). Several additional monensin-drug combinations have been considered (117-119). A brief review has been published on the effects of monensin on feed efficiency in cattle (120).

The reason for the increased feed efficiency has not

been wel it is ar sults in rumen ac tive pro valerio ionic an studies increase importan blood gl did not but it d Some wor efficien however, from a t (135). microbes in vive cellulos ferences not Yet

Seve

safely w

effects (

been well established. From the results of several workers it is apparent that treatment of cattle with monensin results in changes in rumen acid distributions. The total rumen acid concentration remains unchanged, but the relative proportions of acetic, butyric, isobutyric, and valeric acids decreased while the proportions of propionic and isovaleric acids increased (121-125). In vitro studies did not always agree with the in vivo results of increased propionate (126-129). Other physiologically important compounds affected by monensin intake included blood glucose (130,131), urea, and insulin (130). Monensin did not affect the total rumen nitrogen or sodium (132), but it decreased the production of bovine α -amylase (133). Some workers have speculated that monensin increased feed efficiency by decreasing ruminal methane production (134); however, this decreased production does not seem to result from a toxic effect of monensin on the methanogenic flora (135). Indeed, no changes in the numbers of any ruminal microbes have been observed with the intake of monensin in vivo (136,137). In vitro, however, monensin inhibits cellulose digestion by microorganisms (138). The differences between the in vivo and in vitro results have not yet been reconciled.

Several studies have shown that monensin may be used safely with gestating animals (139-141). No deleterious effects of monensin on beef reproduction have been noted

Cor of mone reports carcas ensin y An ind of ani: and ha These that m the fe was th or its ment o iicier. Monens (148), biotic dysent to be

A]

to som

both a

of mon

Ma

(142).

(142).

Considerable interest has been shown in the effects of monensin on beef cattle carcass composition. Several reports from the manufacturers of the drug indicated that carcass quality and characteristics of animals fed monensin were not different from those of controls (143-145). An independent account, however, stated that carcasses of animals fed monensin were graded lower than controls and had a higher incidence of liver condemnation (146). These latter results are consistent with the findings that monensin was essentially quantitatively excreted in the feces, and that at the time of slaughter the liver was the only edible tissue to contain residues of monensin or its metabolites (147).

Although the most widespread use of monensin in treatment of mammals is to increase weight gain and feed efficiency, the drug also has some therapeutic value.

Monensin has been used to control coccidiosis in calves (148), lambs (149-151), and rabbits (152,153). The antibiotic has recently been used to effectively combat swine dysentery (154). On the other hand, monensin has proved to be toxic to horses (155,156). The toxicity of the drug to some organisms has prompted the use of monensin as both an insecticide and an acaricide (157).

Many of the foregoing papers dealing with the use of monensin in biological or agricultural experiments

tended not to consider the chemistry of the antibiotic. Indeed, in a number of cases no distinction was made between monensin, which exists as a carboxylic acid, and its sodium salt. It is, however, apparent that an understanding of the chemistry of monensin should enable one to better understand the results of the life-science experiments.

1.3. ASSAYS OF MONENSIN

An obvious link between the agricultural experiments and the chemistry of monensin is the analysis for the drug in feeds. An automated photometric microbiological assay for monensin in poultry rations was proposed (158), modified and collaboratively tested (159), and later rendered still more sensitive (160). A colorimetric method which used 3% vanillin in 0.5% $\rm H_2SO_4$ in methanol (161) was found to be simple, fast, sensitive, reproducible, and applicable to monensin in feeds, premixes, fermentation broth, and crystalline samples. A variation of the colorimetric method used densitometric scanning of thin-layer chromatography plates by a reflectance technique (162). Two additional microbiological assays have been recommended (163,164).

that

(16

men:

the

(3:

οχί.

st:

F16

00:

MO:

(1

is do

ŧς

ĉ.

ŗ,

5

1.4. PHYSICOCHEMICAL PROPERTIES OF MONENSIN

The crystal structure of monensin showed the acid to have a cyclic conformation in the solid state (6). Pressman suggested that the molecule could be linear in solution (165), but careful studies of monensin solutions in chloroform by infrared spectroscopy showed conclusively that the acid also has a cyclic structure in solution (166). From the results of membrane ion-transport experiments, Pressman concluded that monensin transports alkali metal ions by means of complex formation (165). the molecular structure of the silver salt of monensin (Figure 3), shows that the cation is surrounded by six oxygen atoms of the deprotonated monensin (1,167). Crystal structure data on the thallium (I), sodium, potassium, and rubidium salts of monensin indicate that these complexes should be very similar in structure to the silver complex (167). The structures of the silver salts of monensin, nigericin, and dianemycin have been compared (168,169); the monensin complex, which is a dihydrate, is fairly rigid and has a smaller internal cavity than does the anhydrous nigericin complex; dianemycin appears to be a rather more flexible ligand than the two other antibiotics. Monensin and its alkali metal ion complexes have been further studied by high resolution mass spectrometry (170).

Figure 3. The crystalline structure of the silver salt of monensin (167). (Reproduced with the permission of the copyright holder.)

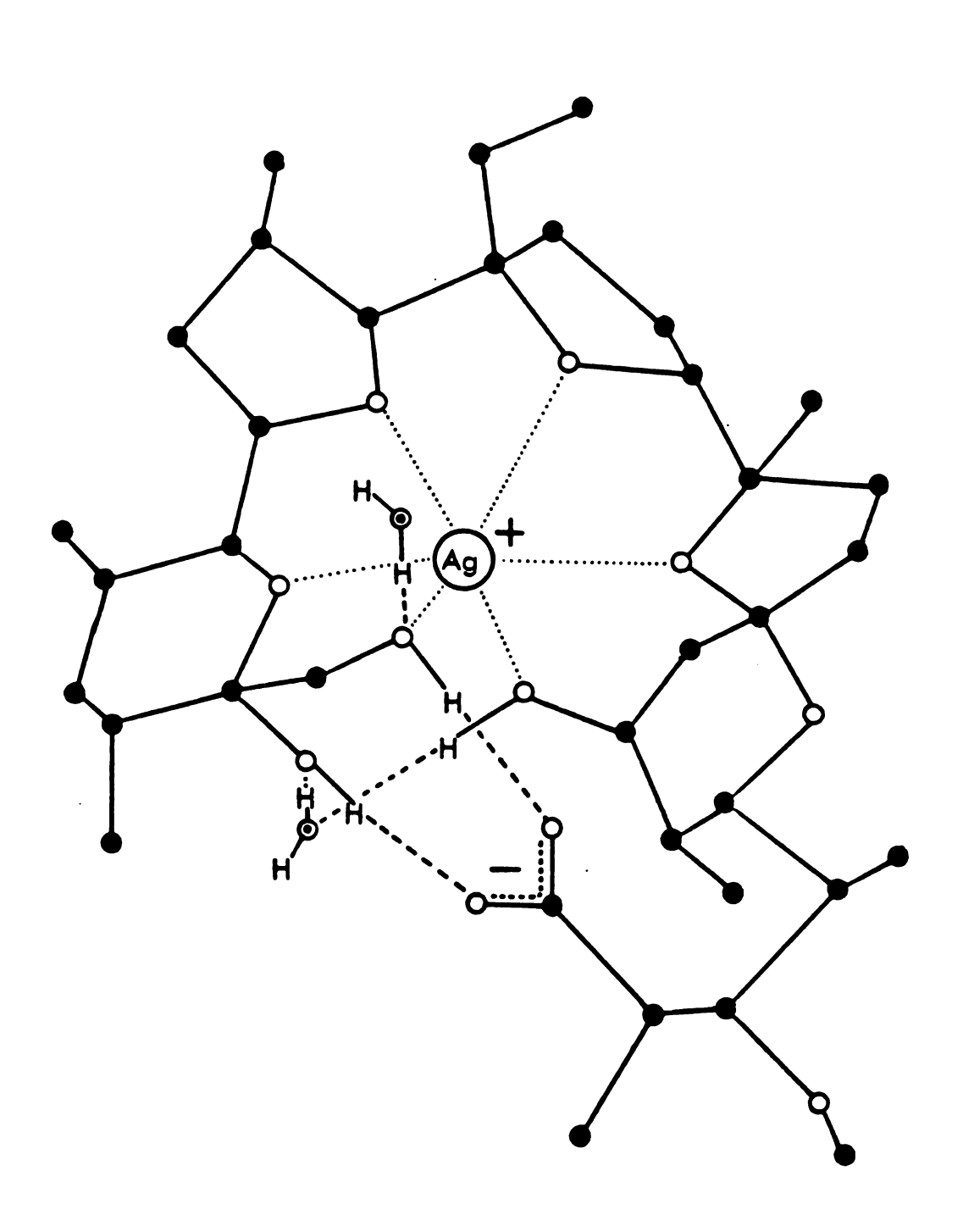


Figure 3

Solution studies on monensin salts have centered on the most stable complexes, namely, those with sodium and potassium. Haynes, Pressman, and Kowalsky monitored the complexation of sodium ion by monensin by using 23Na nuclear magnetic resonance spectroscopy (171). cluded that there exists very little covalent interaction between the metal ion and the oxygen atoms of the ligand. The complex dissociation rate constant in methanol was estimated to be less than 100 s^{-1} . This early estimate has been supported by Degani, who determined the complex dissociation rate constant to be 63 s^{-1} in methanol (172). The latter ²³Na nmr study gave activation enthalpy and entropy values of 10.3 Kcal·mol⁻¹ and -15.8 cal·mol⁻¹. deg⁻¹, respectively, for the complexation reaction (172). Proton nmr was used to study the monensin sodium complex (173,174) as well as the free acid (174).

A number of workers have determined values for formation constants of deprotonated monensin complexes with cations. By titration of monensin with tetramethylammonium hydroxide, Pressman obtained the pKa value of 7.95 in 90% ethanol at 30°C (175). Lutz et al. (166) determined formation constants for sodium and potassium complexes by using ion-selective electrodes in methanol. A computerized microcalorimeter was used to determine ΔH° , ΔG° , and ΔS° for the complexation of sodium and potassium by monensin in methanol (176,177). Relaxation methods which used a

temperat
the comp
methanol
cence of
to the Tr
rescence
constant
for mone
ensin wi
The resu
absolute
A se
Gertenba

A similar ion by Ercase, the

two kind

tion rea

anion was

temperature-jump technique gave an approximate value for the complexation constant of sodium ion with monensin in methanol (178). Cornelius et al. observed the fluorescence of Tl(I) in methanol (179). Addition of ionophores to the Tl(I) solution resulted in a decrease in the fluorescence which the authors used to calculate formation constants. Equilibrium constants were obtained directly for monensin with Tl(I) ions and competitively for monensin with sodium, potassium, rubidium, and cesium ions. The results for all the formation constants determined in absolute methanol are listed in Table I.

A second kind of monensin complex was suggested by Gertenbach and Popov (174). From a series of potentio-metric and spectroscopic measurements they concluded that two kinds of complex can exist in solution. The complexation reactions are,

A similar proposal was made for complexes of potassium ion by grisorixin in methanol (180). In the grisorixin case, the complex of the metal ion with the antibiotic anion was about 100 times as strong as the complex with the protonated ligand.

Table 1. Formation Constants of Monensin Complexes with Univalent Cations in Anhydrous Methanol log $K_{f f}$ ($K_{f f}$ in Laole $^{-1}$).

Li (a, Iv ^b)	+ e z	+ <u>w</u>	*4g	* <u>*</u>	+ ₽	→ 8
3.3±0.1	5.85 (166 ^c , I)	3.3±0.1 5.85 (166 ^c ,I) 4.58 (176,II)	4.2 (179,111)	3.72 (179,111)	3.72 (179,111) 4.41 (179,111)	8.2±0.2 (a,1)
	6.1 (177,11)	4.40 (166,1)	4.58:0.05 (8,1)		3.75±0.05 (a,1) 5.31±0.05 (a,IV)	
	>6 (178.V)	4.98 (166,1)	4.5 ±0.2 (a.IV)	4.5 ±0.2 (a,IV) 3.7 ±0.1 (a,IV) 5.2 ±0.1 (a,III)	5.2 ±0.1 (a, III)	
	4.86 (179,111)	4.86 (179,111) 4.70 (177,11)				
	6.72±0.05 (.,	6.72±0.05 (a.1) 4.94 (176, 11)				
	>4.7 (a, IV	(a, IV) 4.49 (179, III)				
		>4.7 (a, IV)				
		5.18±0.05 (0,1)				

This work.

b Technique.

^CReference.

I. Potentiometry; II. Calorimetry; III. Fluorescence; IV. Cyclic Voltammetry; V. Relaxation.

COMOLUSI

The

of inter
However,
of the d

of the m

mains to

CONCLUSIONS

The antibiotic monensin has generated a great deal of interest from both biological and chemical viewpoints. However, physical chemical data on the solution chemistry of the drug are still lacking. In particular, the nature of the metal ion complex with the protonated ligand remains to be investigated.

CHAPTER 2

EXPERIMENTAL MATERIALS AND METHODS

2.1. MATERIALS

2.1.1. <u>REAGENTS</u> - Hydrochloric acid (Mallinckrodt), 70% perchloric acid (G. F. Smith Chemical Co.), tetra-n-butylammonium hydroxide, 25% in methanol (Matheson, Coleman, Bell), and tetramethylsilane (Aldrich) were used as received. Benzoic acid (Matheson, Coleman, Bell, reagent ACS) was dried at 110°C for 24 hours. Lithium acetate (Fisher, purified) was used as received, but anhydrous lithium perchlorate (K and K) was dried at 180°C for 48 hours. Sodium fluoride (Fisher, certified ACS), sodium chloride (Fisher, certified ACS), sodium perchlorate (G. F. Smith Chemical Co.), sodium bromide (Fisher), and sodium iodide (Fisher, certified ACS) were all dried at least 24 hours at 150°C, while sodium carbonate (Fisher, certified ACS) was dried overnight at 110°C.

Potassium chloride (Fisher), potassium bromide (Fisher), and potassium hydrogen phthalate (Fisher, primary standard) were dried at 110°C for 24 hours, but potassium iodide (Fisher, certified ACS) and potassium thiocyanate (Fisher, certified ACS) were dried at 50°C under vacuum. Rubidium bromide (Alfa, ultrapure) was dried at 130°C for 24 hours, while rubidium iodide (Alfa, 99.9%) and rubidium acetate (Alfa, 99%) were recrystallized from methanol; the iodide was dried at 150°C, the acetate at 60°C under vacuum.

While cesium perchlorate (Alfa, 99%), cesium bromide

(Alfa, ul were drie crystalli Inc.) and Recrystal Thallium water and chloride ultrapure silver re mitmate (ture unde Punts obtained armonium for 22 ho Was first ty the as ty the ad under vac tutylammo Water, th acetate a tion of t the salt 18 hours.

rre e

(Alfa, ultrapure), and cesium iodide (Alfa, ultrapure) were dried at 60°C under vacuum, it was necessary to recrystallize cesium thiocyanate (Rocky Mountain Research, Inc.) and cesium acetate (Alfa, technical) from methanol. Recrystallized salts were dried under vacuum at 50°C. Thallium (I) perchlorate (K and K) was recrystallized from water and dried at 110°C for 24 hours. Thallium (I) chloride (Alfa, ultrapure) and thallium (I) acetate (Alfa, ultrapure) were dried under vacuum at 40°C. Anhydrous silver perchlorate (G. F. Smith Chemical Co.) and silver nitrate (Baker, AR) were dried over P205 at room temperature under vacuum for at least 72 hours.

Purified tetramethylammonium bromide (Eastman) was obtained from Mr. Pierre-Henri Heubel. Tetra-n-butyl-ammonium bromide (Eastman) was dried at 50°C under vacuum for 2^{\(\text{L}\)} hours. Tetra-n-butylammonium perchlorate (Eastman) was first precipitated from acetone and then from methanol by the addition of water and then precipitated from methanol by the addition of diethyl ether; the product was dried under vacuum at room temperature for 48 hours. Tetra-n-butylammonium iodide (Aldrich) was recrystallized from water, then from a solvent mixture containing 95% ethyl acetate and 5% of ethanol (190 proof). After a precipitation of the salt from methanol by the addition of ether, the salt was dried at room temperature under vacuum for 48 hours.

The anion exchange resin was Dowex 1X2, 50-100 mesh

(Baker) in tatch proce deionized v than 5. Th air-dried a to the hydr with 32 met Wash, porti aqueous mit the present til no chla packed as a length by 2 tion of base armonium ioc basio eluent The cat: (Baker) in i Water, and a anion exchan Verted to th Washing with until the spe resin was pac length. Expe

a methanolic

(Baker) in the chloride form. The resin was washed in a batch process three times with 6M aqueous HCl and then with deionized water until the wash liquid showed a pH greater than 5. The resin was further washed with acetone and air-dried at room temperature. Conversion of the resin to the hydroxide form was effected by exhaustive washing with 3M methanolic sodium hydroxide solution. After each wash, portions of the spent liquid were neutralized with acueous nitric acid and tested with silver nitrate for the presence of chloride ion. Washing was continued until no chloride ion could be detected. The resin was packed as a methanolic slurry into a column 40 cm in length by 2.1 cm diameter. In the experimental production of base, a methanolic solution of tetra-n-butylammonium iodide was passed through the column and the basic eluent was collected.

The cation-exchange resin, Dowex 50W-X8, 50-100 mesh (Baker) in its hydrogen ion form, was washed with acid, water, and acetone and dried in the same manner as the anion exchange resin. After drying, the resin was converted to the tetra-n-butylammonium form by exhaustive washing with 1M tetra-n-butylammonium bromide solution until the spent wash liquid was no longer acidic. The resin was packed into a 2.1 cm diameter column of 40 cm length. Experimental production of base was by passing a methanolic solution of sodium hydroxide through the

column and by collecting the basic eluent.

Monensin was received as the sodium salt by the generous gift of the Eli Lilly Company (QA 166H Lot 261FF5, also Elanco Lot X-30162). The salt purity was labelled as 880 mg/g and extensive purification was necessary. The brown impurity was fairly insoluble in methanol and could be removed by filtering a hot methanolic solution of the salt; in some cases methanol-washed Celite 545 (Fisher) was used as a filter aid to prevent the clogging of glass fritted funnels by the gelatinous brown material. After the filtration step, monensin sodium salt (MonNa) was twice precipitated from methanol by the addition of water. A further precipitation of MonNa from ether by the addition of petroleum ether, followed by drying at 110°C, resulted in a white powder with properties which agreed with those previously described (174).

The free acid form of monensin (MonH) was obtained by shaking a chloroform solution of MonNa with an aqueous 0.1 M hydrochloric acid solution. Evaporation of the organic phase gave a white powder which was further purified by two precipitations from methanol by the addition of water. Filtration of these precipitates was greatly facilitated by a digestion period of about 12 hours. By drying the precipitate at 40°C under vacuum for 24 hours one obtained a white product with the properties previously described (174). A mixture of products was obtained when

- 1.0 \underline{M} acid was used instead of 0.1 \underline{M} acid in the initial step.
- 2.1.2. SOLVENTS Methanol (Fisher, ACS) intended for use in measurements was twice distilled over magnesium turnings; water content of the product was less than 75 ppm by Karl Fischer titration. Chloroform (Mallinckrodt, AR) and deuterated chloroform (Aldrich Diaprep, 99.9%) were used as received. Solvents used in reagent preparation and purification were used as received and included acetone (Drake), ethyl ether (Drake), petroleum ether, boiling range 30-60°C (Mallinckrodt, AR), and ethyl acetate (Mallinckrodt, AR).

2.2. METHODS

2.2.1. ELECTROCHEMISTRY

2.2.1.1. Cyclic Voltammetry - Cyclic voltammograms were obtained with a Princeton Applied Research Model 174 polarographic analyzer and recorded on a Houston Instruments Model 2000 x-y recorder. Voltage measurements were made with respect to a methanolic saturated calomel electrode (SCE) with KCl as the supporting electrolyte; a platinum wire spiral was used as auxiliary electrode and a hanging mercury drop as working electrode. All measurements were carried out in 0.16 M tetra-n-butylammonium

as the s was comp genated solution after bu apparent With bub presatur Both determi: In the d ion was ing cond formatic from the Petitive observe: tion. Was the remeasu complex of the ! viduall;

due to .

steps.

Section

hydroxid

hydroxide solution in methanol, the hydroxide served both as the supporting electrolyte and to ensure that monensin was completely deprotonated. The solutions were deoxygenated by passing a slow stream of pure nitrogen and the solution volumes were readjusted with degassed solvent after bubbling. The necessity for volume readjustment is apparent from Figure 4, which shows that solvent loss with bubbling was significant even when two fritted presaturators were used.

Both direct and indirect methods were used for the determination of formation constants by cyclic voltammetry. In the direct method, the half-wave potential of Tl(I) ion was observed at constant metal concentration and increasing concentration of the monensin anion (Mon⁻), and the formation constant of the Tl + Mon - complex was calculated from the $\Delta E_{1/2}$ values (see below). In the indirect competitive method, the Tl(I) half-wave potential was first observed as a function of an increasing ligand concentration. A solution of a salt $M^{+}X^{-}$ of a different metal was then added, and the Tl(I) half-wave potential was remeasured. Knowing the formation constant of the Tl(I) complex, it was simple to calculate the formation constant of the M⁺Mon⁻ complex. The experiment was run on individually prepared solutions rather than as a titration, due to the solvent losses accrued during the degassing steps. The details of the data reduction are given in Section 3.2.

Figure 4. Loss of methanol from the titration cell at room temperature (23°C) with nitrogen gas bubbling through the solvent at a rate of 40 ml·min⁻¹.

*, no gas flow; •, dry gas; □, gas passed through a single fritted bubbler in methanol before reaching cell; o, gas passed through two bubblers before cell.

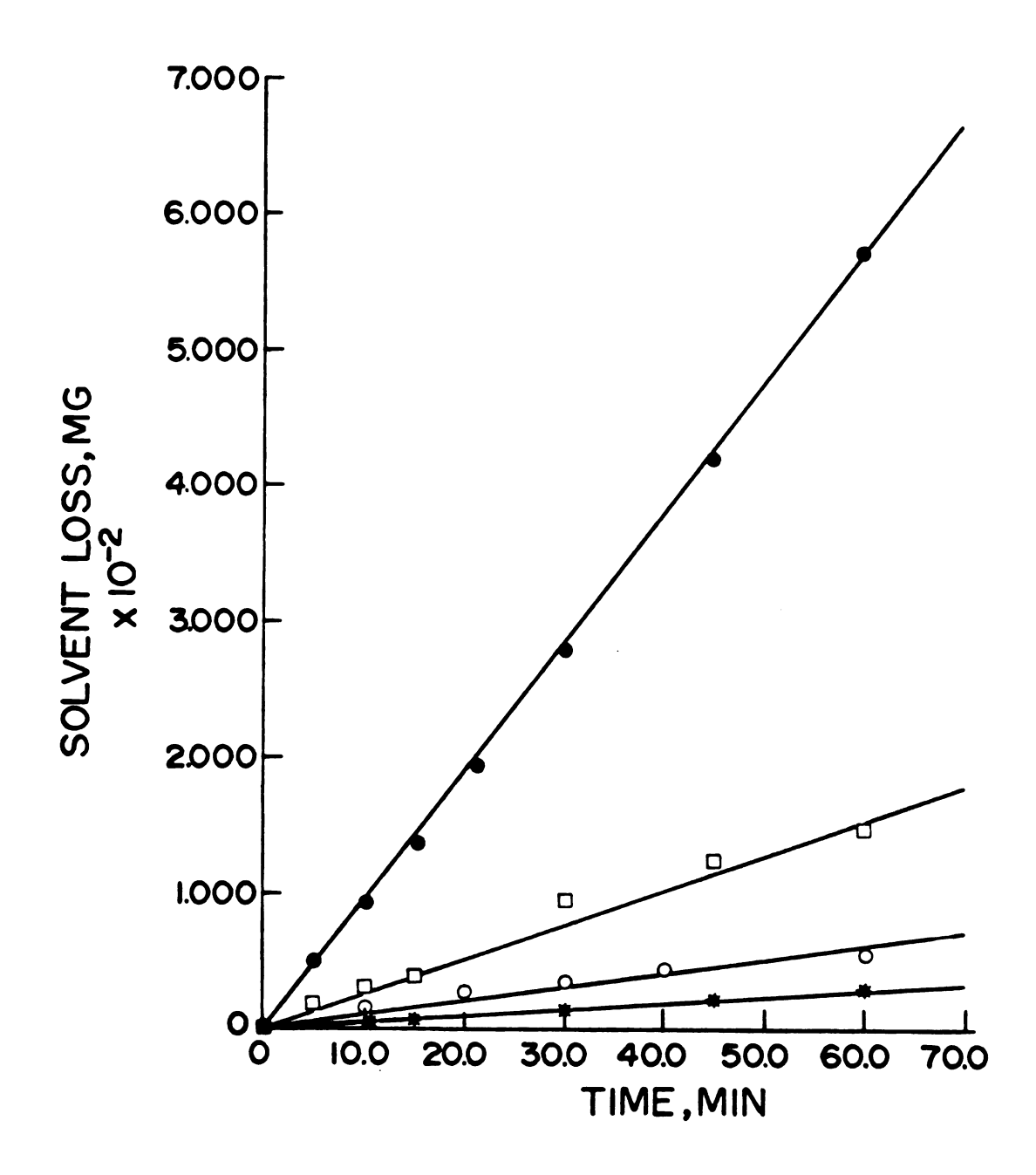


Figure 4

obtain

polare

voltam

to the

ing th

rated

of Hg

the dr

six se

Wire w

Were c

Teasur

soluti

Edded

thermo

each /

in and

- 2.2.1.2. Polarography Polarograms were also obtained with the Princeton Applied Research Model 174 polarographic analyzer and recorded as were the cyclic voltammograms. Voltage measurements were with respect to the methanolic SCE; this electrode was made by replacing the aqueous KCl filling solution of an SCE by a saturated methanolic solution of that salt. A head of 50 cm of Hg provided a mass flow rate of about 65 mg Hg/min at the dropping mercury electrode, with a drop time of about six seconds at the Tl(I) half-wave potential; a platinum wire was used as auxiliary electrode. The measurements were carried cut in 0.1 M tetra-n-butylammonium perchlorate solution in methanol, with tetra-n-butylammonium hydroxide added to depretonate the monensin, if desired.
- 2.2.1.3. <u>Conductimetric Titrations</u> Conductance measurements were carried out in methanol solutions by using a Beckman Model RC-18A conductivity bridge. The cell, which has been described by Greenberg (181), was thermostatted at 25.00±0.02°C in a water bath; several minutes were allowed for temperature equilibration after each volume addition.
- 2.2.1.4. <u>Potentiometry</u> All potentiometric titrations were done with glass ion-selective and pH electrodes in anhydrous methanol solutions. Corning NAS 11-18 sodium

ion, 276 were pre (182). with sat electrod (Corning a much than and Was fed tage fo: 3130) F3 Cutput (Analogi in a ray Tit thermos 5-m2 bu tempera Were ma sclutic was pur acid-ba measure

lem, th

to encl

 I_n

ion, 276220 monovalent cation, and 476105 pH electrodes were preconditioned to methanol as described by Frensdorff (182). The reference electrode was silver-silver chloride with saturated KCl as the supporting electrolyte; this electrode was constructed with a "thirsty quartz" junction (Corning Vycor brand 7930 acid-leached quartz) which shows a much lower transfer of potassium ion into the solution than any other junction used. Output from the electrodes was fed into a high-impedance operational amplifier voltage follower; use of a MOSFET operational amplifier (RCA 3130) provided an input impedance greater than $10^{12}~\Omega$. Output of the voltage follower was measured with an Analogic 2546 digital voltmeter; potentials could be read in a range of $\pm 2.0~V$ with $\pm 0.1~mV$ accuracy.

Titrations were carried out in an all-glass cell thermostatted to ±0.1°C. Titrant was added from 2- or 5-ml burets. In cases where titrant and reaction vessel temperatures differed significantly, volume corrections were made for thermal expansion and/or contraction of solutions. The titration cell, while essentially airtight, was purged with nitrogen to remove carbon dioxide during acid-base titrations. During ion-selective electrode measurements, where formation of carbonates is not a problem, the cell was not purged with nitrogen.

In order to reduce electrical noise, it was necessary to enclose the titration assembly in a grounded Faraday

tion mix ncise ir The formed a of 0.16 temperat supporti methanc] generat: the salt titrated equatic: are give In t for the butylamm and the sclution of the f to inclu electros Titz

out as f

a soluti

butylamm

cage. I

cage. An air-driven magnetic stirrer was used for solution mixing since electrical stirrers introduce electrical noise into the cage.

The titrations with ion-selective electrodes were performed as follows: with all electrodes in place, 20 ml of 0.16 M tetra-n-butylammonium hydroxide solution was temperature equilibrated in the cell for 30 min. The supporting electrolyte was then "titrated" with the methanol solution of the metal salt of interest, thus generating an electrode calibration curve. After all of the salt solution was added, the final solution was backtitrated with a solution of the ligand. The necessary equations for calibration and equilibrium calculations are given in Section 3.3.

In the case of silver complex, the calibration curve for the NAS 11-18 electrode was obtained with tetra-n-butylammonium perchlorate as the supporting electrolyte, and the final solution of Ag⁺ ions was titrated with a solution of monensin-sodium complex, MonNa. Calculations of the formation constants were done iteratively in order to include the effects of the liberated Na⁺ ion on the electrode response.

Titrations which used glass pH electrodes were carried out as follows: with all electrodes in place, 20 ml of a solution containing $2x10^{-3}$ M $HClO_{\mu}$ in 0.15 M tetra-n-butylammonium perchlorate was temperature equilibrated

in the with te equival for the could t if desi bration ammoniu In ence of perchic Was 0.1 same ca medium, tion of the aci final c Meis te armor.iu

The for the tase ti

4.5. Nit:

tion was

in the cell for 30 min. The strong acid was then titrated with tetra-n-butylammonium hydroxide solution to the equivalence point, thus generating the calibration curve for the glass electrode as the free H⁺ ion concentration could be calculated at each point. Aliquots of acid and, if desired, salt solutions were added to the final calibration solution and the acid titrated with tetra-n-butyl-ammonium hydroxide solution.

In the acid-base titrations of monensin in the presence of K^+ , Rb^+ , or Cs^+ , where precipitation of metal perchlorates was a problem, the supporting electrolyte was 0.15 \underline{M} tetra-n-butylammonium iodide. Although the same calibration procedure was used as in the perchlorate medium, account had to be made of the incomplete dissociation of HI. Also, due to the presence of the $ClO_{\overline{4}}^-$ ions, the acid and the salt could not be added directly to the final calibration solution and, therefore, the titrations were performed in a second aliquot of 0.15 \underline{M} tetra-n-butyl-ammonium iodide.

The necessary equilibria and mass-balance equations for the calculation of equilibrium constants from acid-base titration data are considered in detail in Section 4.5.

Nitrogen gas used to purge the titration cell solution was freed from oxygen, carbon dioxide, and water. The gas was passed through fritted glass bubblers in

solution barium and fin

instrum

duced t

is shown

Mostek :

Eenerato

Instrume

(Texas :

The curi

ment and

a temper

(Intersi

the inte

circuits in the c

Duri

provided Was open

Pulses 11

solutions of cobalt (II) sulfate and a basic solution of barium chloride, then through a drying tower of Drierite, and finally bubbled through methanol before being introduced to the titration cell.

2.2.1.5. Coulometry - A block diagram of the instrument constructed for constant-current coulometry is shown in Figure 5. The crystal time base was controlled by a 1.000 MHz crystal oscillator in conjunction with a Mostek MK 5009 counter time-base circuit. The pulse generator was designed around a 555 timer chip (Texas Instruments), and the gate was comprised of NAND gates (Texas Instruments, SN7400). Five of seven 7490 decade counters were multiplexed to provide a five-digit display. The current source was designed by M. Rabb of this department and consisted of a 741C operational amplifier, with a temperature-compensated Zener diode to provide an accurate and stable voltage reference. A solid-state switch (Intersil DG 191) was used to limit residual current in the intervals between current passages. Details of the circuits and construction of the coulometer can be found in the operating manual (183).

During experiments (run mode) the crystal time base provided a train of pulses at 10.00 KHz. When the gate was opened, the decade counters recorded the number of pulses in the train until the gate was closed, thus

Figure 5. Block diagram of the constant - current coulometer.

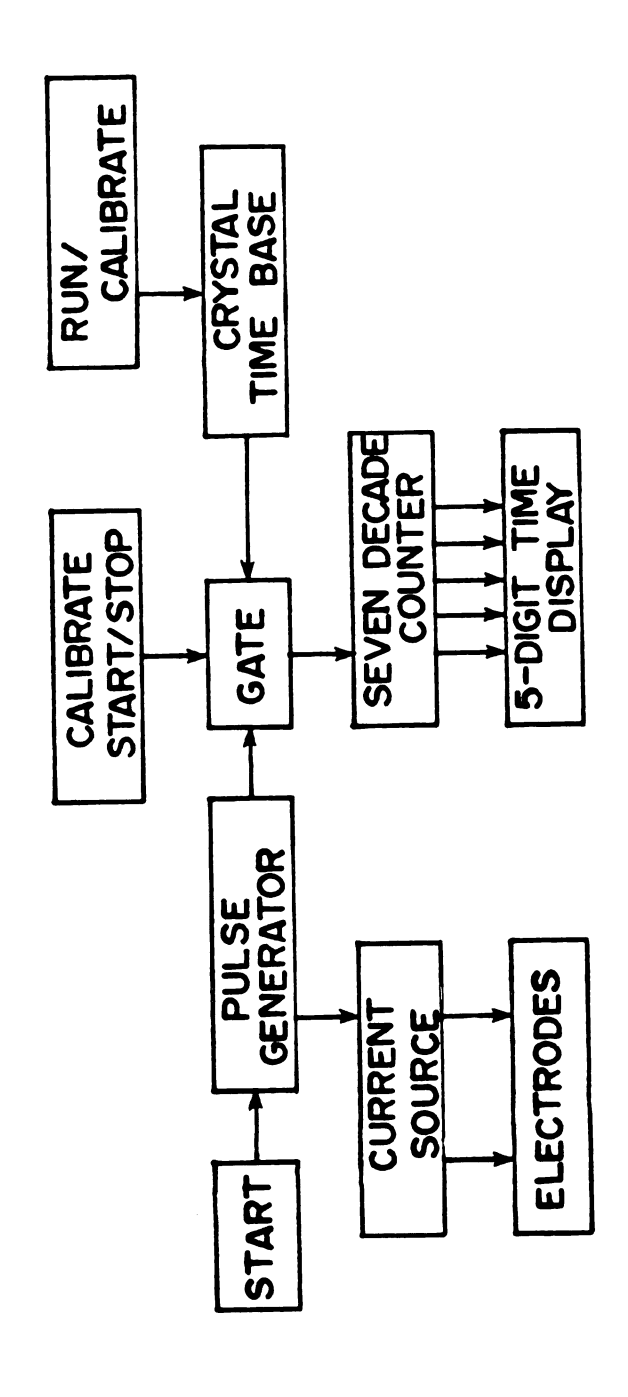


Figure 5

providin was open start s presele simulta: the gate corded · open, a: had flo digit d The time ta cisely start s elapsed for abo to a re Ęŗ.6

time ba time. of 1 us

stabil:

electro
cylinde

was open. In operation, the experimenter depressed the start switch, which turned on the pulse generator for a preselected time of 100 ms to 10 s. The pulse generator simultaneously turned on the current source and opened the gate. Thus, as shown in Figure 6, the counters recorded the length of time during which the gate had been open, and which was identical to the time that the current had flowed. The elapsed time was read out on the fivedigit display.

The coulometer also had a mode for calibrating the time base. In the calibrate mode the time base was precisely divided to a frequency of 100 Hz. The calibrate start switch served to open the gate manually and the elapsed time was displayed. Typically the gate was opened for about 10^{4} s and the measured elapsed time was compared to a reference time.

The instrument specifications were as follows: the time base was accurate to better than 0.5 ppt of the actual time. The current rise and fall times were on the order of 1 μ s, and the residual current was about 2 nA. Current stability was estimated to be ± 1 ppt.

Coulometric base generation was performed with platinum electrodes. The generating electrode was a platinum mesh cylinder 3 cm high and 3 cm in diameter. The counter electrode, platinum foil 1 cm by 1.5 cm, was placed in a

Figure 6. Waveforms typical of a single coulometric titration step.

____\

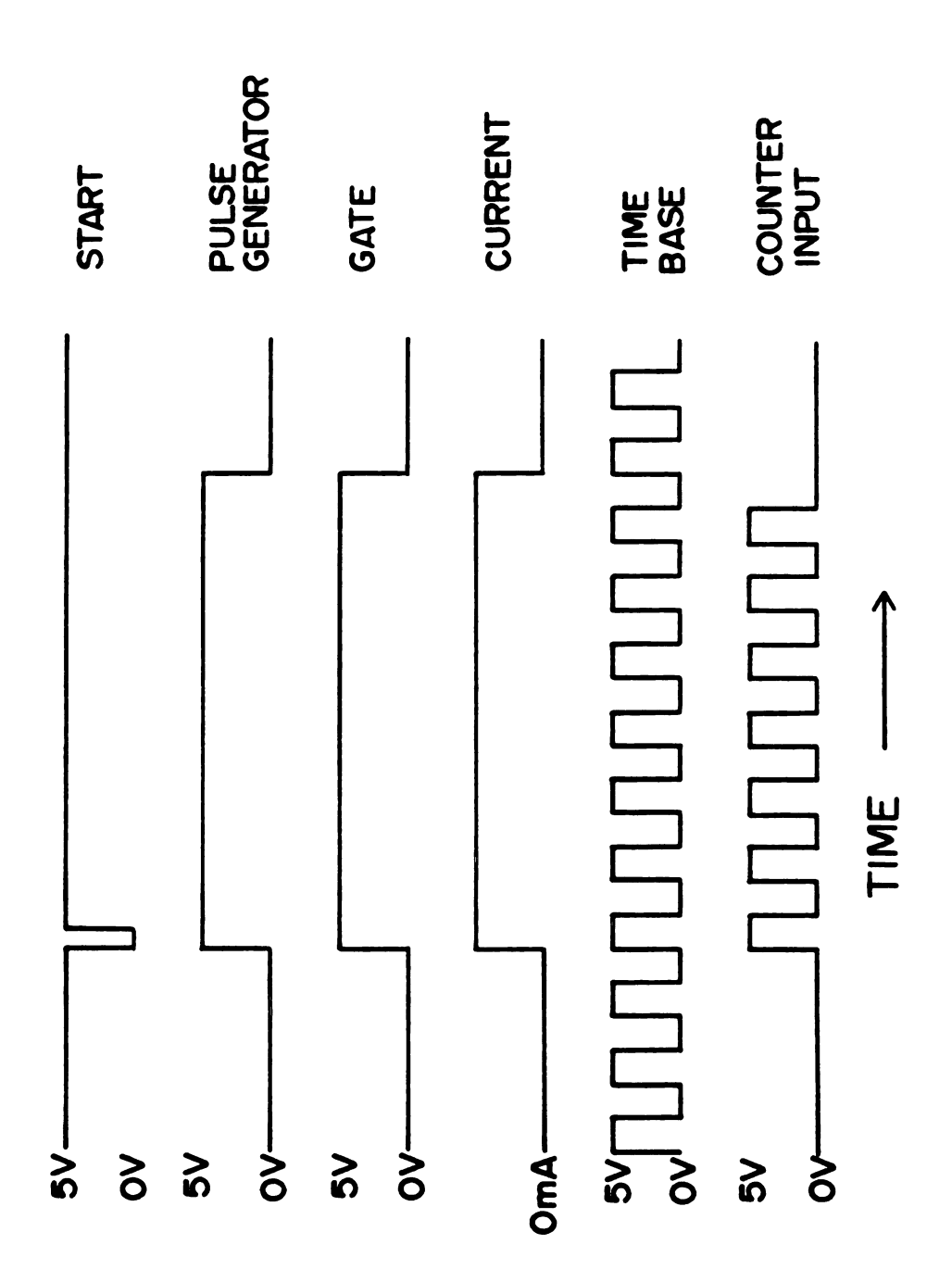


Figure 6

glass tu anion ex Ionios 1 at the t

2.2.

4000-600 457 and 2 tions and

sodium or done by t

300 nm we

Merotek

measured recorded om square

modified of driven mag

For the me

Was at 230

glass tube and separated from the sample solution by an anion exchange membrane in the ${\rm ClO}_4^-$ form (Cl form membrane, Ionics 103-PZL-183). Solutions were stirred vigorously at the time of base generation.

2.2.2. SPECTROSCOPY

- 2.2.2.1. <u>Infrared</u> Spectra covering a range of 4000-600 cm⁻¹ were obtained by means of Perkin Elmer Models 457 and 237B grating infrared spectrophotometers. Solutions and Nujol mulls of solid samples were placed between sodium chloride mull plates. Wavelength calibration was done by using standard polystyrene bands.
- 2.2.2.2. <u>Ultraviolet-visible</u> Spectra from 200-800 nm were obtained in square 1.0 cm quartz cells on a Microtek Unicam SP.800 spectrophotometer.
- 2.2.2.3. <u>Fluorescence</u> Fluorescence spectra were measured on an Aminco-Bowman Spectrophotofluorometer and recorded on a Houston Model 2000 x-y recorder. The 1.0 cm square stoppered quartz cells were positioned in a modified cell-holder which allowed the use of an air-driven magnetic stirrer for solution mixing in the cell. For the measurements of the Tl(I) fluorescence, excitation was at 230 nm, and the emission was monitored from 300 to

500 nm. Mirrors were used on the back sides of the cell to reflect exciting radiation back through the cell as well as to augment collection of the emitted light.

2.2.2.4. <u>Nuclear magnetic resonance</u> - Proton nmr spectra were taken on a Varian A56/60D spectrometer, using calibrated chart paper and sideband-calibrated sweep widths. All chemical shifts were referenced to TMS.

Carbon-13 spectra were obtained on a Varian CFT-20 spectrometer, using an internal deuterium lock and complete proton decoupling. As in the proton spectra, all shifts were referenced to TMS as internal standard.

Alkali metal and thallium nmr spectra were obtained on a highly modified Varian DA-60 spectrometer in the Fourier Transform mode. Data acquisition was done by a Nicolet 1083 computer. The instrument had a magnetic field of 1.409 Tesla and employed an external proton lock. Experimental conditions are given in Table II. Chemical shifts were not corrected for bulk diamagnetic susceptibility. The shifts were referenced to the solutions listed in Table II.

2.2.3. OTHER ANALYSES

2.2.3.1. <u>Gas Chromatography</u> - A Varian Aerograph Model 420 was used with helium carrier gas and thermal conductivity detection. Porapak QS, 80-100 mesh (Waters

	Table II.	Experimental	Conditions	for	Metal	Ion	NMR.
--	-----------	--------------	------------	-----	-------	-----	------

Nucleus	Resonance Frequency, MHz	External Reference Solution
7 _{Li}	23.32	4.0 M Liclo ₄ in H ₂ O
23 _{Na}	15.87	3.0 M NaCl in H ₂ O
39 _K	2.80	sat'd KNO2 in D20
133 _{Cs}	7.87	0.5 M CsBr in H ₂ O
205 _{Tl}	34.61	2.5 <u>M</u> TlOAc in H ₂ O

Associates) was packed by vibration and tamping into a stainless steel column of dimensions 2 feet x 1/4 inch. Samples were introduced by means of microliter syringes (Hamilton).

- 2.2.3.2. <u>Water Analysis</u> Karl Fischer titrations were done by a Photovolt Aquatest II titrimeter.
- 2.2.3.3. X-ray Analysis In single-crystal X-ray diffraction studies the crystal was mounted on a glass fiber with epoxy glue. Diffraction data were collected at room temperature (23°C) with a Picker FACS-I automatic diffractometer using Zr-filtered Mo Ka radiation. The single-crystal X-ray work was carried out by Drs. D. L. Ward and K.-T. Wei of this department (184).

Picker i 40 mm ra diffract tape and nine how Powdered referen sin² e,

Powe

water, contain of meta knowns.

ment commonochritanmama
PM tube

11, 670

°s, 852

With a 1

runs for

provide

Powder diffraction data were collected by using a Picker instrument equipped with a Guinier camera with 40 mm radius. The powdered samples for the transmission diffraction patterns were mounted on Scotch transparent tape and exposed in vacuo to Cu K α radiation for about nine hours. X-ray generation was at 35 KV and 18 mA. Powdered platinum mixed with the samples served to generate reference lines. Film line spacings were converted to $\sin^2\theta$, d, and $\sin\theta/\lambda$ values with a computer program provided by Dr. H. A. Eick.

2.2.3.4. Flame Analysis - Methanolic sample solutions were diluted to desired concentrations with distilled water, and care was taken that all standard solutions contained very nearly the same amounts of methanol and of metal salts (other than the analyte) as did the unknowns. Flame analyses were performed on a Heath instrument consisting of an EU-703-70 flame unit, EU-700 scanning monochromator, and EU-701-30 PM module containing a Hammamatsu R446 UR PM tube. The 300-850 nm range of the PM tube allowed analysis of the following wavelengths:
Li, 670.7 nm; Na, 589.2 nm; K, 766.5 nm; Rb, 780.0 nm;
Cs, 852.1 nm; T1, 377.8 nm. The analyses were obtained with a hydrogen-air flame (1 psi:15 psi) with duplicate runs for standards and unknowns.

Elmer RM used for

melting determi

to 300°

a CDC 6

equilit

Details

constar

- 2.2.3.5. <u>Mass Spectrometry</u> A Hitachi Perkin Elmer RMU-6 spectrometer with electron impact source was used for mass spectrometric analysis.
- 2.2.3.6. <u>Melting Point Analysis</u> A Fisher-Johns melting point apparatus was used for all melting point determinations. The instrument was calibrated from 40°C to 300°C by means of melting point standards (Hoover).
- 2.2.3.7. <u>Data Reduction</u> Data were analyzed on a CDC 6500 computer by using two major programs, a non-linear least-squares program, KINFIT4 (185), and a general equilibrium-solving program, MINIQUAD 76A (186-188). Details on the use of these programs for equilibrium constant calculations are given in the Appendices.

CHAPTER 3

METAL ION COMPLEXES WITH THE MONENSIN ANION, MON-

The

Several

the Mon

ments i

to calc

yet non

combini

...

In

ensin c

metry a

both by

copic d fluores

3.2. _P

Pol

T1(I)-K

of Ling.

of the

been pre

3.1. INTRODUCTION

The object of these studies was to gain an insight into the selectivity of the deprotonated monensin (Mon⁻) ionophore and thus it was desirable to measure the complex formation constants for Mon⁻ with various metal ions. Several workers have determined formation constants for the MonM type complexes, but agreement among the measurements is not good. Furthermore, it was necessary to know the stoichiometry of the complexation reaction in order to calculate equilibrium constants from experimental data, yet none of the previous studies have determined the combining ratio of ligand and metal ions.

In the present studies, the stoichiometry of the monensin complex with Tl(I) was determined by cyclic voltammetry and polarography. Formation constants were measured both by cyclic voltammetry and by potentiometry. Spectroscopic determinations of formation constants, based on Tl(I) fluorescence and metal ion nmr, were also considered.

3.2. POLAROGRAPHY AND CYCLIC VOLTAMMETRY

Polarographic technique was used to characterize the Tl(I)-Mon system in order to determine whether the method of Lingane (189) could be used to find the stoichiometry of the complex. Derivation of the Lingane equation has been presented in many texts and need not be shown here.

Lingane
the election
sibility
plot of
as show
also ha
and thu
Secondl
concent
could b

The

one ct

for the

Us

Which Tl(I)

ot mon

The requirements for successful application of the Lingane method to labile complexes are several. First, the electrode reaction must be reversible; the reversibility of the Tl(I)-Mon system was demonstrated by the plot of $log(i/(i_d-i))$ as a function of applied potential, as shown in Figure 7. This plot is not only linear, but also has a nearly Nernstian slope of 1.66 x 10^{-2} mV⁻¹, and thus confirms the reversibility of the reaction. Secondly, large excesses of ligand were used so that the concentration of free ligand at the electrode surface could be assumed to be equal to that in the bulk solution. Finally, it was assumed that the diffusion current constants for the complexed and free metal ion were nearly the same.

Using the assumptions considered above for the reaction

$$MX_{j} \neq M + jX$$

one obtains Lingane's equation

$$\Delta E_{1/2} = (E_{1/2})_{complex} - (E_{1/2})_{free}$$

$$= \frac{-2.303RT}{nF} \log \beta_{MX_{i}} \frac{-2.303RT}{nF} j \log C_{X}$$
 (3)

which predicts that the measured half-wave potential of T1(I) should shift to a more negative value in the presence of monensin. This predicted shift was indeed observed,

20

10

Figure 7. Reversibility plot for a polarogram of a solution of 5.0 x 10^{-4} M TlClO $_4$ and 5.95 x 10^{-3} M Mon in anhydrous methanol. The points are measured values and the line is a least-squares fit.

901

-1

-2

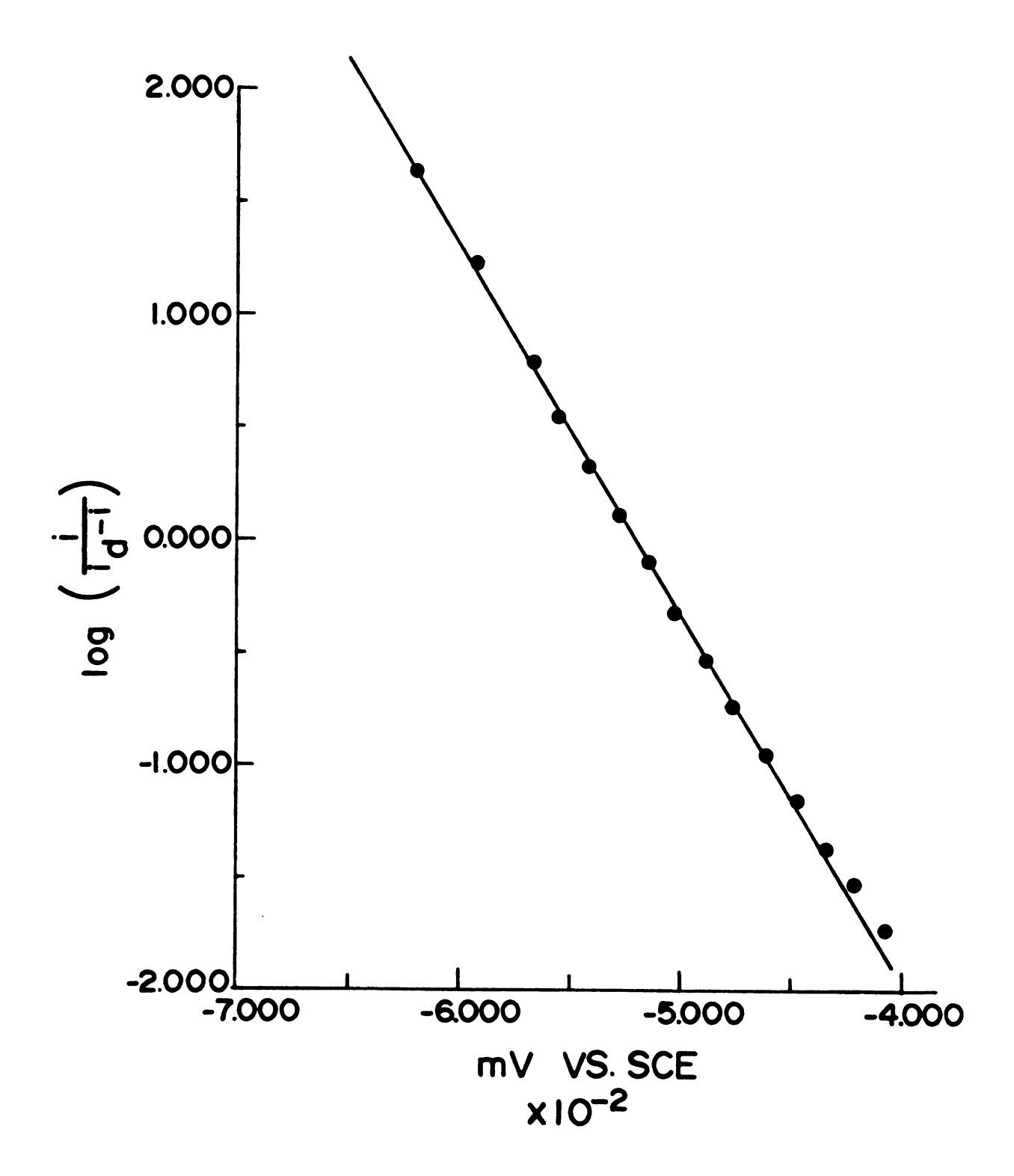


Figure 7

Aft bility system, complex Reversi separat tial sw Cor ΔE_{1/2} , ratio, slope a The 9. It comple: same st 72*, K state ; (170). Су stabil: metal : conver: close 4

as Tl(

a modi:

as show

as shown in Figure 8.

After these initial studies have shown the applicability of Lingane's method to the study of the Tl(I)-Monsystem, cyclic voltammetry was used to determine the complex stoichiometry and to measure formation constants. Reversible electrode reactions, as ascertained by peak separations of 55 to 70 mV, could be obtained with potential sweep rates of 20 mV·s⁻¹ or less.

Consideration of Equation (3) shows that a plot of $\Delta E_{1/2}$ versus -log C_X should be linear. The combining ratio, j, of ligand to metal may be determined from the slope and the formation constant β_{MX} , from the intercept.

The results of such an experiment are shown in Figure 9. It is evident from the slope of 69 mV that only a 1:1 complex, Mon⁻Tl⁺, is formed. This 1:1 complex has the same stoichiometry as the various Mon⁻ complexes of Ag⁺, Tl⁺, K⁺, Rb⁺, and Na⁺ which have been studied in the solid state by x-ray crystallography (167) and mass spectrometry (170).

Cyclic voltammetry was also used to determine the stability constants of Mon complexes with several alkali metal ions. The reduction waves of these ions cannot be conveniently observed in methanol as they appear too close to (or beyond) the solvent reduction wall. However, as Tl(I) ion is reduced at much more positive potentials, a modification of the Ringbom and Eriksson method (190,

Figure 8. Representative polarograms in anhydrous methanol solution. I, the supporting electrolyte, 0.1 $\underline{\text{M}}$ tetra-n-butylammonium perchlorate; II, 2 x 10^{-4} $\underline{\text{M}}$ TlClO₄ in supporting electrolyte; III, 2 x 10^{-4} $\underline{\text{M}}$ TlClO₄, 4.9 x 10^{-3} $\underline{\text{M}}$ Mon⁻ in supporting electrolyte.

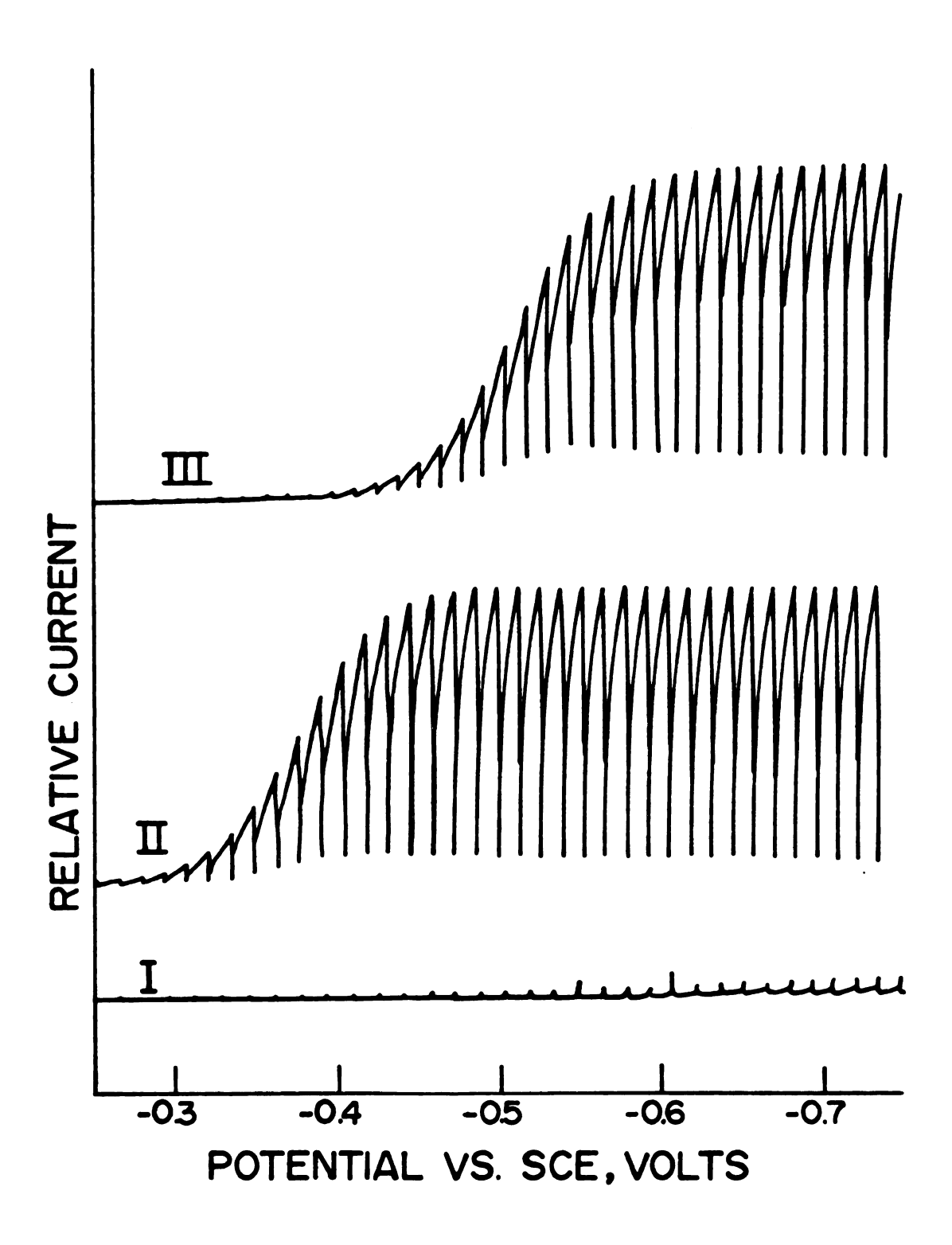


Figure 8

Figure 9. Lingane plot of $\Delta E_{1/2}$ as a function of log [Mon⁻] for the Mon⁻ - Tl⁺ system in absolute methanol. The line is a least-squares fit through the observed points (218). (Reproduced with the permission of the copyright holder.)

- 2

-1

Half-wave Shift, mV

-

-

•

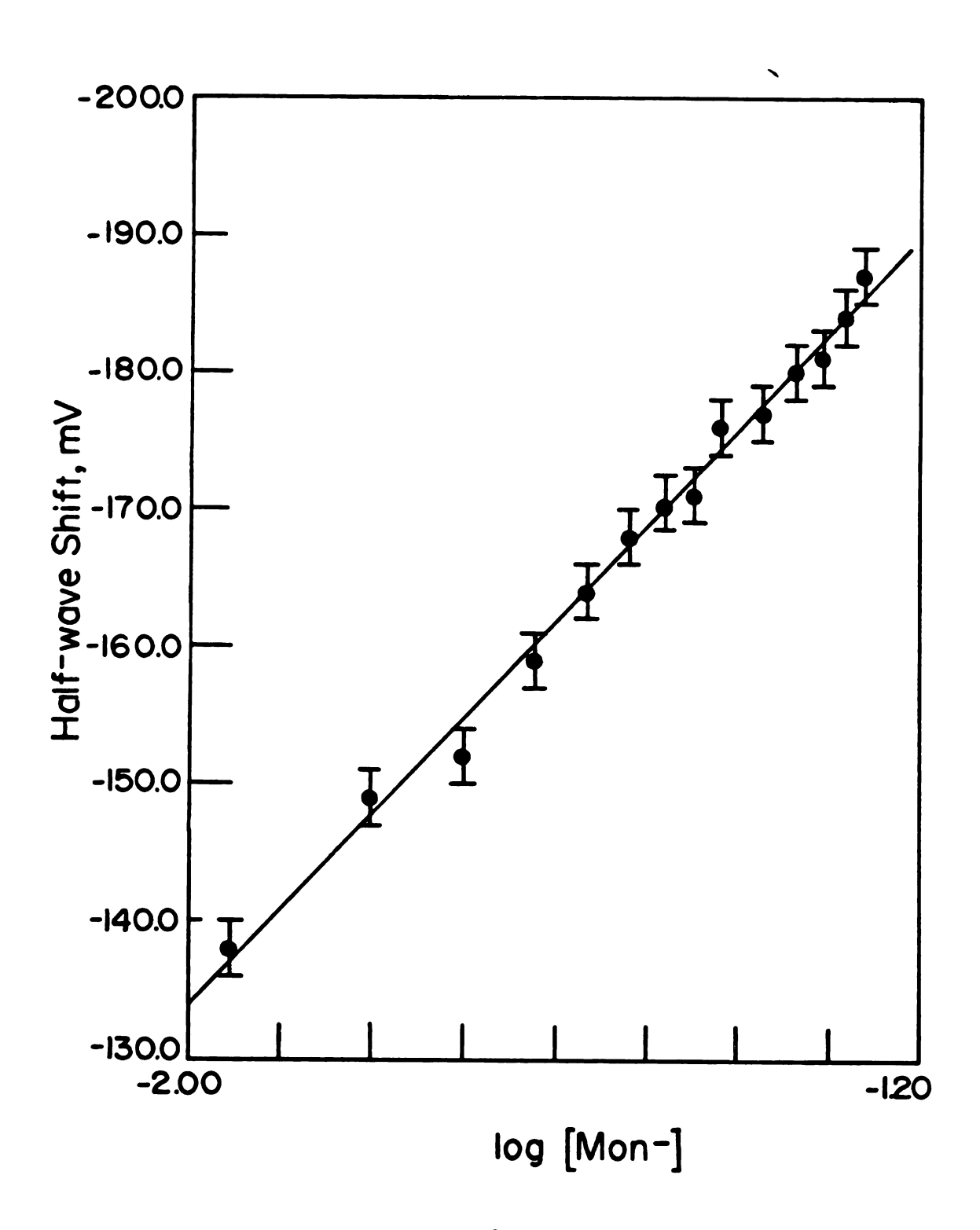


Figure 9

It has a tion of potential concents of free reduction using a ligand of tial at equation plex, where the concents of the conce

191) ca:

From the ing (6) substitu

and [M+]

191) can be used to determine the formation constants. It has already been seen that addition of Mon to a solution of Tl(I) ions results in a shift of the halfwave potential to more negative values as the free ligand concentration is increased. The addition of another complexable metal ion should decrease the concentration of free ligand, and the halfwave potential of the Tl(I) reduction should revert to more positive values. By using a curve such as the one shown in Figure 9, the free ligand concentration is obtained from the halfwave potential at any point in the titration. Using mass balance equations and the formation constant for the MonTl complex, K_f^{Tl} , we obtain

$$C_{M+} = [MonM] + [M^{+}]$$
 (4)

$$C_{Mon}^- = [Mon^-] + [MonM] + [MonT1]$$
 (5)

$$[MonT1] = K_{\mathbf{f}}^{\mathbf{T}1} [Mon^{-}] [\mathbf{T}1^{+}]$$
 (6)

$$C_{T1}^{+} = [MonT1] + [T1^{+}]$$
 (7)

From the value of the free ligand concentration and solving (6) and (7), one gets a value for [MonTl], after which substitution into (4) and (5) gives values for [MonM] and [M $^+$], thereby enabling the calculation of $K_{\mathbf{f}}^{\mathbf{M}}$.

tratic

Th

limit

ments

where

and th

to ser

for as

in the

Th

effect

the De

Where

Was fo

a valu

result

rectio

retry

result

obtain

The technique for competitive determination of concentration formation constants as applied here has an upper limit of log $K_{\mathbf{f}}^{\mathbf{M}} \approx 4$. It was found that for accurate measurements it was necessary that $C_{\mathbf{M}^+} > C_{\mathbf{Mon}^-}$. In the cases where $C_{\mathbf{M}^+} < C_{\mathbf{Mon}^-}$ and $K_{\mathbf{f}}^{\mathbf{M}}$ is appreciable, [MonM] $\approx C_{\mathbf{M}^+}$, and the determination of [M⁺] by Equation (2) is subject to serious error. However, $C_{\mathbf{M}^+}$ cannot become too large, for as [Mon⁻] approaches zero, so does the observed shift in the halfwave potential.

The formation constants were corrected for activity effects by the calculations of activity coefficients from the Debye-Huckel equation

$$\log \gamma_{\pm} = -\frac{[1.823 \times 10^{6}/(DT)^{3/2}]|Z_{+}Z_{-}|\sqrt{I}}{1 + [5.029 \times 10^{9}/(DT)^{1/2}]a\sqrt{I}}$$
(8)

where the <u>a</u> parameter was taken to be 5×10^{-8} cm. It was found that at 25° C the mean activity coefficient had a value of 0.422 and, therefore, serious errors would result from the usual practice of ignoring activity corrections.

The formation constants determined by cyclic voltammetry are shown in Table I. Further discussion of these
results will be given later in comparison to those results
obtained by other measurement techniques.

After

The :

Ag/AgCl,

and the c

At consta the cours

charges v

also rema

given by,

where Eo,

3.3. POTENTIOMETRY

After the preliminary values of the formation constants had been obtained by cyclic voltammetry, more precise values of these constants were determined by potentiometric titrations.

The potentiometric measurement cell was as follows:

Ag/AgCl//salt solution/glass electrode sensitive to M+

and the cell potential is given by

$$E = E_{glass}^{\circ} + \frac{RT}{nF} \ln a_{M} - E_{Ag/AgCl} + E_{j}$$

$$= E_{cell}^{\circ} + \frac{RT}{nF} \ln a_{M} + E_{j}$$

$$= E_{cell}^{\circ} + E_{j} + \frac{RT}{nF} \ln C_{M} + \frac{RT}{nF} \ln \gamma_{M} + (9)$$

At constant ionic strength γ_{M^+} should be a constant; in the course of the titration if the solution composition changes very little, the junction potential, E_j , should also remain constant. Therefore the cell potential is given by,

$$E = E_{cell}^{\circ \prime} + \frac{RT}{nF} \ln C_{M}^{+}$$
 (10)

where E° is the sum of standard, junction and asymmetry

potentia It s titratio

electrod done at to be ca

protes a

potentia

surement

moving t

reduces

asymmetr

0 -14...

The curves v

and co-w

fecting calibrat

tions to

taminant

the limi

from the

tion fro

Electrod

16.

potentials.

It should be noted that the entire calibration and titration procedure was performed without removing the electrodes from solution. Thus the calibrations were done at constant ionic strength, allowing the electrodes to be calibrated as concentration, rather than activity, probes according to equation (10). Concentration calibration removes the uncertainty involved in relating potentials of buffer solutions of known activity to measurements done at different ionic strengths. By not removing the electrodes from solution one also substantially reduces the possibility of changes in the glass electrode asymmetry potential and in the junction potential.

The electrode calibration procedures gave calibration curves which deviated from ideality at $\sim 10^{-5}$ M. Midgley and co-workers (192,193) have described the factors affecting the linearity of glass ion-selective electrode calibration curves and concluded that the major contributions to nonideal calibrations were from interfering contaminants and reagent blank and, at concentrations near the limit of detection, dissolution of alkali-metal ions from the glass membranes. In the present work the contribution from the dissolution of glass was considered to be negligible compared to the effects of the first two causes. Electrode calibration curves were fitted to the equation

$$E = E^{\circ i} + m \log (C_{M^{+}} + R)$$
 (11)

where E and E°' have their usual meanings, m is the slope of the Nernstian plot, and R is the effective residual cation concentration contributed by the impurities in the solvent. The parameters varied were E°', m, and R. The calculated value of the slope, m, was used in subsequent calculations rather than assuming a theoretical slope of 2.303 $\frac{RT}{nF}$ for the Nernstian plots. A typical calibration curve is shown in Figure 10.

For Na⁺, Ag⁺, K⁺, and Rb⁺ ions the electrode responses were nearly Nernstian. The excellent electrode response to the sodium ion over a temperature range of 0-45°C is illustrated in Figure 11. In the case of Cs⁺ ion, calibration gave lower slopes than expected, while with Li⁺ ion no usable calibration curves could be obtained.

After titration of the calibration solution with the ligand, the calculation of the concentration formation constants was straightforward. Since in the titration the residual cation concentration from the solvent is negligible with respect to the total metal concentration, the amount of ligand used to complex this residual cation is likewise negligible. Thus by arrangement of Equation (11), the free metal concentration is defined by

$$[M^{+}] = 10^{\left(\frac{E - E^{\circ}}{m}\right)}$$
 (12)

Figure 10. Calibration curve for the ion - selective electrode in absolute methanol. The solid curve is the calculated calibration curve and the solid circles are experimental points (218). (Reproduced with the permission of the copyright holder.)

AGC!

.

-2

-4

-6

-8

-10

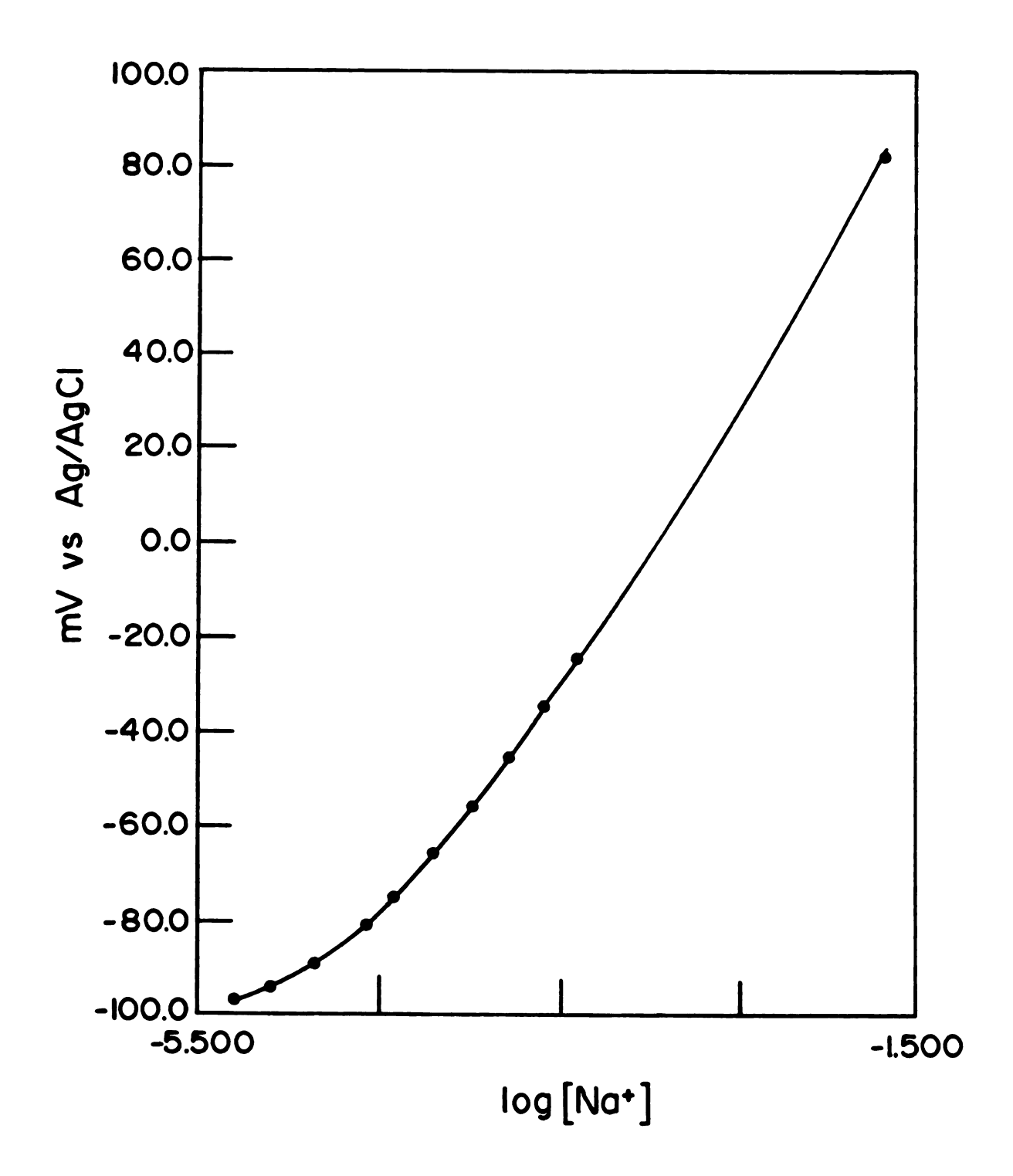


Figure 10

Figure 11. Temperature dependence of the slope \underline{m} in the Nernstian equation $E = E^{\circ}' + \underline{m} \log [Na^{\dagger}]$. Solid line is the calculated temperature dependence (218). (Reproduced with the permission of the copyright holder.)

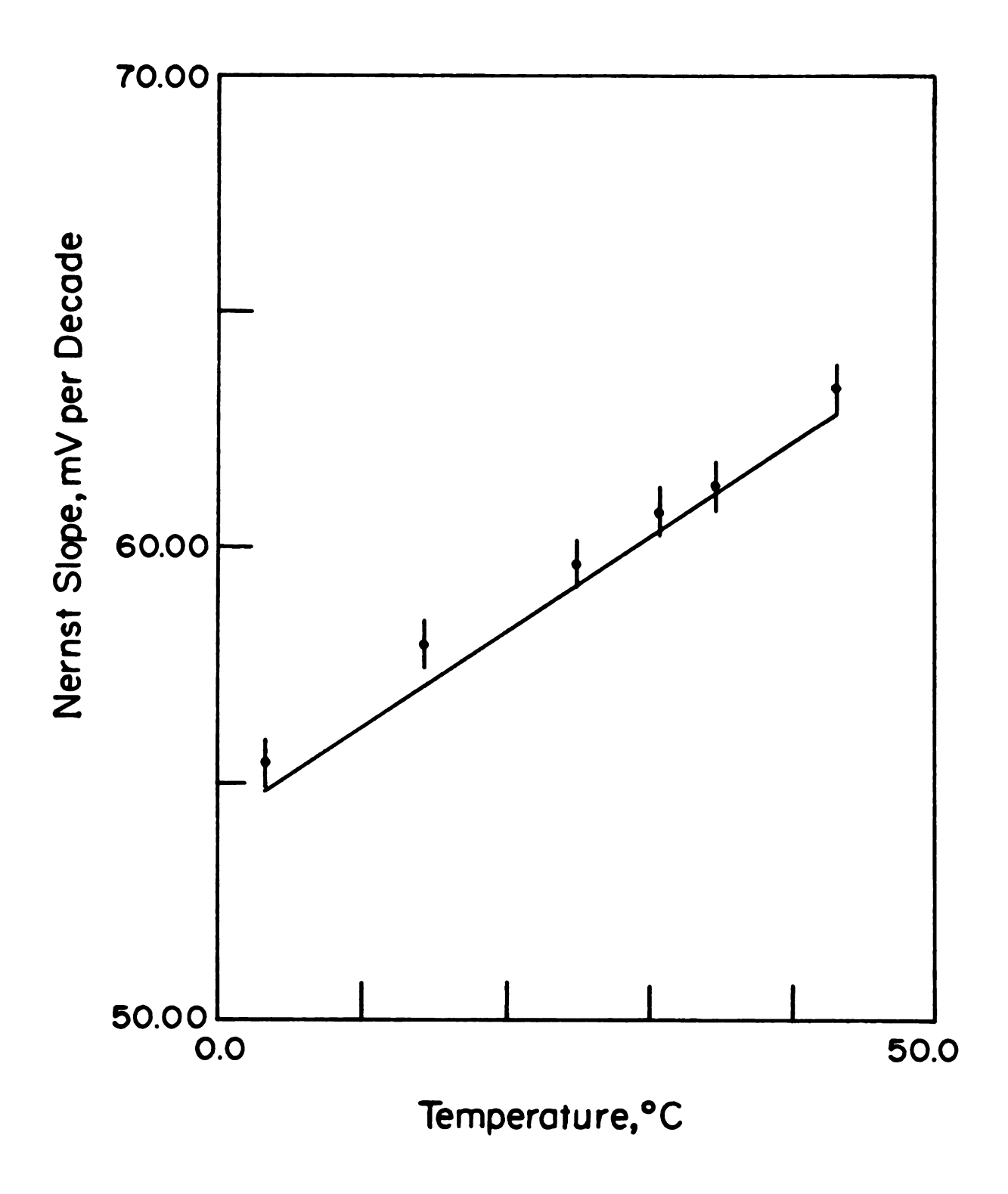


Figure 11

realiz

result

obtain

We have also mass balance

$$[MonM] = C_{M+} - [M^+]$$
 (13)

$$[Mon^{-}] = C_{Mon^{-}} - [MonM]$$
 (14)

Before the equivalence point, the condition [MonM] C_{Mon} leads to large errors in the calculation of [Mon] by Equation (14). Therefore, in the analysis of the titration described, only data after the equivalence point were used as input to the program MINIQUAD.

A typical titration curve is shown in Figure 12. The agreement between the calculated and observed results is good and shows little systematic error.

The results of the potentiometric titrations corrected for activity effects are given in Table I. It should be noted that the standard deviations reported for the formation constants are substantially greater than those produced by the computer curve-fitting since the program MINIQUAD gave estimates of lower error than could be realized experimentally. Discussion of the potentiometry results will be given later in comparison to the results obtained by other methods.

Figure 12. Potentiometric titration curve for the Mon - Na system in absolute methanol. . , calculated points; •, observed points (218). (Reproduced with the permission of the copyright holder.)

6.0

5.0

4.0

3.0

2.0

1.0

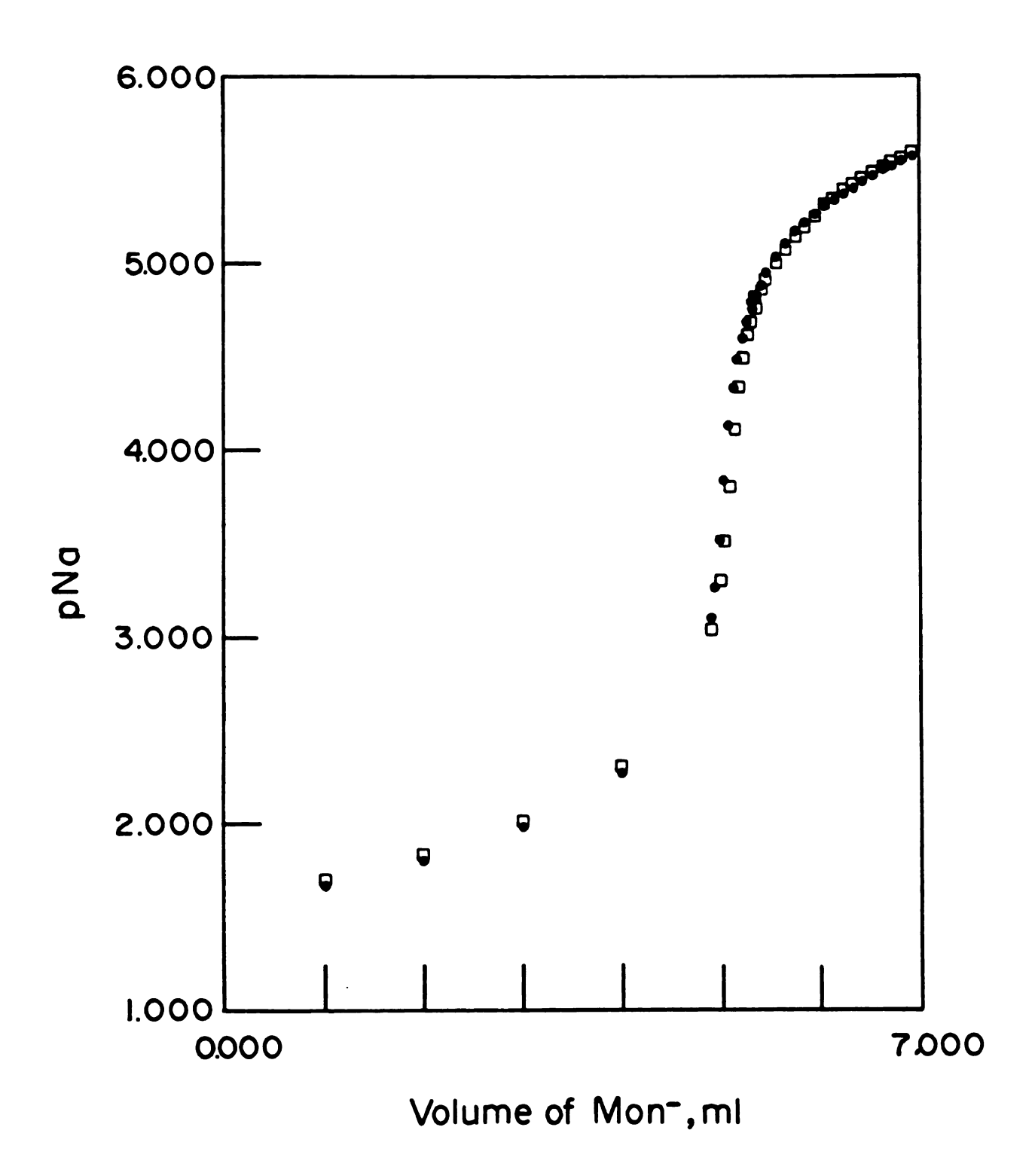


Figure 12

3.4. FLUORESCENCE

Fluorimetry was used in an attempt to verify the formation constants of monensin complex which were determined by cyclic voltammetry and potentiometry. The fluorescence of Tl(I) ion was used to determine the formation constant of the MonTl complex, but no equilibrium constants for the alkali-metal monensin complexes were obtained by the fluorimetric technique.

The method of determining complexation constants is based on the quenching of T1(I) fluorescence in methanol solutions when a ligand is added. Cornelius et al. (179) found that the quenching was effected by several types of ligands including crown ethers and such naturally occurring ionophores as valinomycin, the actins, and nigericin group anions. These workers eliminated the possibility that the quenching could be due only to collisional process, as they observed that the quenching of Tl(I) fluorescence was reversed by the addition of other metal ions which can be complexed by the ligand. Thus they concluded that the complexation of Tl(I) was responsible for its decreased fluorescence. In the case where Tl(I) is titrated with Mon one also observes the quenching phenomenon, as seen in Figure 13. A typical mole ratio plot based on such data is shown in Figure 14 and confirms the 1:1 combining ratio of ligand to metal as determined by cyclic voltammetry. Figure 13. Quenching of the fluorescence of a 1.15 x 10⁻⁴

M T1ClO₄ solution in methanol by Mon⁻. The ligand to metal mole ratios are as follows: curve 1, 0.00; 2, 0.0627; 3, 0.1402; 4, 0.1733; 5, 0.3098; 6, 0.4758; 7, 0.5680; 8, 0.7376; 9, 0.8446; 10, 0.9147; 11, 1.062; 12, 1.346; 13, 1.579; 14, 2.290; 15, baseline.

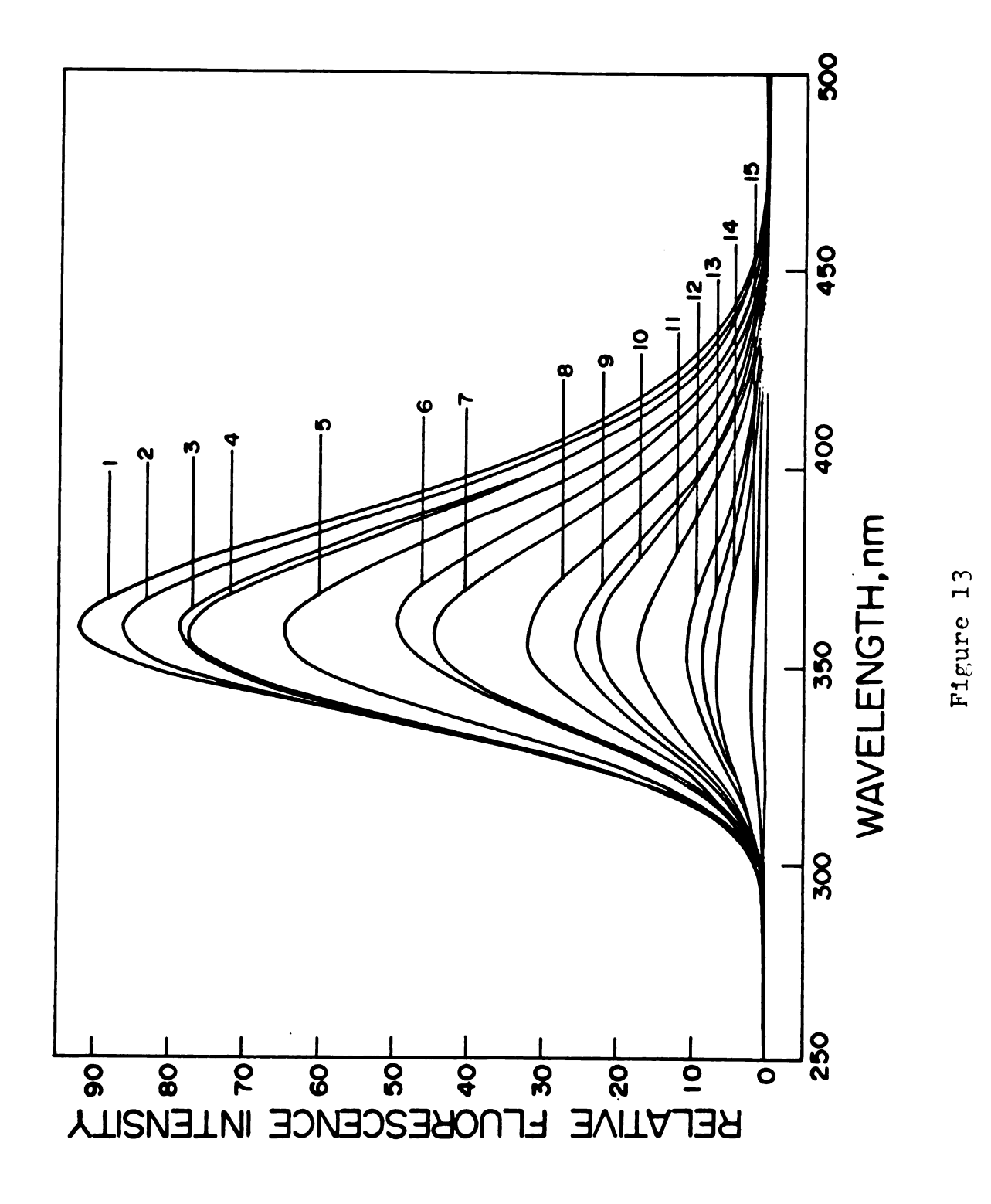


Figure 14. Fluorescence intensity at 360 nm as a function of the ligand to metal mole ratio in the titration of 3.000 ml of 1.15 x 10^{-4} M TlClO $_4$ with 1.268 x 10^{-3} M Mon $^-$ in absolute methanol. The data have been corrected for dilution and background fluorescence and normalized to 100 for the fluorescence of Tl $^+$ in the absence of Mon $^-$.

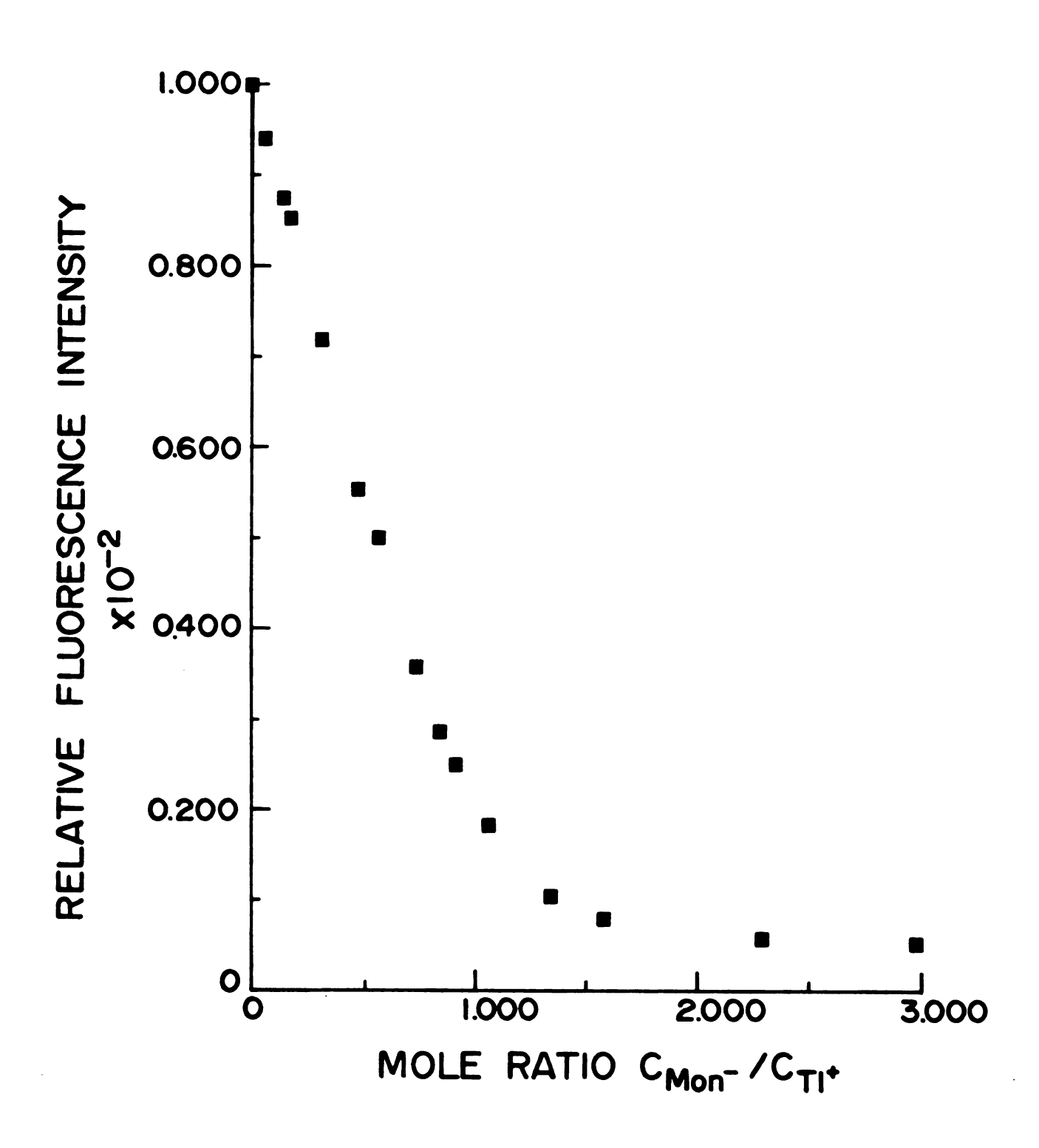


Figure 14

For calculation of formation constants the Tl(I) fluorescence signal is used as a measure of the free metal ion. Then the necessary equations are

$$C_{Mon}^{-} = [Mon] + [MonT1]$$
 (15)

$$C_{T1} + = [T1^{\dagger}] + [MonT1]$$
 (16)

$$[MonT1] = K_{f}^{T1} [T1^{+}] [Mon^{-}]$$
 (17)

Only data in the region of the mole ratio plot around 1:1 are suitable for the calculation of the formation constant. When the metal ion is in great excess of the ligand, the condition [MonTl] $\approx C_{Mon}$ leads to errors in the calculation of [Mon] by Equation (15). When the ligand is in excess of the metal ion, however, a different kind of problem is encountered. It is apparent from Figure 13 that in the course of the titration the fluorescence maximum shifts to lower wavelengths; this shift is especially evident when a large excess of ligand has been added. The shift is due to the growth of a new peak at 343 nm due to the monensin anion, as shown in Figure 15. That this peak may indeed be attributed to the ligand is ascertained by the linear increase in fluorescence at 343 nm with Mon addition illustrated in Figure 16. The growth of this ligand peak causes the fluorescence intensity

Figure 15. Fluorescence spectra of (1) 1.047 x 10^{-4} \underline{M} TlClO $_{4}$ and (2) 3.594 x 10^{-3} \underline{M} Mon solutions in methanol.

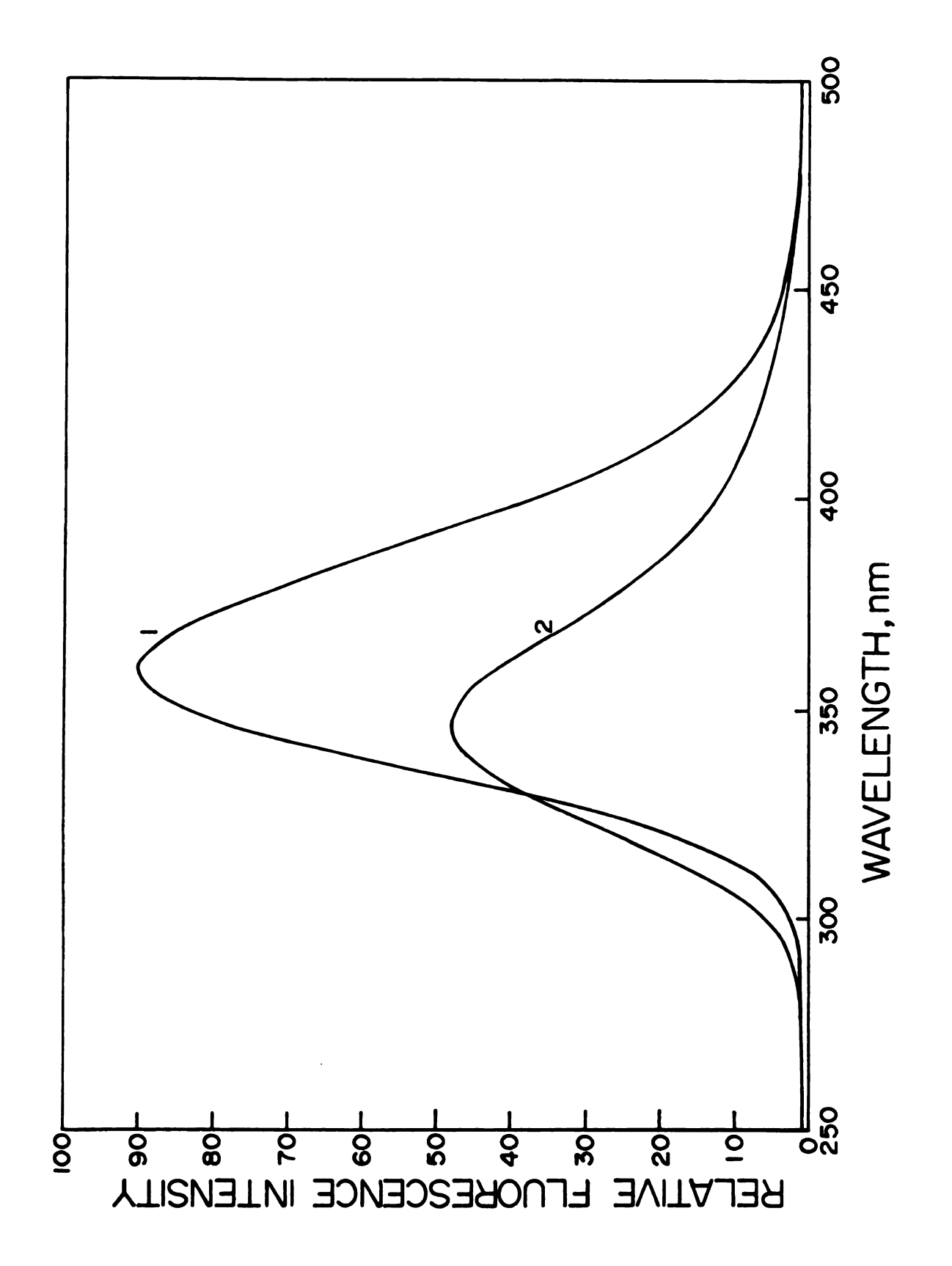


Figure 15

Figure 16. Relative fluorescence intensity at 343 nm as a function of the Mon-concentration. The data have been corrected for dilution and background fluorescence.

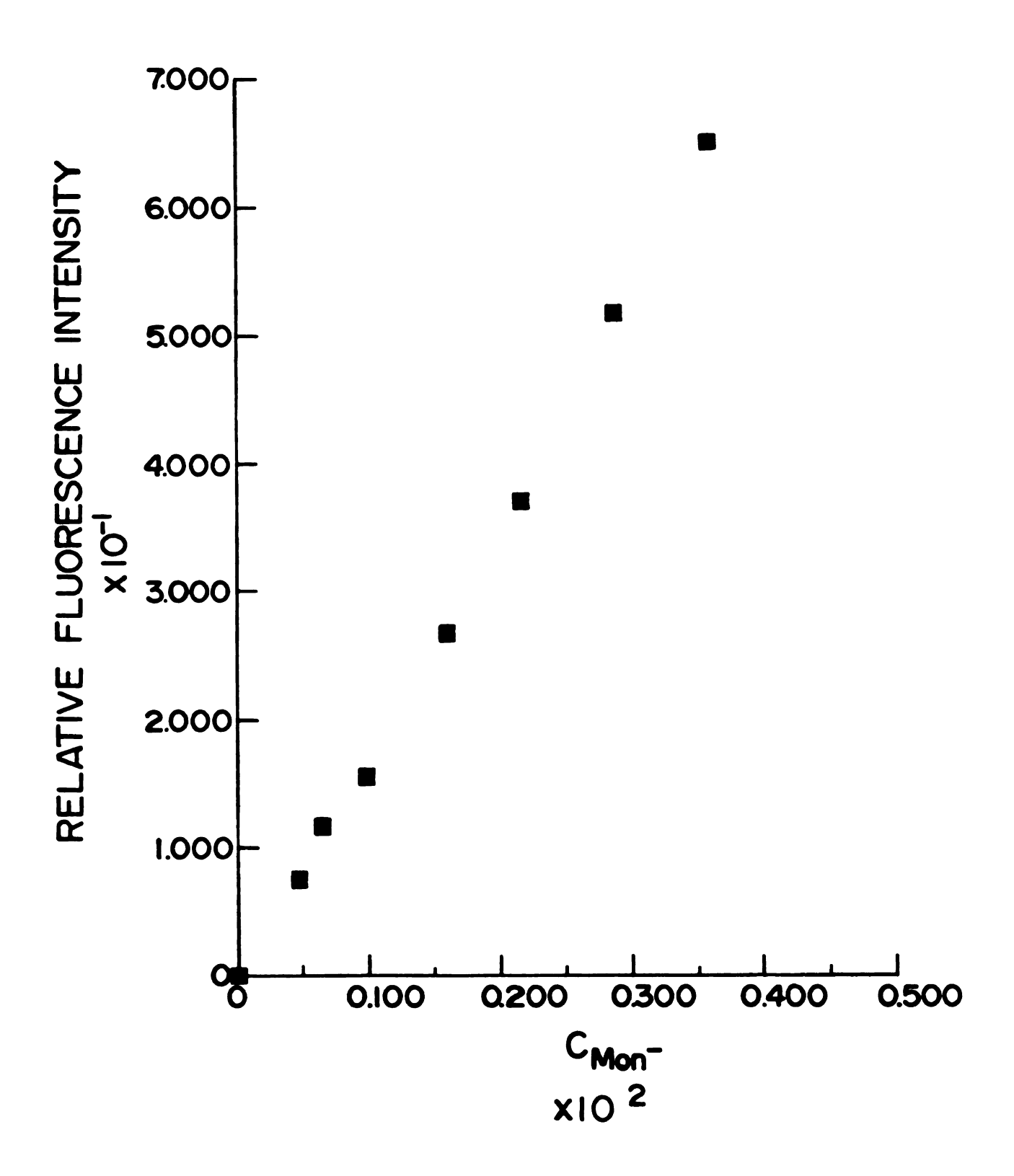


Figure 16

at 360 nm to decrease more slowly than would be expected from the decrease in Tl(I) fluorescence alone, and thus interferes with the determination of [Tl⁺]. Due to the limitations just described, only data between ligand to metal mole ratios of 0.7 to 1.6 were used for calculations of the formation constant. The value obtained for the complexation constant of MonTl is presented in Table I.

The fluorescence data were relatively imprecise and, therefore, the competitive method for determining formation constants of alkali metal ions with monensin was not considered to be useful.

3.5. METAL ION NMR

Although metal ion nmr, particularly that of the alkali metals, has enjoyed considerable success in the characterization of tetrazole (194), glutarimide (195), crown and cryptand (196) complexation, the technique has not proved nearly so useful in the studies of complexes of metal ions with the monensin anion. For example, when Mon was added to a 0.1 M solution of LiClO $_{\rm H}$ in methanol, the chemical shift change from a ligand to metal mole ratio of zero to unity was only 0.1 ppm. This chemical shift change is experimentally significant and confirms the cyclic voltammetric results that there is some MonLi

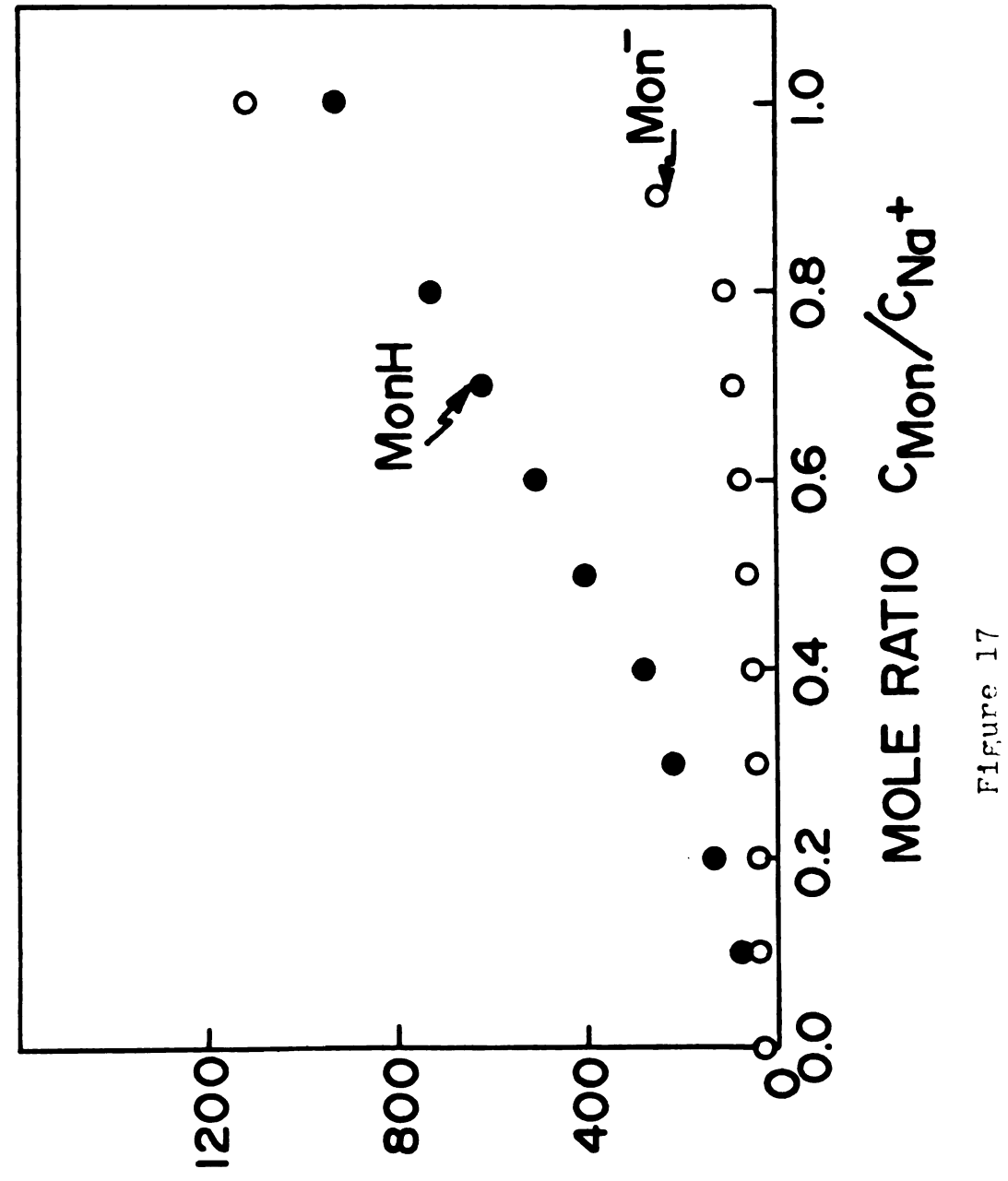
complex formation; however, the small chemical shift change limits the accuracy with which a formation constant could be determined by the nmr method. The small shift indicates either that the MonLi complex is not very strong or else that the free and complexed lithium ions have nearly the same chemical shift. The addition of the ligand to Li⁺ ion solution did not result in any significant broadening of the ⁷Li resonance.

Very different results were obtained in the study of sodium complexes by ²³Na nmr. As shown in Figure 17, the addition of the monensin anion to solutions of sodium ion in methanol produces line-broadening in the observed resonance. The increased linewidth must be due to a fast quadrupolar relaxation at the nucleus, resulting from complexation by an unsymmetrical ligand. The extreme broadness of the lines severely limits the accuracy with which resonance frequency can be measured and, thereby, precludes the use of ²³Na nmr measurements for calculation of formation constant for the MonNa complex.

Similar line-broadening was observed in the ²⁰⁵Tl nmr experiments involving addition of Mon⁻ to Tl(I) solutions. The broadening could not be due to efficient quadrupolar relaxation in this nucleus of spin 1/2. Yet at a ligand to metal mole ratio of only 0.24 the observed linewidth had increased to 1850 Hz compared to only 40 Hz for the free metal ion. Obviously no mole ratio studies

Figure 17. Changes in the linewidth of the $^{23}\mathrm{Na}$ resonance with the addition of monensin.





could be carried out to calculate the MonTl complexation constant.

Addition of Mon- to Cs⁺ ion solutions in methanol resulted in a 77 ppm paramagnetic chemical shift change and minimal line-broadening over a ligand to metal mole ratio of zero to unity.

3.6. FORMATION CONSTANTS

Formation constants for MonM complexes which have been determined in this work are given in Table I. All formation constants are corrected for activity effects. The agreement among the results obtained by potentiometry, cyclic voltammetry, and fluorescence is good. The results are compared to those of other workers in Table I; formation constants obtained in this work are slightly higher than those of Simon et al. (166,176,177). The present results do not agree well with those obtained by Cornelius et al. (179) by using Tl(I) fluorescence, especially in the cases of strong complexes. Hughes and Man (197) stated that Tl(I) fluorescence was not suitable for characterizing the interaction of that metal ion with ligands because the fluorescence method led to much higher values of formation constants than those measured electrochemically. The results of Cornelius et al., however, are rather too low in comparison to the cyclic voltammetric

values and the current fluorescence results. It should be further noted that the early results obtained by fluorescence (179) do not reflect the marked selectivity of Mon⁻ in its complexation of metal ions.

Several workers have qualitatively described the selectivity of the Mon⁻ ionophore. The results are shown in Table III. All authors are in general agreement, except with regard to the strength of the MonLi complex. Our studies indicate only a small degree of complexation of Li⁺ by Mon⁻. These results are in agreement with those of Pinkerton and Steinrauf (167).

Stabilities of the monensin - alkali metal complexes are strongly dependent on the size of the cation. Figure 18 shows a quantitative representation of the Mon selectivity. At least among the alkali ions, the relationship between the ionic dimensions and the cavity size of the ligand seems more important than other factors as the solvation energy or the polarizability of the cation. This relationship is consistent with the molecular structure of the MonM complexes, as the monensin complex is rigid and relatively inflexible (168). As seen in Figure 18, the stabilities of the Ag and Tl complexes are less influenced by the ionic radii than those of the alkali metal complexes, probably due to an increased covalency in the ion-ligand bonds.

The stability of the sodium complex is quite

Table III. Selectivity Order for MonM Complexes.

Order	Method	Ref.
Na + > K + > Tl + > Rb + > Cs + > L1 +	Electrochemical	Present Work
$Na^+ > K^+ > Rb^+ > Cs^+$	Two-phase Systems	165
$Na^+ > K^+ \sim L1^+ > Rb^+ > Cs^+$	Membranes and Liquid Crystals	217
Na	Model Transport Systems	917
$Na^+ > K^+ > Li^+ > Rb^+ > Cs^+$	Monensin as Carrier in Liquid Membrane Electrode	166
Na > K > T1 > Rb > Cs +	Tl(I) Fluorescence	179

Figure 18. Selectivity of the Mon⁻ complexation reaction for the alkali, Tl⁺, and Ag⁺ ions (218). (Reproduced with the permission of the copyright holders.)

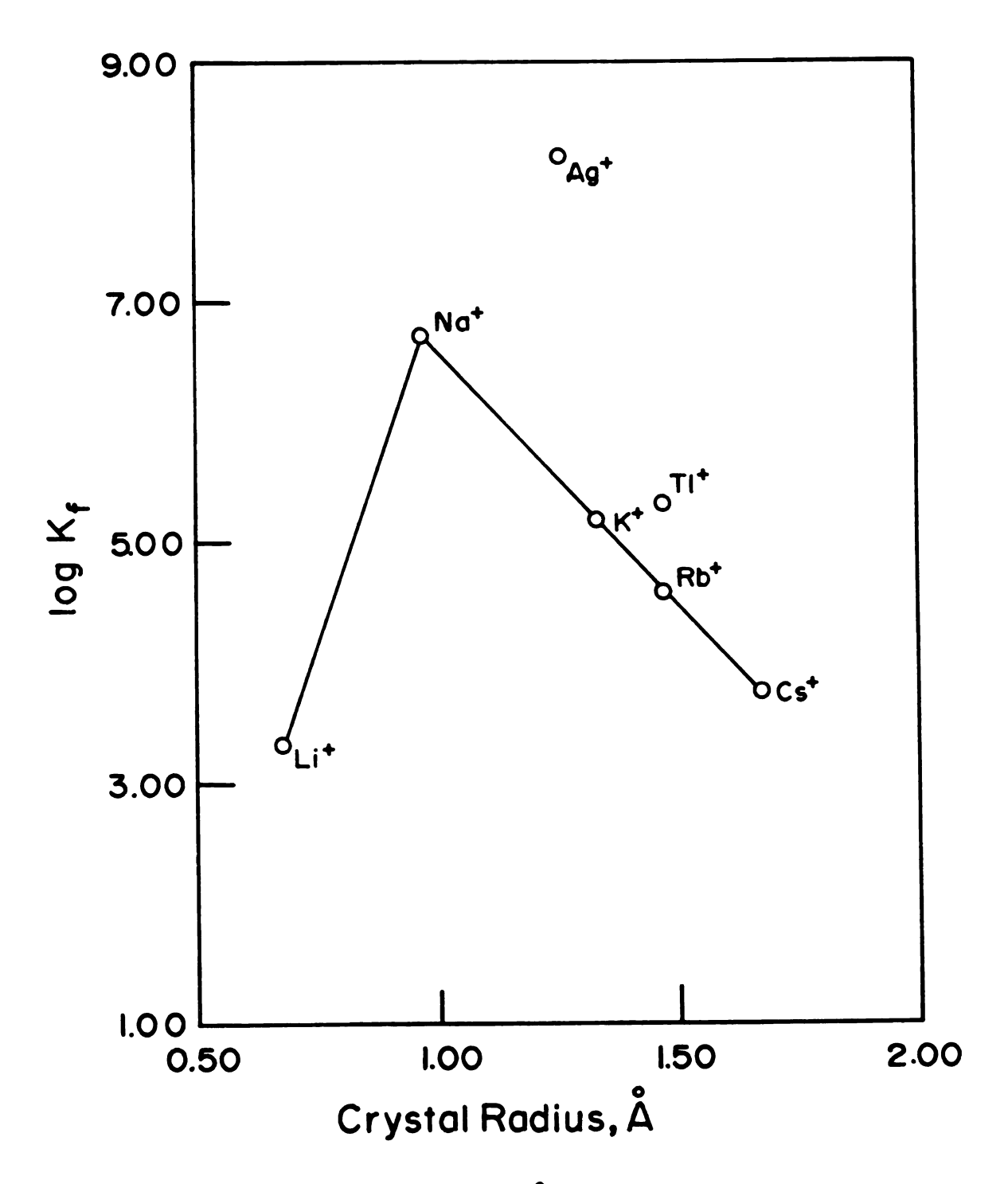


Figure 18

respectable, but it is considerably below the stabilities of Na⁺ complexes with diazapolyoxamacrobicyclic ligands (cryptands, Figure 19) in which a cation is located in the interior of a three-dimensional cavity formed by three polyether strands connected to two nitrogen bridgeheads (198). Thus for Na⁺ in 95% methanol log K_f for the C221·Na⁺ complex is 8.84 and for the C222·Na⁺ complex is 7.21 (199). The lower stability of the MonNa complex is not surprising since, in contrast to the cryptand, Mon⁻ ion does not have a pre-formed molecular cavity.

3.7. CONCLUSIONS

Formation constants for complexes of monovalent metal ions with the monensin anion Mon were determined by cyclic voltammetry, potentiometry, and fluorimetry. The values for the complexation constants emphasized the selectivity of monensin for Na over the other alkali metal ions and for Ag over all the other monovalent metal ions. For the alkali metal ions the size of the cation seems to determine the strength of the complex.

Figure 19. Structures of representative cryptands.

CHAPTER 4

COMPLEXES WITH THE ACID FORM OF MONENSIN, MONH

4.1. INTRODUCTION

The monensin complexes discussed thus far have been those which involved the anionic form of the ligand, Mon, but it was also of interest to study reactions of monensin which involved the acid form, MonH. The most obvious reaction involving protons is the acid dissociation of monensin. Prior to the work of Gertenbach and Popov (174) this reaction had only been studied in mixed solvents such as 66% dimethylformamide (1) and 90% ethanol (175). Gertenbach and Popov estimated the pKa of monensin in anhydrous methanol but did not determine the thermodynamic value of this equilibrium constant.

In similar solution studies, they proposed that complexes of alkali metal and alkaline earth ions can be formed by reaction of the metal ion with the protonated form of monensin according to the equilibrium

$$MonH + M^{+} + MonM + H^{+}$$
 (18)

It was the purpose of the present work to investigate more thoroughly the above reaction and to characterize it in terms of the possible paths of the reaction, the structures of the products, and the stabilities of the complexes.

4.2. DETERMINATION OF THE pK OF MONENSIN

The determination of the acid dissociation constant of monensin was carried out by acid-base titration in anhydrous methanol. While the techniques for the determination of acidity constants have been used extensively, especially in aqueous systems, they could not be applied directly in the case of monensin. A major problem was in the proper choice of titrant. The acid dissociation reaction is

$$MonH \neq Mon^- + H^+$$
 (19)

and it is evident that if the acid were titrated with a base containing a complexable metal ion, the equilibrium in Equation (19) would necessarily be shifted to the right, and therefore monensin would appear to be a stronger acid than is really the case. The titrant must, in consequence, contain only cations which are not complexable; the alkylammonium cations are suitable for this purpose.

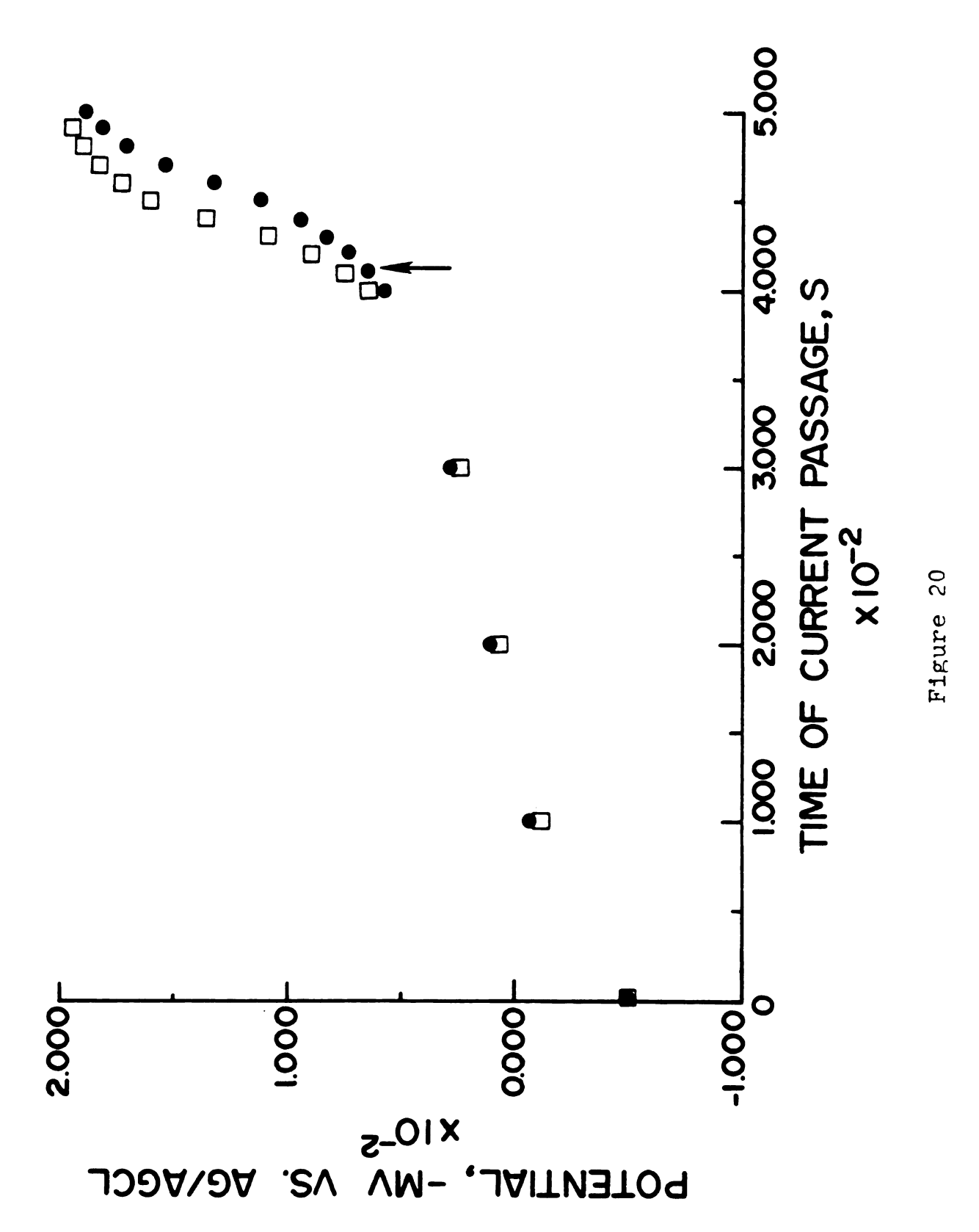
Alkylammonium hydroxide titrants have been used previously for titrations in nonaqueous solvents. Early use was made of tetra-n-butylammonium hydroxide (200-203) although several other alkylammonium cations have been employed (204). As there was some question regarding the long-term stability of tetra-n-butylammonium hydroxide (TBAH) in methanol solution (205), several methods were considered for the preparation of the reagent.

Preparation of TBAH by ion-exchange was not very satisfactory. Passage of tetra-n-butylammonium iodide through an anion-exchange column in the hydroxide form resulted in solution contaminated with iodide ions. Similarly, passage of sodium hydroxide through a cation exchange column in the tetra-n-butylammonium form gave a product which contained appreciable amounts of sodium ion. As neither of these contaminants could be tolerated in acidbase titrations, the ion-exchange preparations were not pursued further.

In situ coulometric generation of the base also presented problems. This manner of base preparation was recommended by Fritz and Gainer (206) for studies in butanol and acetone and evaluated by Cooksey et al. (207) for work in isopropanol solutions. In the present study the major difficulty was that, in acid-base titrations which employed coulometric base generation, the calculated and observed endpoints did not agree; the observed endpoint time was always longer than expected. The magnitude of the endpoint error depended somewhat on the supporting electrolyte which was used in the counter-electrode compartment. As shown in Figure 20, the use of perchlorate medium in the electrode compartment gave an endpoint error on the order of 10 percent, while the bromide medium gave a corresponding error of only four percent. These results can be interpreted in terms of the electrode reactions.

Figure 20. Endpoint errors in the coulometric titration of benzoic acid in anhydrous methanol solutions.

□, titration data from bromide medium; •, titration data from perchlorate medium. The arrow indicates the calculated endpoint.



In the presence of traces of water the predominant counterelectrode reaction in the perchlorate medium is

$$2H_2O \stackrel{?}{\leftarrow} 4H^+ + 4e^- + O_2$$
 (20)

while in the bromide medium it is

$$2Br^{-} \stackrel{?}{=} 2e^{-} + Br_{2}$$
 (21)

Thus in perchlorate medium as the base is generated in the reaction vessel, acid is produced in the counterelectrode compartment. During current flow, the mobile H+ ions tend to move from the counter-electrode compartment into the sample cell and cause the extended endpoint error. As no acid is generated in the bromide medium, the endpoint problem is not as severe; the residual error is believed to be due to reducible impurities in the solvent. Fritz and Gainer (206) also reported solvent blanks of a few percent which they removed by pre-electrolysis of the solvent before the analyses, however, since their measurements were determinations of total acid quantity, only the endpoint location was critical. In the present work the potentials at each titration point were important and therefore pre-electrolysis was not considered appropriate as it would introduce unknown quantities of base into the solution.

Since the base could not be prepared in sufficient purity, recourse was made to a commercially available titrant. In order to alleviate fears of possible decomposition, the base was used to titrate standard benzoic acid in methanol and the results were compared to literature values. The experimentally determined value at 25°C was $pK_a = 9.35 \pm 0.05$ for K_a in units of moles·1⁻¹. This value is in excellent agreement with the literature value of $pK_a = 9.38$, which is the mean of several concurring determinations (208-212).

The volumetric titration technique was further applied to the titration of monensin in methanol solution. The necessary equations are analogous to those of the titration of Na⁺ by Mon⁻, except that the acid-base electrode calibrations were fit to the equation

$$E = E^{\circ} + \frac{RT}{nF} \ln (a_{H} + R)$$
 (22)

where the Nernst slope was not fit as an adjustable parameter, but rather calculated from theory. After calibration the equations are

$$[H^{+}] = 10^{\left(\frac{(E - E^{\circ}) nF}{RT}\right)}$$
 (23)

$$C_{H^+} = [H^+] + [MonH]$$
 (24)

/

$$C_{Mon}^{-} = [Mon^{-}] + [MonH]$$
 (25)

Only data in the buffer region were used as input to the program MINIQUAD.

Titration of monensin yielded a value of $pK_a = 10.30$ \pm 0.05. This value is in fair agreement with the value of $pK_a = 10.15$ obtained by Gertenbach and Popov (174); the latter work, however, did not incorporate activity corrections.

4.3. EVIDENCE FOR THE EXISTENCE OF MonHM+ COMPLEXES

In their original suggestion that monensin in its free acid form could complex metal ions, Gertenbach and Popov (174) discussed the results of several experiments. They found that MonH solubilizes sodium perchlorate in chloroform up to a 1:1 ligand to metal mole ratio. At a mole ratio of unity the ¹H nmr spectrum of the solution was characteristic neither of the free acid nor of the deprotonated sodium complex, MonNa. At the same mole ratio they observed that the infrared spectrum showed a carbonyl vibration at 1704 cm⁻¹ characteristic of the -COOH group; the MonNa complex shows a carbonyl band at 1560 cm⁻¹, which is characteristic of the deprotonated carboxyl group. In the present work, the ¹³C nmr spectrum of the solution containing equimolar MonH and sodium perchlorate has a peak at 178.8 ppm which is characteristic of the -COOH

group. By comparison, the protonated carboxyl group of MonH gives a resonance at 177.8 ppm, while the deprotonated carboxyl group of MonNa gives a peak at 188.2 ppm. These data give further evidence that in chloroform solution the sodium ion forms a complex with the neutral monensin molecule, in which the ligand retains the carboxyl proton.

A potentiometric study by Gertenbach and Popov also served to emphasize that the acid remains protonated during complex formation. Addition of sodium perchlorate to monensin in methanol resulted in a release of protons into the solution, yet the infrared spectra indicated that the 1704 cm⁻¹ band did not disappear. The proposed reaction was

$$MonH + Na^{+} \stackrel{?}{\nearrow} MonNa + H^{+}$$
 (26)

and an overall equilibrium constant of about unity was calculated.

The experimental value of unity for the overall equilibrium constant of reaction (26) is surprising. For that reaction, $K_{eq} = K_a \times K_f$ and using the best values obtained to date, $pK_{eq} = 3.58$. Because of this discrepancy, work was done to ascertain the validity and/or completeness of reaction (26).

Conductance studies were initiated to determine the extent of reaction (26). If the reaction proceeds

significantly to the right, the high mobility of the released protons should lead to high conductance as the sodium ion is added to the monensin solution. A typical conductimetric titration is given in Figure 21. It shows that the addition of the sodium ion to a solution of MonH resulted in lower conductance than did the addition of the salt to methanol alone. These results argue strongly against the release of appreciable amounts of proton; on the contrary, they indicate that a charged species is formed which has a lower mobility than the sodium ion.

Corroborating evidence on the relatively small release of protons was found from potentiometric pH measurements. It was found that when the sodium ion was added to a solution of monensin in methanol, the ratio of free proton to total sodium was on the order of 10^{-2} , which indicates that reaction (26) does not proceed significantly to the right.

In light of the previous experimental results, several reaction paths are possible.

Path 2
$$K_{f}^{\dagger}$$
 $\uparrow \downarrow$ $MonHNa^{\dagger}$ $\downarrow MonNa + H^{\dagger}$ $\downarrow MonNa + H^{\dagger}$ $\downarrow MonNa + H^{\dagger}$ $\downarrow MonNa + H^{\dagger}$

Either of the paths could explain the potentiometric results. In path 1, monensin dissociates to some extent,

Figure 21. Conductimetric titrations of methanol solutions with 5.684 x 10^{-3} M NaClO $_{4}$ solution. • represents NaClO $_{4}$ addition to 50.00 ml of methanol, x represents NaClO $_{4}$ addition to 50.00 ml of 2.360 x 10^{-3} M MonH solution in methanol.

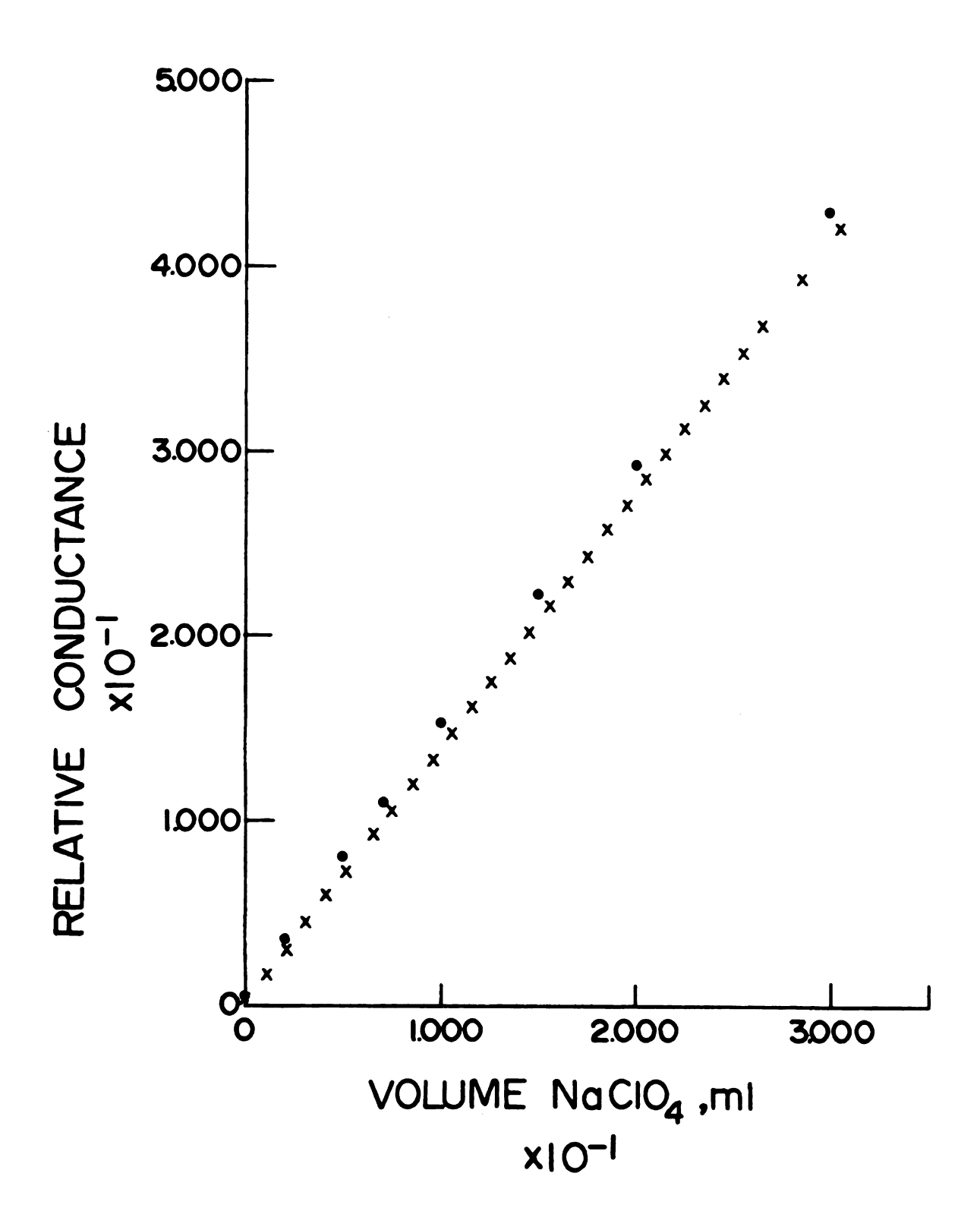


Figure 21

but the degree of dissociation is enhanced by complexation of sodium ion by the monensin anion with a net increase in solution acidity. By path 2 the solution also becomes more acidic with sodium ion addition, provided that $K_a^* > K_a$ and that K_f^* is non-zero.

Neither of these mechanisms contradicts the ir spectra which indicate that monensin remains protonated; the sensitivity of infrared measurements is low and, since only a small fraction of monensin is in the form of MonNa, the decrease in intensity of the 1704 cm⁻¹ band would not be appreciable. The conductance results, however, indicate path 2, with the formation of the large charged complex, MonHNa⁺, which would be likely to have a lower mobility than the sodium ion.

Other evidence for the existence of a metal-ion complex other than MonM came from acid-base titrations. In the titration of monensin by sodium hydroxide in methanol, if the K_a of the acid is known the K_f for the formation of MonNa can be calculated. Such calculations give log K_f^{*4} , which does not agree with the value of log K_f = 6.72 determined by ion-selective electrode measurements. Thus, the presence of another complex is indicated.

Spectroscopic studies also proved to be valuable in demonstrating the presence of a second complex besides

MonM. By measuring Tl(I) fluorescence with addition of the monensin free acid one obtains a mole ratio plot shown

in Figure 22. The fluorescence intensity does not decrease to baseline with monensin addition as it does in basic solution (cf. Section 3.4). Furthermore, there is a definite break in the curve at unity mole ratio; such a break would be expected in the case of reaction (27) path 2, but not of path 1.

Metal ion nmr studies were also diagnostic. As shown in Figure 17, the addition of MonH to the sodium salt solutions resulted in drastic line-broadening of the ²³Na resonance, while the addition of the monensin anion produced much narrower lines, especially at low ligand to metal mole ratios. If in the addition of MonH the only complexation reaction were by path 1, one would expect only minimal line-broadening due to the formation of MonNa; as marked line-broadening is observed, a different sodium complex must be formed.

Similar mole ratio studies based on ¹³³Cs and ²⁰⁵Tl nmr measurements are shown in Figures 23 and 24 and indicate that in these cases upon addition of MonH the metal ion also undergoes a change in environment. What is particularly important is that the ²⁰⁵Tl signal did not broaden and disappear as it did in basic solution. The fact that the results which are obtained in neutral solution differ from those obtained in basic solution argues again for the formation of metal ion complexes other than those with the deprotonated ligand.

Figure 22. Fluorescence intensity at 360 nm as a function of the ligand to metal mole ratio in the titration of 3.000 ml of 1.120 x 10^{-4} M TlClO $_4$ with 1.991 x 10^{-3} M MonH in absolute methanol. The data have been corrected for dilution and background fluorescence and normalized to 100 for the fluorescence of Tl $^+$ in the absence of MonH.

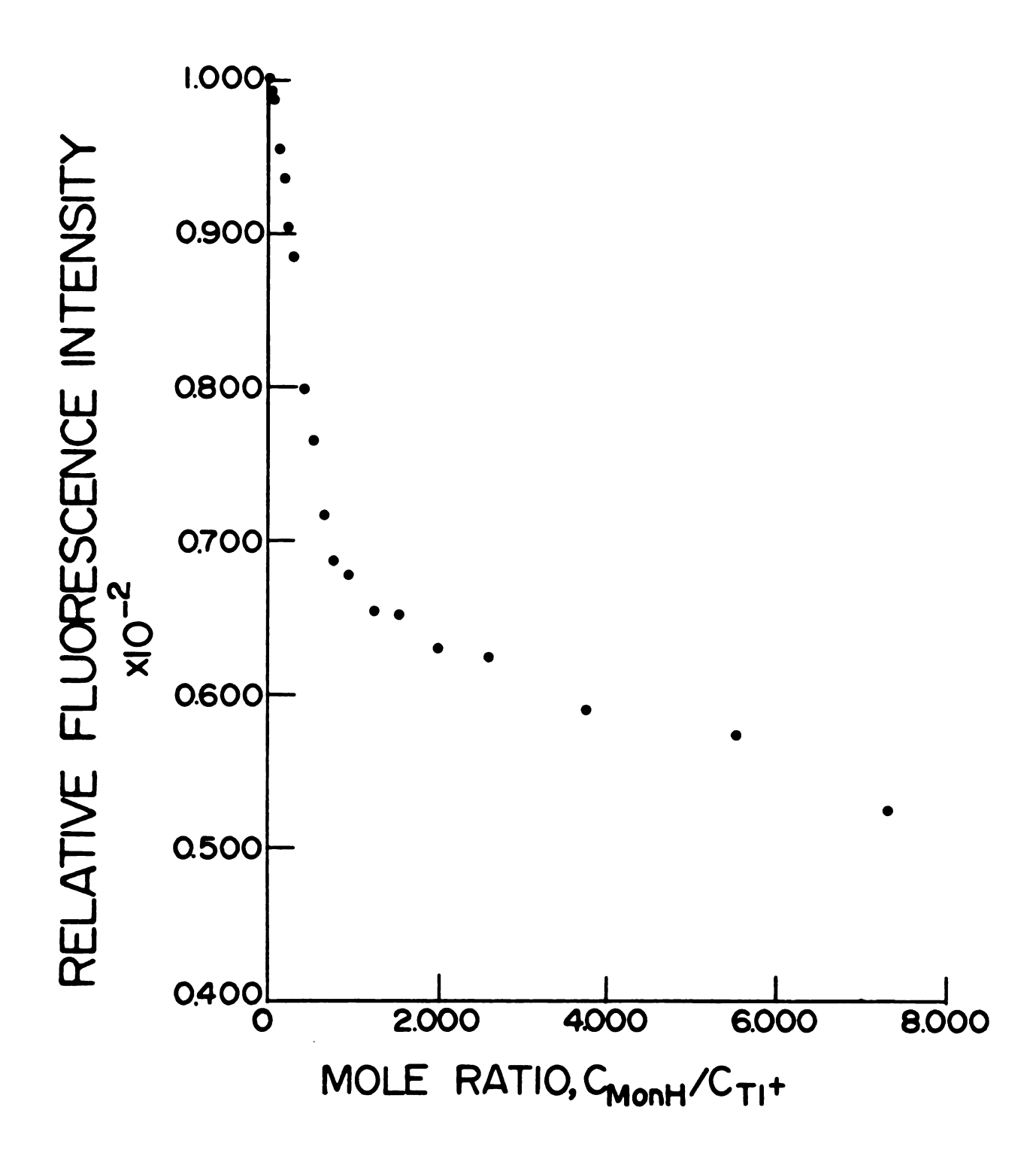


Figure 22

Figure 23. Chemical shift of 0.100 \underline{M} CsSCN in anhydrous methanol as a function of the MonH - metal mole ratio.

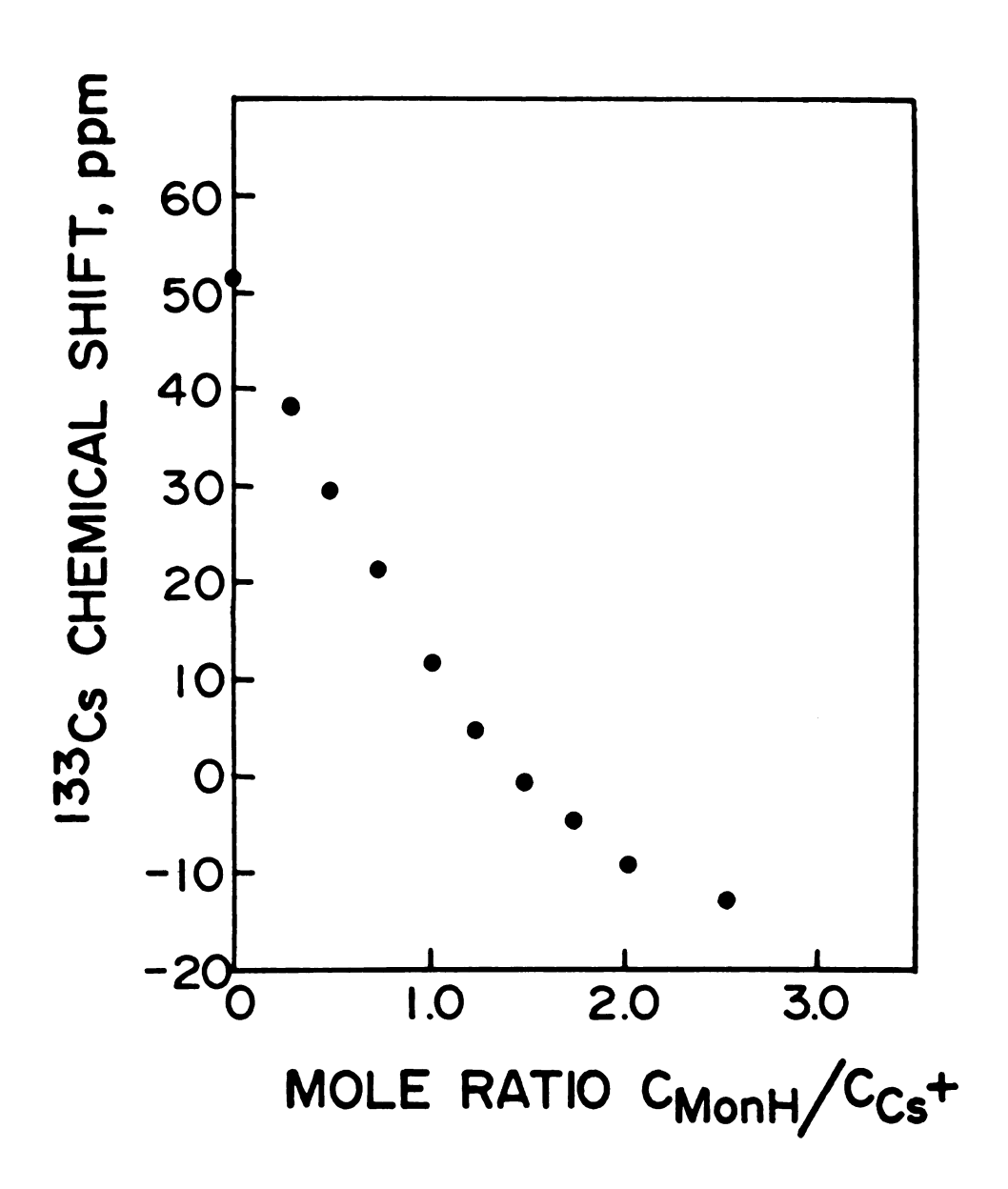


Figure 23

Figure 24. Chemical shift of 1.13 x 10^{-2} $\underline{\text{M}}$ TlClO $_{4}$ in anhydrous methanol as a function of the MonH-metal mole ratio.

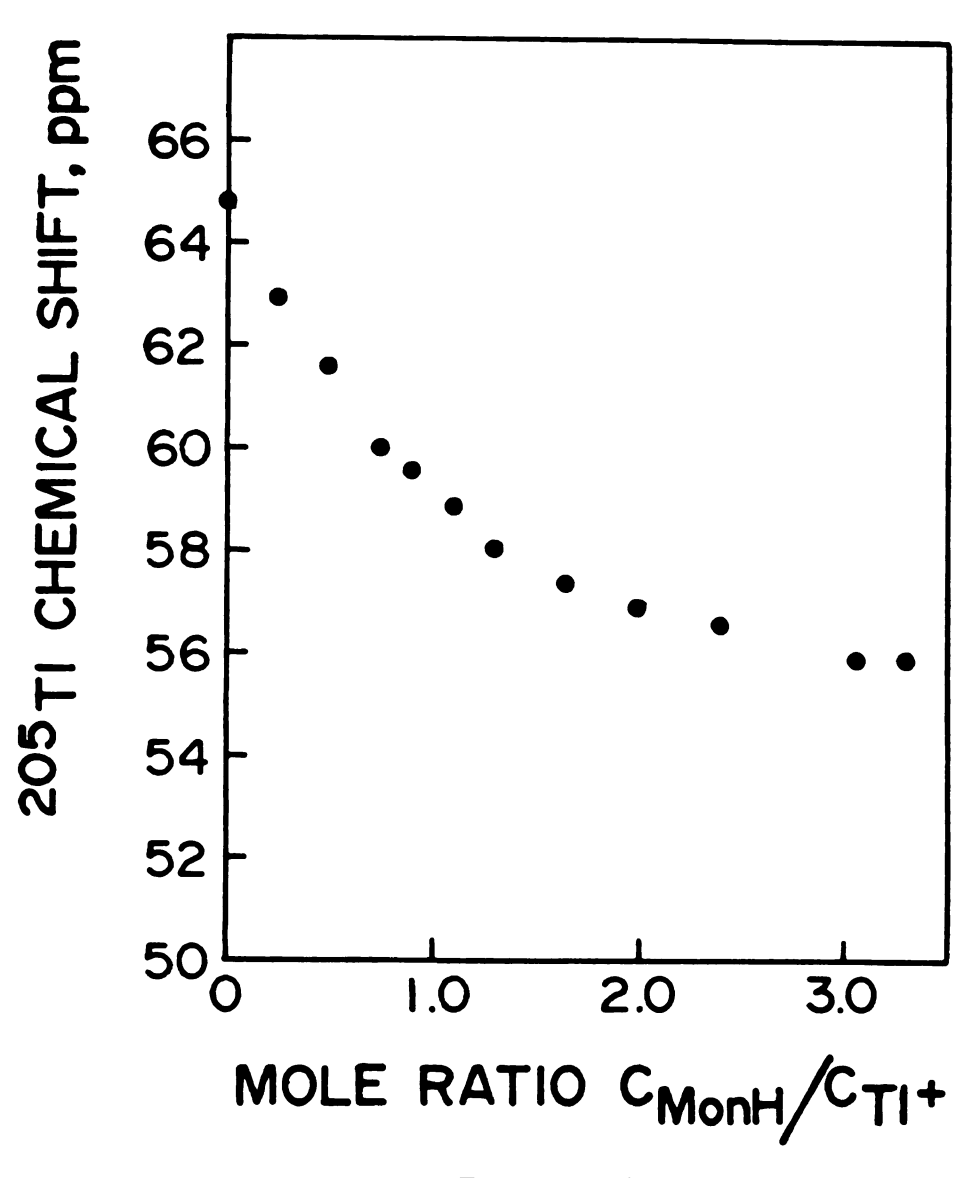


Figure 24

4.4. CHARACTERIZATION OF THE COMPLEX INVOLVING MonH and M+

In attempts to characterize the new type of complex formed with the free acid form of monensin and a metal ion, solid complexes were prepared and isolated. The structures were studied by a variety of physicochemical methods both in the solid state and in solution.

Complexes of the alkali metal salts were prepared by mixing equimolar quantities of metal salt in methanol and monensin free acid in chloroform. The mixed solvent was rapidly removed under vacuum by using a rotary evaporator, since slow evaporation of the solvent often led to monensin decomposition. The resultant product was either recrystallized from a 1:1 mixture of ethyl ether and petroleum ether (30-60°C) or precipitated from ether by the addition of petroleum ether. This procedure was successful only for complexes involving sodium and potassium salts, as the reaction gave a mixture of products with salts of lithium, rubidium and cesium. In the case of sodium fluoride a mixture of monensin free acid and monensin sodium salt was obtained; this result was taken to indicate that HF is a weaker acid than monensin in this solvent system.

The liquefaction points of the solid complexes (Table IV) indicate that the new complexes are neither monensin free acid nor the sodium salt. Since the new complexes

Table IV. Melting Points for Several Monensin Complexes.

Complex	Melting Point, °C
MonH	114-117
MonHNaCl	188-190*
${ t MonHNaClO}_4$	183-184*
MonHNaBr	188-190*
MonHNaI	199-201*
MonNa	267 - 269

^{*}Liquefaction point.

decomposed before melting, the values given in Table IV cannot be considered true melting points.

Infrared analysis of the complexes provided some useful information. All of the new sodium complexes showed absorption bands around 1704 cm⁻¹, indicating that the ligand is present in the acid form. A comparison of the carbonyl regions of the infrared spectra of the three monensin species is given in Figure 25. It is apparent that the new complex, which contains both sodium and bromide ions, also contains the protonated ligand. Furthermore, the spectrum does not show an absorption band around 1640 cm⁻¹ which is present in the spectrum of the monohydrated acid and, to a lesser extent, in the dihydrated MonNa and which is believed to be due to water of crystallization. absence of water in the MonHNaBr complex is also indicated in Figure 26, where, in contrast to both MonH and MonNa, it is apparent that this new complex exhibits no bands above 3400 cm^{-1} . A comparison of the hydrogen-bonding region in the infrared spectra of several complexes is shown in Figure 27. It is striking that all of the complexes contain a common band around 3375 cm⁻¹; this band may reflect a similar hydrogen-bonding pattern for closing the monensin ring in all of these complexes. Other peaks in this O-H stretching region reflect the differences in hydrogen-bonding to the various anions involved in the solid complexes.

Figure 25. Infrared spectra of Nujol mulls of several monensin species.

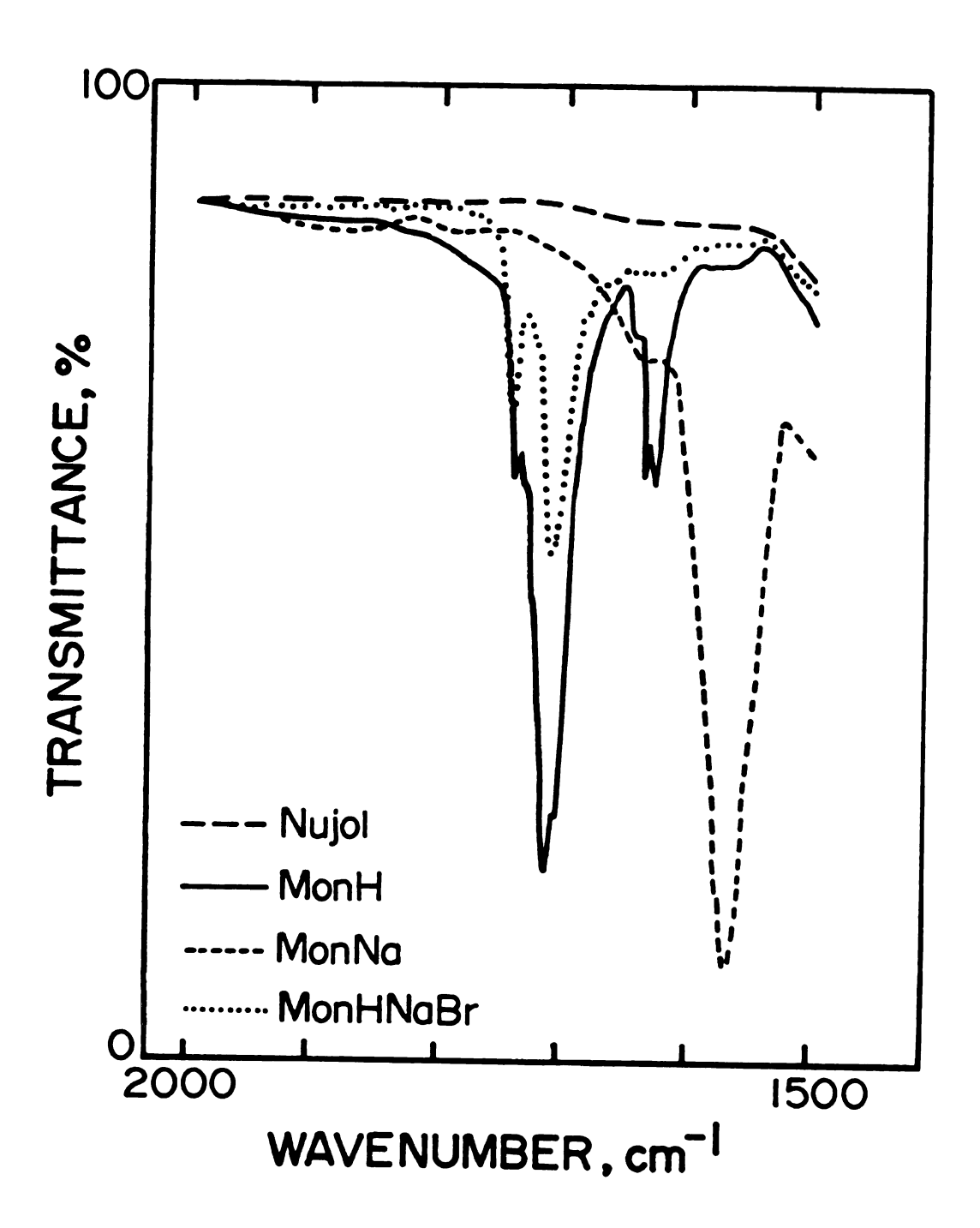


Figure 25

Figure 26. Comparison of the O-H stretching regions in the infrared spectra of Nujol mulls of three monensin species. — -, Nujol; — -, MonH; ---, MonHNaBr; ..., MonNa.

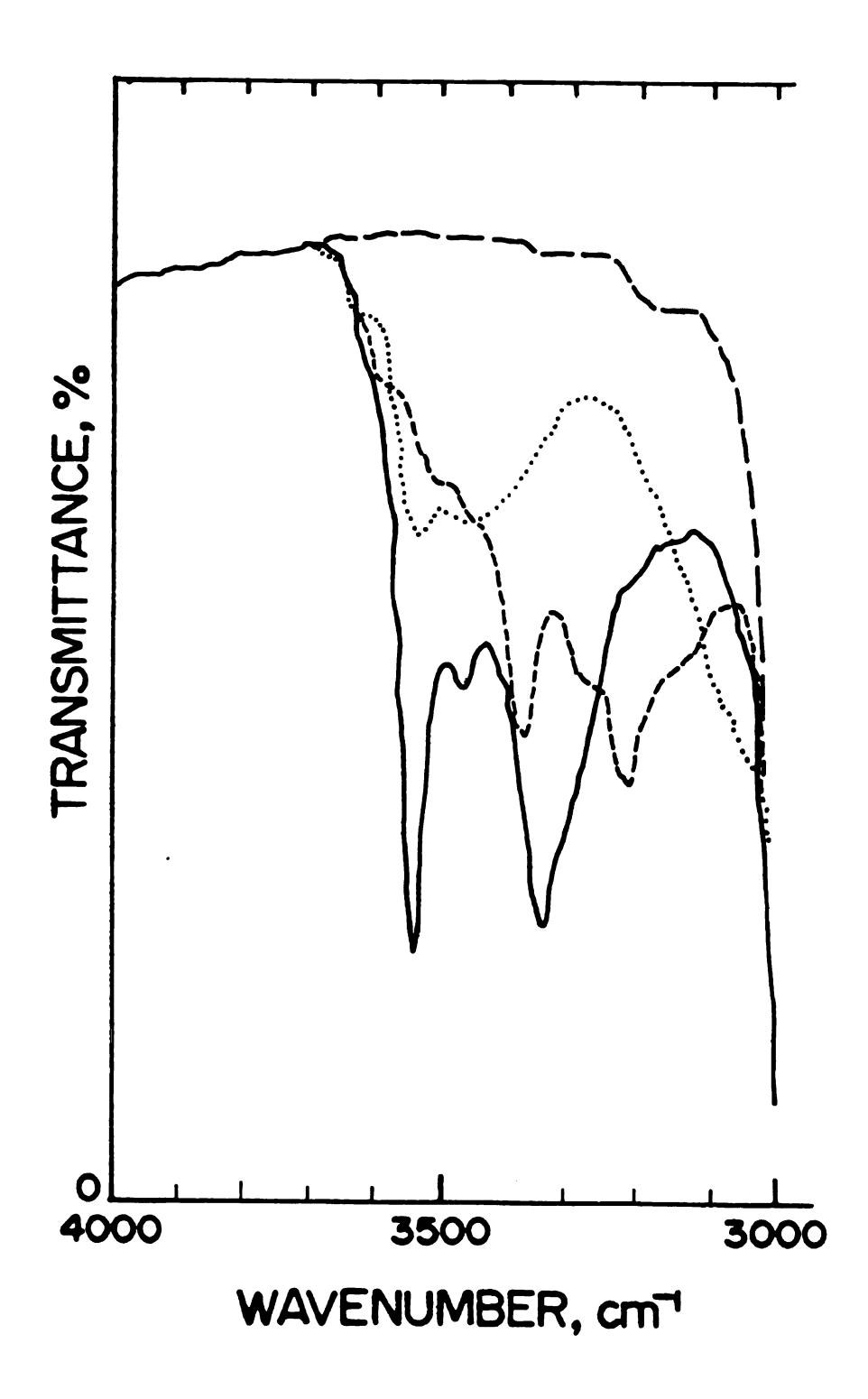


Figure 26

Figure 27. Comparison of the O-H stretching regions in the infrared spectra of Nujol mulls of MonHNaX complexes. --, X=Br; ---, X = Cl; ----, X = I; \cdots , X = ClO $_4$.

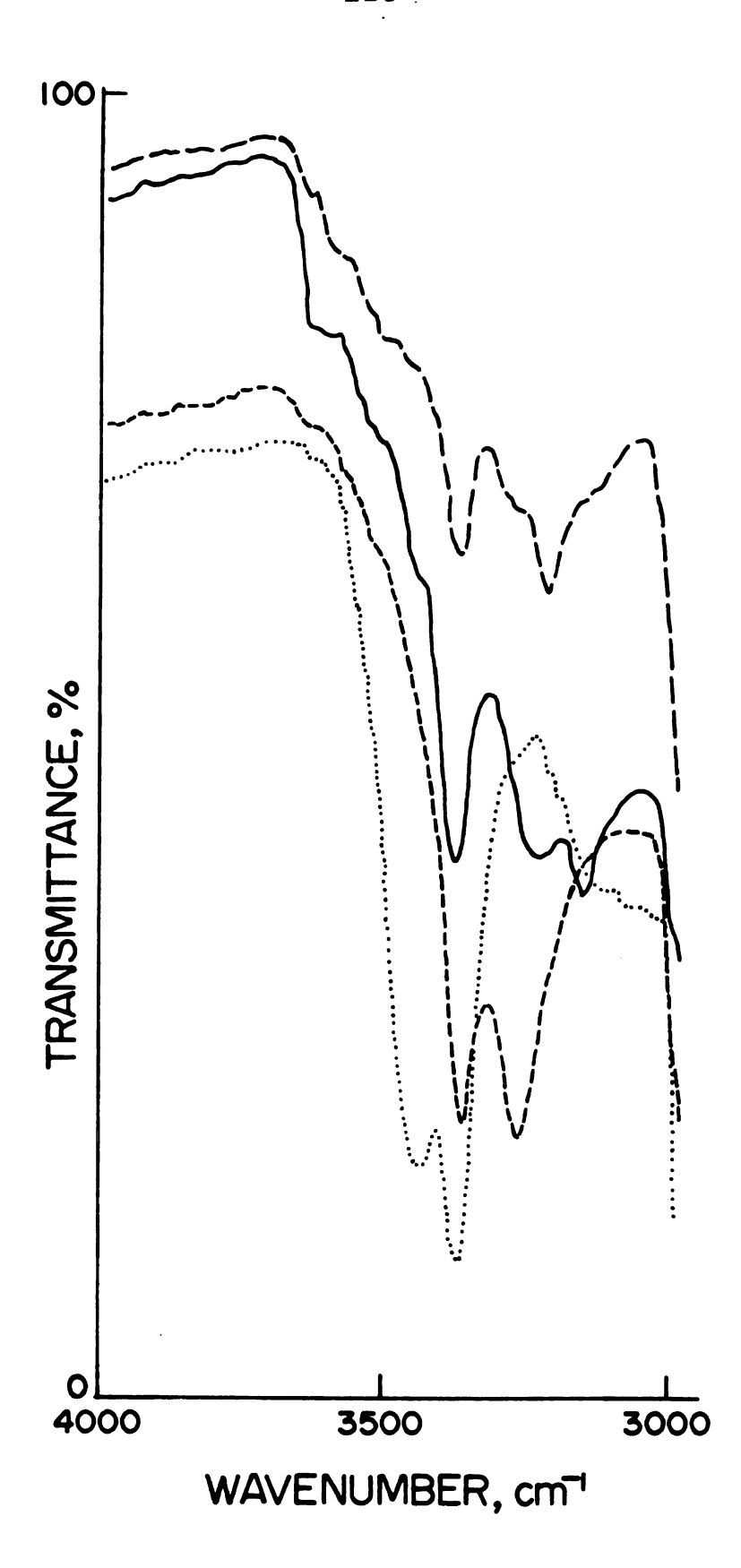


Figure 27

X-ray crystallographic studies on the MonHM⁺ complexes provided support for the interpretation of potentiometric and spectroscopic results (184). Single-crystal studies proved particularly useful. The unit cell parameters of several monensin species are given in Table V. In each monensin species the number of monensin molecules per unit cell is four, and the unit cell volumes differ as expected for the different cell contents. Attempts to measure unit cell dimensions for MonHNaCl and MonHNaI by powder diffraction methods were unsuccessful. It had been thought that the diffraction patterns of these two sodium halide complexes might be similar enough to that of MonHNaBr so that hkl indices could be assigned to the strongest lines. However, the patterns were sufficiently different to make the determination of unit cell parameters impossible by this method.

The crystal structure of the monensin sodium bromide complex (184) is shown in Figure 28. As postulated from previous measurements, the structure contains both a bromide ion and a neutral monensin molecule coordinated to a sodium ion. The sodium ion is coordinated in a distorted octahedral manner to four ether and two alcohol oxygen atoms of monensin. Two intramolecular hydrogen bonds join the ends of the monensin molecule, while two other hydrogen bonds are to the bromide ion. Data on the coordination of the sodium and bromide ions are given in

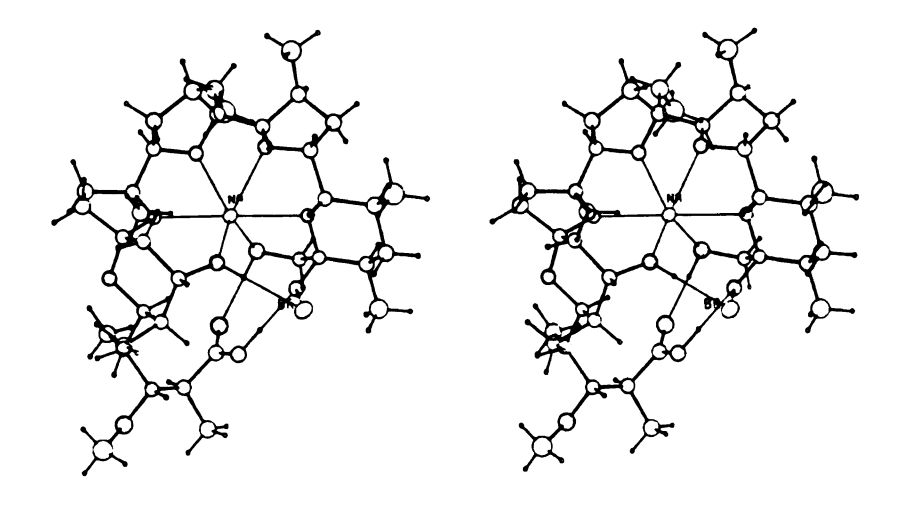
(Reproduced Comparison of Cell Parameters of Structures of Monensin (184). with the permission of the copyright holder.) Table V.

	Na ⁺ Br ⁻ Complex	Ag+ Salta	Free Acid ^b	Na ⁺ ClO ₄ Complex
ದ	16.618(4)Å	16.46	15.15	17.832(9)
٩	18.702(4)	18.81	23.61	22.257(10)
v	12.923(3)	12.73	10.65	10.367(6)
space group	P2 ₁ 2 ₁ 2 ₁			
Vol	4016.3	3941.4	3809.4	4114.5

aReference (167).

^bReference (5).

Figure 28. Two stereo views of the crystal structure of
MonHNaBr (184). (Reproduced with the permission of the copyright holder.)



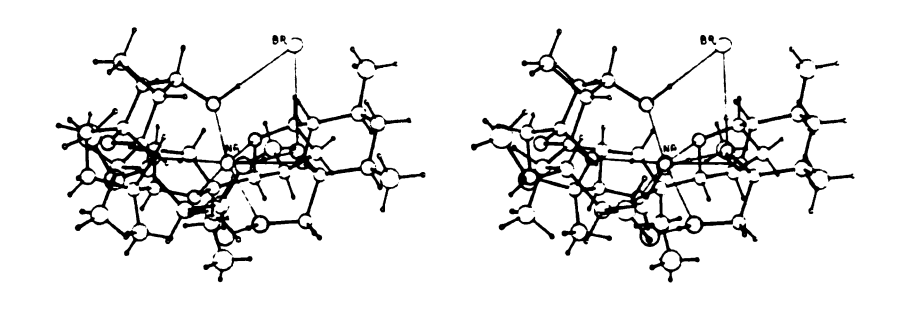


Figure 29 and Table VI.

The configuration and structure of the monensin molecule in the complex are very similar to those reported for the free acid (6) and for the silver salt (167). The carbon skeleton of the sodium bromide complex is almost identical to that of the silver salt; the bromide ion coordinates correspond to those of one of the water molecules of the silver salt, but no atom was found corresponding to the other water molecule.

A most striking difference among the three known monensin species is in the scheme of hydrogen bonding, as seen in Figure 30. These very different hydrogen-bonding patterns are consistent with the different infrared spectra obtained for the three compounds and with MonHNaBr containing no associated water, in contrast to MonH and MonNa.

Thus, the solid state characterization showed good consistency with the results obtained from solution studies. However, it was also of interest to examine the stability of the new complexes in solutions.

Complexes of the form MonHM⁺ showed a marked instability in the presence of water. It was found that after shaking a chloroform solution of MonHNaClO₄ against water and separating the phases, perchlorate ion could be precipitated from the aqueous phase by the addition of tetraphenylar-sonium chloride. Also, the material remaining in the

Figure 29. Schematic representation and bond lengths (Å) of Na⁺ coordination in the crystal structure of MonHNaBr. The oxygen atoms are numbered as in Figure 1.

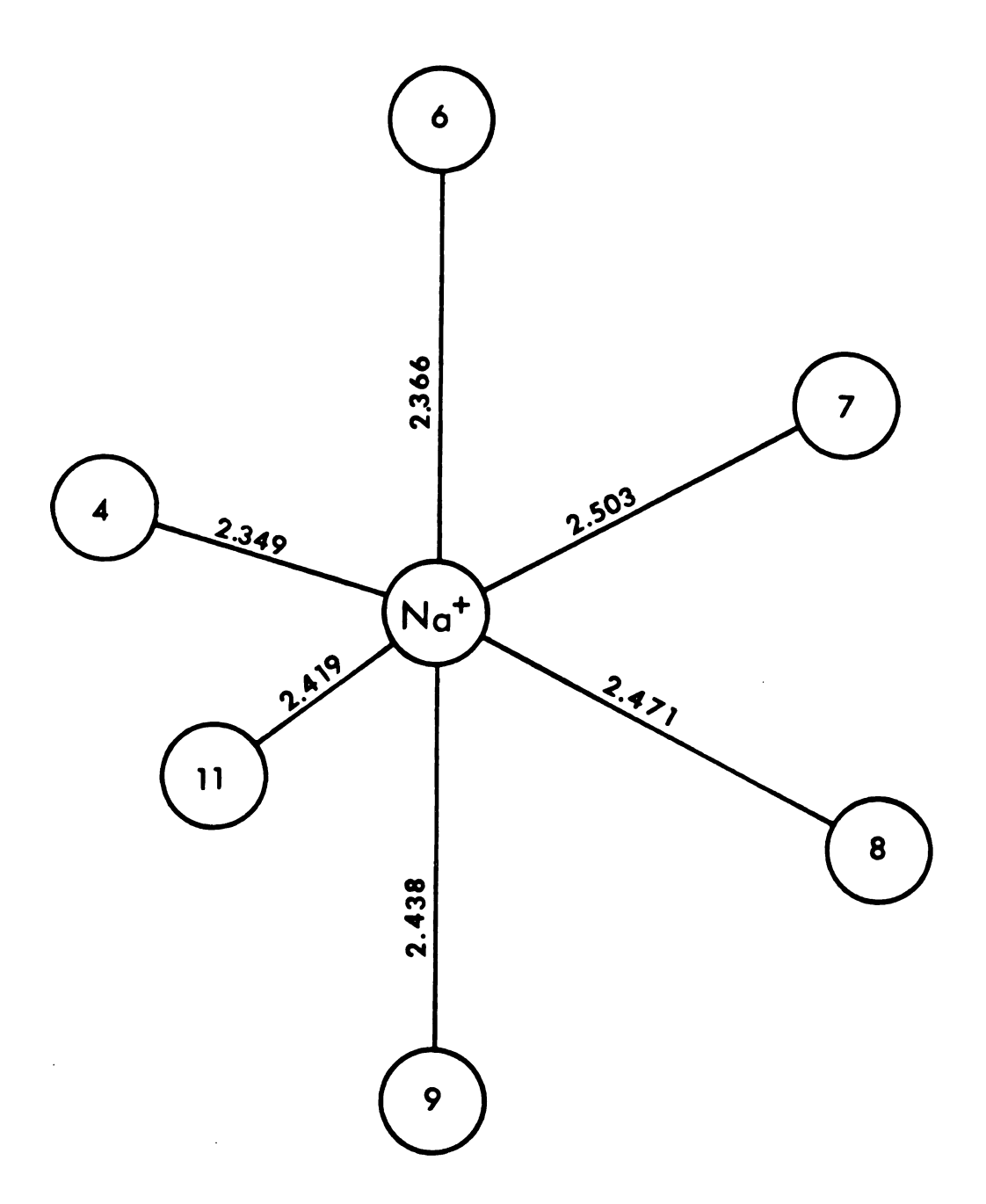
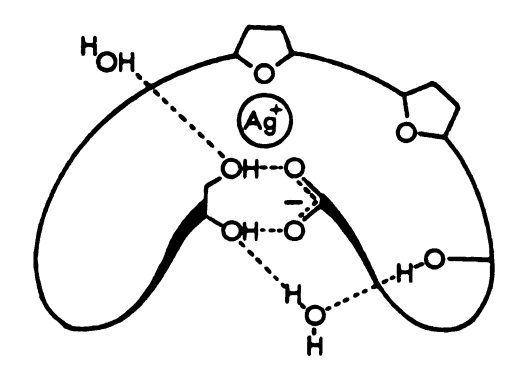


Figure 29

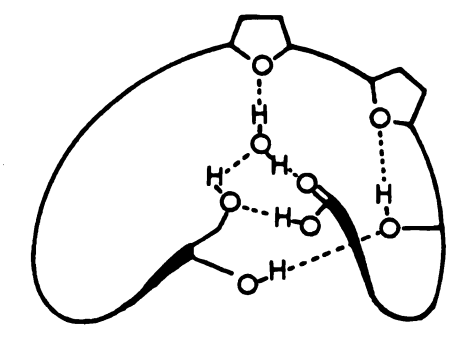
Table VI. Crystal Data on the Sodium and Bromide Ion Coordination in MonHNaBr. The oxygen atoms are numbered as in Figure 1.

	Bond Leng	ths (Å)	
Na-0(4)	2.349	Na-0(8)	2.471
Na-0(6)	2.366	Na-0(9)	2.438
Na-0(7)	2.503	Na-0(11)	2.419
	Bond Ang	les (°)	
0(4)-Na-0(6)	74.1(3)	0(6)-Na-0(11)	116.2(3)
0(4)-Na-0(7)	137.8(4)	0(7)-Na-0(8)	69.5(2
0(4)-Na-0(8)	110.3(3)	0(7)-Na-0(9)	113.9(3
0(4)-Na-0(9)	102.2(3)	0(7)-Na-0(11)	100.0(3
0(4)-Na-0(11)	114.4(3)	0(8)-Na-0(9)	64.7(2
0(6)-Na-0(7)	69.0(2)	0(8)-Na-0(11)	118.8(3
0(6)-Na-0(8)	114.8(3)	0(9)-Na-0(11)	66.7(3
0(6)-Na-0(9)	175.9(3)		
Hydr	ogen-bonding t	o the bromide ion	
		H-Br	0-Br
0(4)-H0(4)-Br		[2.21]	3.216
0(10)-H0(10)-E	Br	[2.17]	3.193

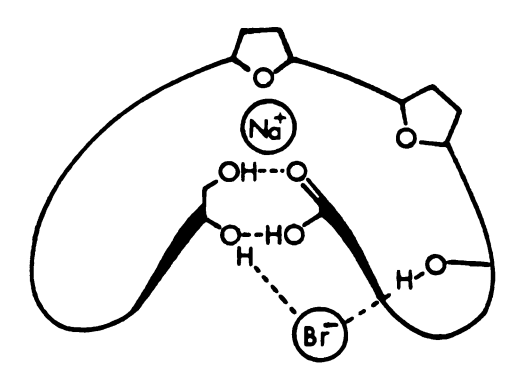
Figure 30. Schematic representation of the crystalline hydrogen-bonding in three monensin species (5). (Reproduced in part with the permission of the copyright holder.)



MONENSIN SILVER SALT



MONENSIN FREE ACID



MONENSIN SODIUM BROMIDE COMPLEX

Figure 30

organic phase had the properties of monensin free acid, indicating that the complex had been decomposed into its starting materials.

The anhydrous nature of the MonHNaClO $_{\downarrow}$ complex combined with its instability in the presence of water provided a path for the preparation of MonD·D $_{2}$ O, in which deuterium was partially substituted for exchangeable protons. Addition of D $_{2}$ O to a methanolic solution of MonHNaClO $_{\downarrow}$ yielded a white precipitate which exhibited the same melting range as MonH. In the infrared spectrum of the solid, two nearly identical hydrogen-bonding patterns were observed, one corresponding to normal bonding, the other appearing at a frequency of about 1000 cm $^{-1}$ lower. The infrared spectrum also showed greater than 50 percent reduction in the intensity of the peak at 1640 cm $^{-1}$ (see Figure 25), confirming the previous conclusion that this peak was due to associated water.

Another type of complex instability was encountered in the course of acid-base titrations. It has already been noted that addition of metal salts to monensin solutions produces an acid-lowering effect as predicted by the proposed equilibria in reaction (27). The increased solution acidity could be titrated with a base such as TBAH; representative titration curves are shown in Figure 31. It was found, however, that the shapes of such titration curves changed as a function of the time elapsed

Figure 31. Titrations of monensin free acid with tetran-butylammonium hydroxide in anhydrous methanol solution with various supporting electrolytes.

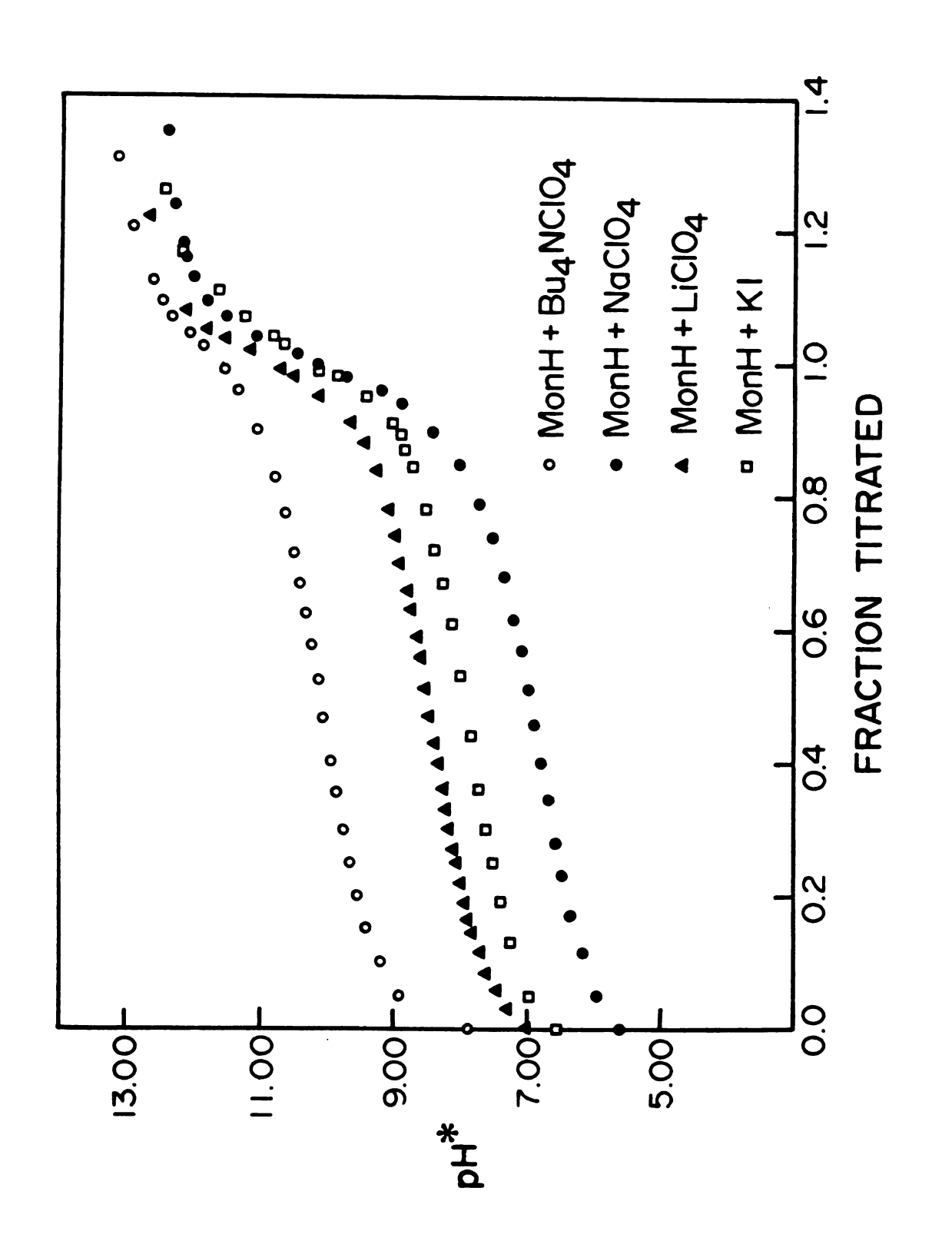


Figure 31

after the mixing of the monensin and metal salt solutions. As seen in Figure 32 with time the solution appeared to contain a mixture of weak and strong acids. The stronger acid component is that expected from monensin in solution with the salt; the origin of the weak acid is undetermined. The reaction product has not yet been identified, but on the basis of infrared measurements, mass spectrometry, melting point, and ¹H nmr analysis it seems to be a mixture of compounds and not any single monensin species.

The time-dependent reaction was found to also be temperature-dependent. As illustrated in Figure 33, the reaction proceeds much faster with increasing temperature. Although titrations were done at various monensin and metal salt concentrations, little information could be obtained on the order of the reaction. Plots such as those shown in Figure 34 have too much error in the time axis to be of much value. As each titration required more than 30 minutes, the error was such that no good comparisons could be made among the several reaction conditions.

The decomposition has been observed in the titrations of monensin in the presence of all of the alkali metal ions. The reaction rate is roughly correlated with the amount of acid-lowering effect, and decreases in the order $Na^+ > K^+ > Rb^+ > Cs^+ > Li^+$. This observation suggests that the decomposition proceeds faster in more acidic solutions. Agtarap et al. (1) observed that monensin was

Figure 32. Titrations of 20.00 ml of 2.012 x 10^{-3} M MonH, 6.115 x 10^{-3} M NaClO₄ with 5.07 x 10^{-2} M TBAH in absolute methanol at 22°C. The titrations were begun 0.0 (•), 3.0 (x), and 21.0 (+) hours after mixing the MonH and NaClO₄ solutions.

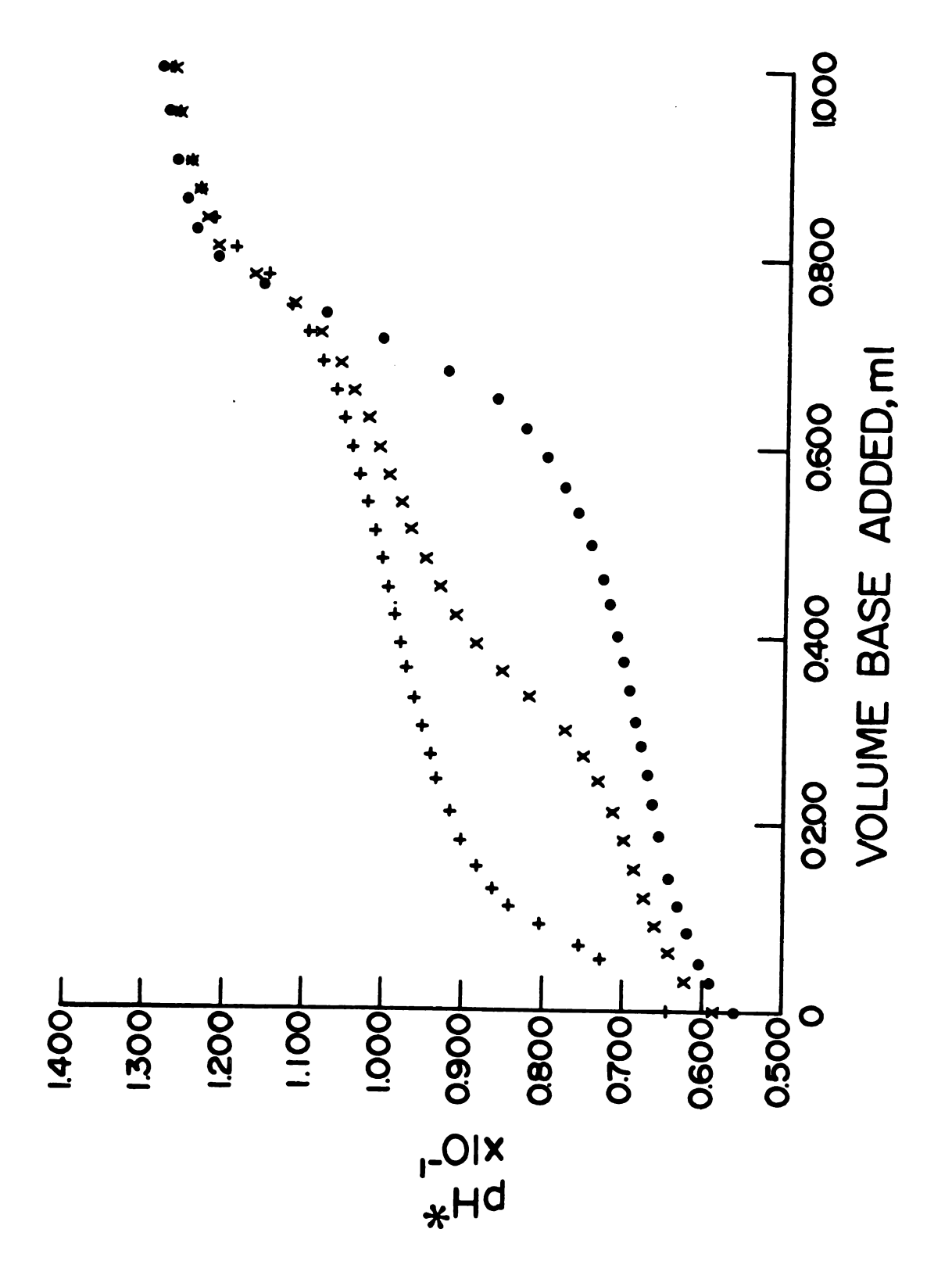


Figure 32

Figure 33. Temperature dependence of the decomposition in methanolic solutions of MonH and NaClO4. The inset defines the two observed endpoints, EPl and EP2. •, 1°C; +, 22°C; x, 35°C.

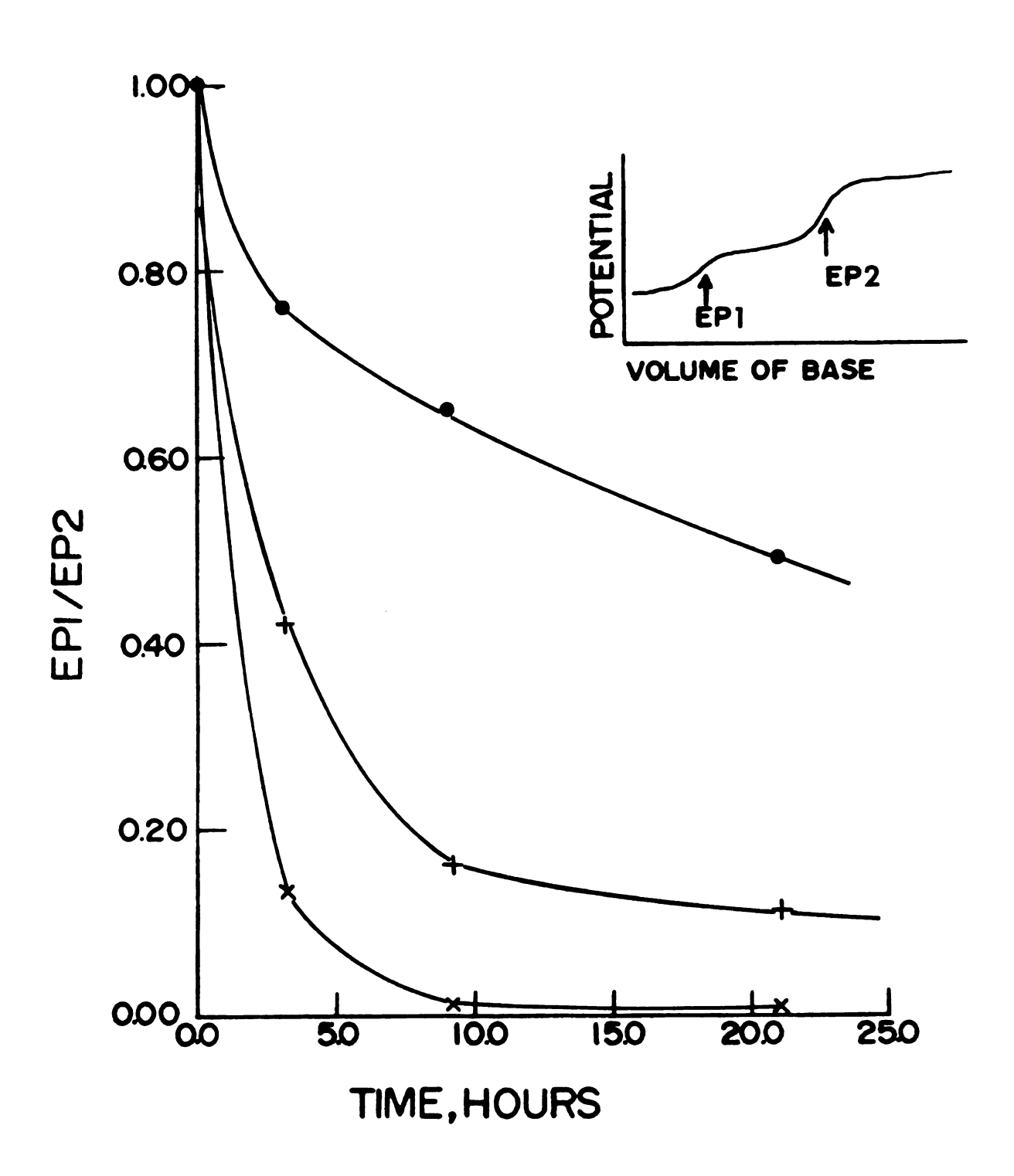


Figure 33

Figure 34. Concentration dependence of the decomposition in methanolic solutions of MonH and NaClO $_{\mu}$ at 22°C. The inset defines the two observed endpoints, EPl and EP2. x, $C_{MonH} = 0.17 \ \underline{M}$, $C_{Na} + 0.50 \ \underline{M}$; *, $C_{MonH} = 0.15 \ \underline{M}$, $C_{Na} + 0.15 \ \underline{M}$; o, $C_{MonH} = 2 \ x \ 10^{-3} \ \underline{M}$, $C_{Na} + 6 \ x \ 10^{-2} \ \underline{M}$; + $C_{MonH} = 2 \ x \ 10^{-3} \ \underline{M}$, $C_{Na} + 1 \ x \ 10^{-3} \ \underline{M}$.

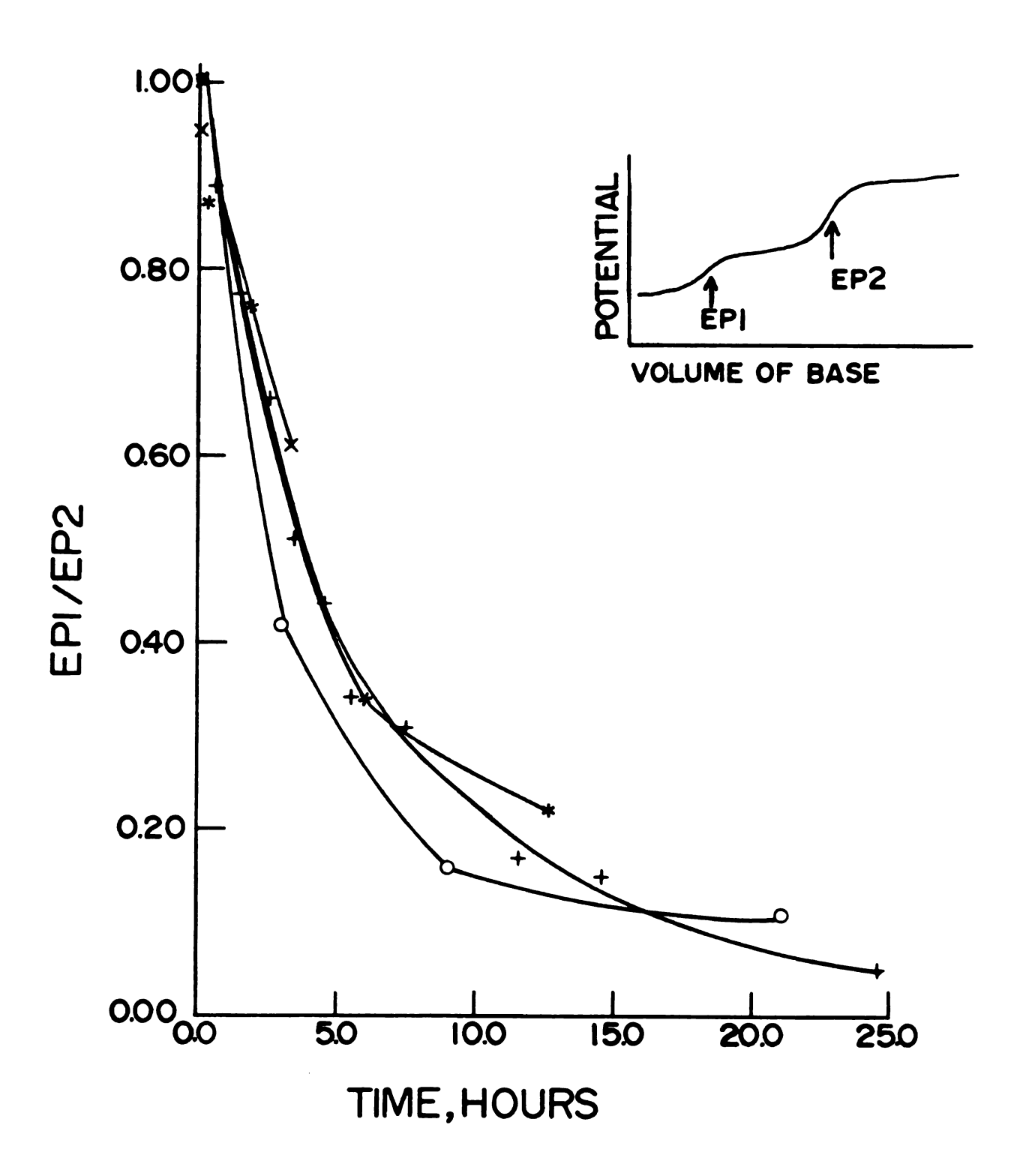


Figure 34

unstable in acid solution, and Agtarap and Chamberlin (4) attributed the instability to hydrolysis of the spiroketal group. The hydrolysis product which they obtained had $\lambda_{\rm max}^{\rm EtOH}$ at 281 nm. In the present work, the action of millimolar HClO4 on millimolar monensin in methanol at room temperature produced a large absorbance increase at 230 nm and a small rise at 280 nm. On the other hand, under the same conditions substitution of NaClO4 for HClO4 produced almost no change in the ultraviolet or visible absorption spectra of monensin.

It is clear that the details of this time-dependent reaction are not known. However, in quantitative measurements the effects of this decomposition reaction must be considered.

4.5. DETERMINATION OF FORMATION CONSTANTS FOR MonHM⁺ COMPLEXES

Several techniques were used in attempts to determine formation constants for the MonHM⁺ complexes in methanol solutions. Fluorescence, metal ion nmr, and cyclic voltammetry were generally unsatisfactory for these quantitative studies, but acid-base potentiometry was suitable for the equilibrium constant measurements.

The quenching effect of monensin on Tl(I) fluorescence is illustrated in Figure 22. In principle this quenching could be related to the complex formation constant but, as

in basic solution, there were complications. The measurements showed a good deal of scatter and were further influenced by a peak at about 322 nm due to the ligand.

Figure 35 shows how the ligand peak grows into the spectrum, causing the fluorescence maximum to shift even at low mole ratios. Thus the conditions were similar to those in basic solutions and reliable formation constants could not be found without extensive dual-wavelength experiments.

Metal ion nmr likewise suffered from the same problems as in basic solutions. Addition of monensin to lithium salt solutions produced little change in the ⁷Li resonance frequency or linewidth; this result was also observed by Gertenbach and Popov (174). In the cases of sodium and potassium salts the increased linewidths so reduced the accuracy of the chemical shift measurements that no quantitative data could be obtained. Even in those cases in which smooth mole ratio plots were obtained (Figures 23 and 24) data interpretation is difficult; in solution one has two ligands, MonH and Mon⁻, and three complexes, MonH, MonM, and MonHM⁺. In addition, for metal ion nmr, one has the additional unknowns of the chemical shifts for the metal complexes. Thus, metal ion nmr was not considered appropriate for these equilibrium constant calculations.

Although cyclic voltammetry of Tl(I) yielded a great deal of information on the complexation reactions involving Mon, little information could be obtained when using MonH

Figure 35. Quenching of the fluorescence of a 1.120 x 10⁻⁴

M T1ClO₄ solution in methanol by MonH. The ligand to metal mole ratios are as follows: curve 1, 0.00; 2, 0.060; 3, 0.118; 4, 0.178; 5, 0.237; 6, 0.296; 7, 0.415; 8, 0.533; 9, 0.652; 10, 0.770; 11, 0.948; 12, 1.245; 13, 1.541; 14, 1.985; 15, 2.578; 16, 3.763; 17, 5.541; 18, 7.319; 19, 23.71.

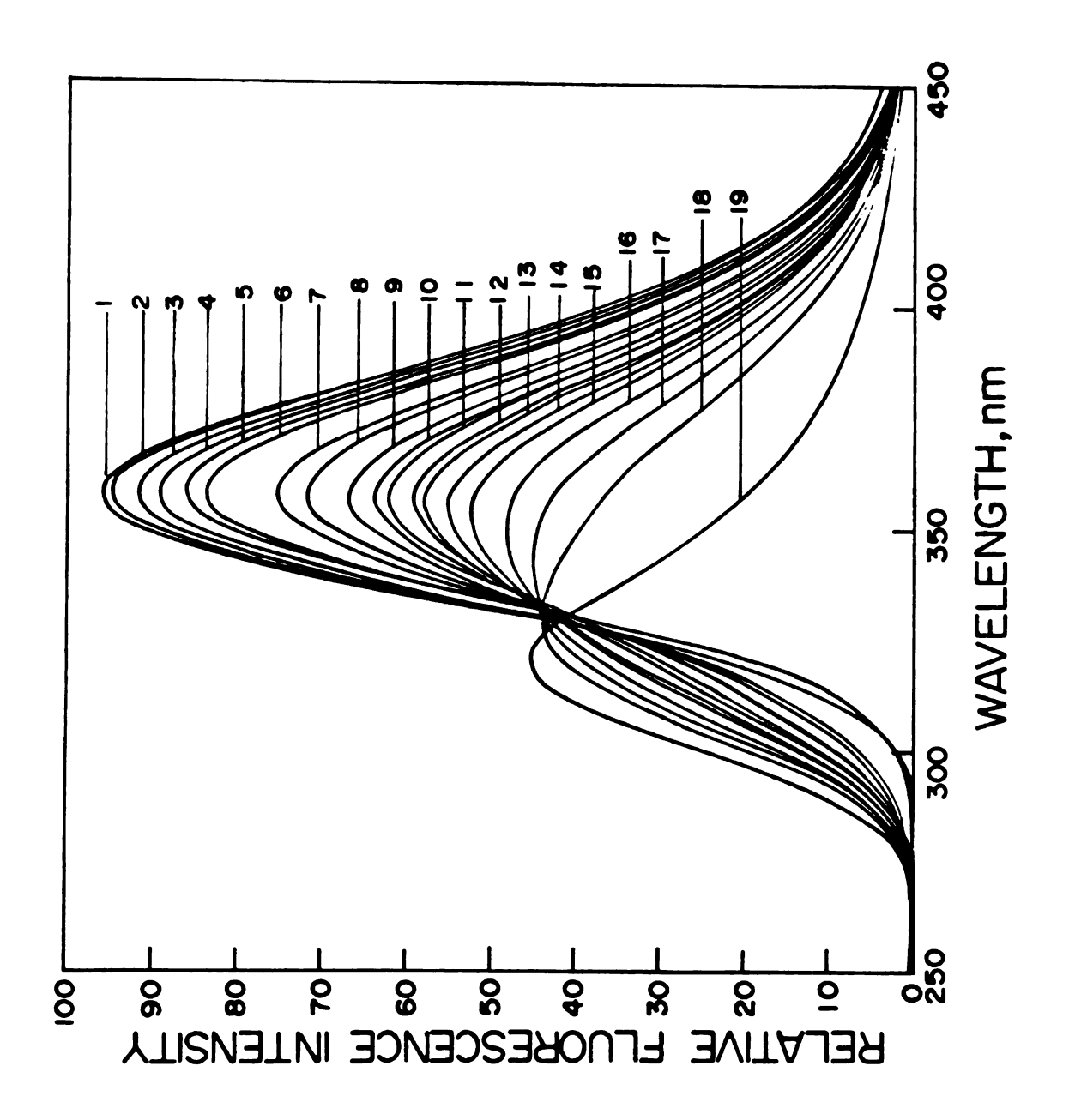


Figure 35

as ligand; the halfwave potential shifts were just too small to be accurately measured.

A technique which is precise, accurate, and applicable to the determination of MonHM complexation constants is potentiometry. Titrations of the acid released by the interaction of monensin with metal salts gave the data for the calculation of equilibrium constants. Experimentally, since the electrode responses were very fast and the measurement electronics very stable, an entire titration could be performed in less than 15 minutes; even so, the curves had to be corrected for a small amount of degrada-The correction involved using data only in the buffer region before the first equivalence point as input to the program MINIQUAD and not the data between the first and second equivalence points. As seen in Figure 32, the two acids, $MonHNa^+$ and the degradation product, have pK_a values differing by almost three units and therefore should be titrated independently of each other.

The titrations of monensin solutions containing the metal ions Li⁺, Na⁺, Ag⁺, or Tl⁺ were carried out in perchlorate medium. The necessary equations are

$$C_{H^{+}} = [H^{+}] + [MonH] + [MonHM^{+}]$$
 (28)

$$C_{M^{+}} = [M^{+}] + [MonM] + [MonHM^{+}]$$
 (29)

$$C_{Mon}^{-} = [Mon^{-}] + [MonH] + [MonHM^{+}] + [MonM]$$
 (30)

$$[MonM] = K_f^M [M^+] [Mon^-]$$
 (31)

$$[MonH] = [H^{+}] [Mon^{-}]/K_a$$
 (32)

$$[MonHM^{+}] = K_{f}^{MonHM^{+}} [MonH][M^{+}]$$
 (33)

The titration results are given in Table VII.

The titrations of monensin in solutions with K⁺, Rb⁺, or Cs⁺ were done in tetra-n-butylammonium iodide (TBAI) medium, due to the insolubility of the metal perchlorate salts. In the halide solution data interpretation becomes extremely difficult because of the number of equilibria involved due to ion-pairing considerations. The necessary mass-balance equations follow:

$$C_{H^{+}} = [H^{+}] + [HI] + [MonH] + [MonHM^{+}]$$
 (34)

$$C_{M^{+}} = [M^{+}] + [MI] + [MonM] + [MonHM^{+}]$$
 (35)

$$C_{Mon}^- = [Mon^-] + [MonH] + [MonHM^+] + [MonM]$$
 (36)

$$C_{TBA}^{+} = [TBA^{+}] + [TBAI]$$
 (37)

$$C_{I^-} = [I^-] + [HI] + [MI] + [TBAI]$$
 (38)

Table VII. Formation Constants for MonHM Complexes in Anhydrous Methanol

Complex	log K _f	
MonHLiClO ₄	K _f ≈ 0	
$\mathtt{MonHNaClO}_{\mathtt{4}}$	2.5 ± 0.1	
$\mathtt{MonHAgClO}_{\mathtt{4}}$	3.7 ± 0.2	
MonHKI	<2	
MonHTlClO ₄	1.7 ± 0.1	
MonHRbI	<2	
MonHCsI	<u><</u> 1	

with the corresponding equilibrium constant expressions

$$[HI] = K_{\mathbf{f}}^{\mathbf{HI}} [H^{+}][I^{-}]$$
(39)

$$[TBAI] = K_f^{TBAI} [TBA^+] [I^-]$$
 (40)

$$[MI] = K_f^{MI} [M^+] [I^-]$$
(41)

$$[MonH] = K_f^{MonH} [Mon^-] [H^+]$$
 (42)

$$[MonM] = K_{\mathbf{f}}^{MonM} [Mon^{-}] [M^{+}]$$
 (43)

$$[MonHM^{+}] = K_{f}^{MonHM^{+}} [MonH] [M^{+}]$$
 (44)

Some of the equilibrium constants have not been accurately determined in methanol solution, particularly the constants $K_{\rm MI}$ and $K_{\rm HI}$. The values of the MonHM⁺ formation constants determined in the iodide medium are estimates at best, and are therefore given only as an order of magnitude in Table VII.

Comparison of the formation constants of MonHM⁺ complexes with those of MonM complexes (see Table I) shows that the selectivity order is the same for both types of complex, but also that the MonHM⁺ complexes are much weaker than their corresponding MonM complexes. The increased stability of MonM complexes is undoubtedly due to the zwitterionic

charge stabilization in those complexes; in a medium of low dielectric constant the neutral MonM molecule would be favored over the charged MonHM⁺ complex. Further discussion of the relative stabilities will be presented in the consideration of the thermodynamics of monensin complexation.

4.6. CONCLUSIONS

The acid dissociation constant of monensin was determined by acid-base potentiometry. The protonated form of the acid was found to complex metal ions and the form of the complexes was determined to be MonHMX where MX is a metal salt. The complexes were characterized both in the solid state and in solution, and formation constants were determined potentiometrically. Protonated complexes are much weaker than the corresponding deprotonated complexes but show the same order of selectivity.

CHAPTER 5

THERMODYNAMICS OF MONENSIN COMPLEXATION

5.1. INTRODUCTION

Currently there are known three monensin complexes, including the proton complex, which are formed according to the reactions

$$Mon^{-} + H^{+} \neq MonH \tag{45}$$

$$Mon^{-} + M^{+} \stackrel{\rightarrow}{+} MonM \tag{46}$$

$$MonH + M^{+} \stackrel{?}{\downarrow} MonHM^{+}$$
 (47)

It has been shown that there are large differences among the equilibrium constants of reactions (45) - (47); it was of interest to investigate the possible bases for these differences. To this end thermodynamic studies were done to determine the enthalpies and entropies of the above reactions.

5.2. THERMODYNAMICS OF MONENSIN COMPLEXATION

The method used for determining the enthalpy and entropy of a reaction was based on the temperature dependence of the formation constant. The straightforward derivation of the necessary equations follows:

$$\Delta G = \Delta H - T\Delta S \tag{48}$$

$$\Delta G = -RT \ln K_{f} \tag{49}$$

$$\Delta H - T\Delta S = -RT \ln K_{f}$$
 (50)

$$\ln K_{f} = -\frac{\Delta H}{R} \left(\frac{1}{T}\right) + \frac{\Delta S}{R}$$
 (51)

Thus a plot of ln K_f as a function of the reciprocal of temperature gives a straight line with slope - $\frac{\Delta H}{R}$ and intercept $\frac{\Delta S}{R}$, provided that the enthalpy is a constant over the temperature range considered.

The experimental realization of formation constant measurements at different temperatures involved the consideration of a variety of temperature effects. For work in molar concentration units, temperature change also alters the concentration, due to volume expansion or contraction. Significant changes in the activity coefficients with temperature were also important. The volume changes not only affected the ionic strength, but temperature effects were also seen in the two constant terms in Equation (8) which are inversely proportional to $(\varepsilon T)^{1/2}$ and $(\varepsilon T)^{3/2}$, respectively. The change in temperature also induced a change in the dielectric constant of the solvent; in the present work the values of Leung and Grunwald (213) were used for the variation of dielectric constant of methanol with temperature.

After activity corrections had been applied, plots of

In $K_{\mathbf{f}}$ versus $\frac{1}{T}$ for reactions (45)-(47) gave straight lines, as shown in Figure 36. The thermodynamic parameters are listed in Table VIII, and those for MonNa are compared to the values obtained calorimetrically by Lutz <u>et al</u>. (177). It is somewhat difficult to compare the two results since the calorimetric method is probably more accurate for the determination of enthalpy of a reaction than the temperature dependence of ln $K_{\mathbf{f}}$. On the other hand, the calorimetric method for the determination of formation constants, in general, becomes unreliable when $K_{\mathbf{f}} > 10^{4}$.

It is interesting to compare the results for the three types of monensin complex. The MonH and MonNa complexes are both enthalpy as well as entropy stabilized, while the MonHNa⁺ complex is enthalpy stabilized and entropy destabilized. The basis for these differences apparently lies in the different reaction types. Reaction (45) is of two charged species combining to form an entirely neutral molecule; reaction (46) consists also of two charged species combining to form a complex, but in the latter case the complex species is not neutral, but rather zwitterionic, since Pinkerton and Steinrauf have shown that the carboxylate group does not participate in bonding to the metal ion (167). Finally, in reaction (47), combination of a charged metal ion and an uncharged ligand results in a charged complex.

The differences among the entropies of complexation

Figure 36. Temperature dependence of $\ln K_{\hat{f}}$ for three monensin complexes in methanol solutions. Curve 1, MonH; 2, MonNa; 3, MonHNaClO₄.

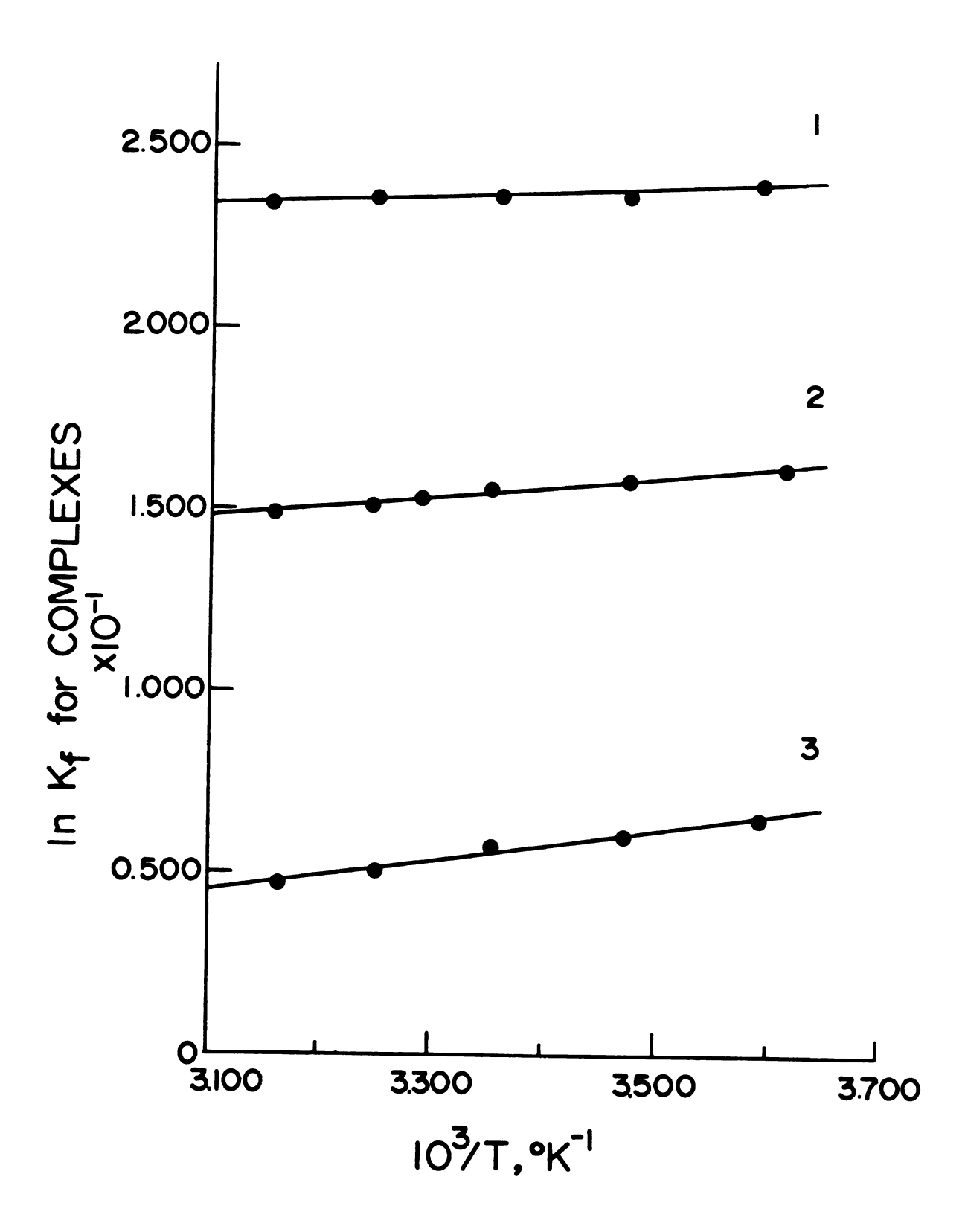


Figure 36

Thermodynamic Parameters for Monensin Complexes. Table VIII.

Complex	ΔH° (Kcal·mole ⁻¹)	ΔS° (Kcal·mole ⁻¹)	ΔG° (Kcal·mole ⁻¹)	log K _f
MonH	-2.4 ± 0.3	39 ± 1	-14.1 ± 0.3	10.30 ± 0.05
MonNa	-5.47 ± 0.24	12.4 ± 0.7	-9.2 ± 0.2	6.72 ± 0.05
MonNa*	-3.87 ± 0.07	14.6	-8.22	6.1 ±0.5
$MonHNaClO_{m{\mu}}$	-8.5 ± 0.6	-17 ± 2	-3.3 ± 0.5	2.5 ±0.1

* Values from Reference (177).

for the three reactions are quite large. The entropy changes on complexation include the effects of three factors: 1) the changes in translational entropy, 2) the changes in solvent structure, and 3) the changes in the rotational and vibrational entropies of the ligand.

The extent of solvation of the metal ion, of the ligand, and of the complex determine the change in translational entropy upon complexation. If one assumes that a charged entity in solution is likely to be more solvated than an uncharged species, it is evident that in reaction (45) a large increase in translational entropy would be expected. In that reaction, two charged, solvated reactants combine to form a neutral, relatively unsolvated product. The increase in translational entropy would thus result from desolvation of both the metal ion and the ligand. A similar, but smaller, increase in translational entropy would be expected in reaction (46), in which the metal ion is desolvated, but the resulting zwitterionic complex should be partially solvated. Finally, it seems that in reaction (47) a smaller increase in translational entropy would be expected since the charged complex should be more highly solvated than the uncharged species.

Solvation of a charged complex such as MonHNa⁺ results in changes in the solvent structure upon formation of the complex. The solvated alkali metal ion is a solvent "structure-breaker" which disorders the solvent

in the immediate vicinity of the ion. In the case of the charged complex, on the other hand, only second-shell solvation effects are important, as the ligand replaces the solvent molecules in the primary solvation sphere of the metal ion. As a result, the solvent structure is more ordered around the "structure-making" organic cation than it is around the alkali metal ion. In the complexation reaction (47), therefore, the observed decrease in entropy is not unexpected.

The third contribution to entropy change in complexation is the change in internal entropy of the ligand. It may be expected that both the vibrational and rotational entropies of the ligand would be reduced upon complexation, as the ligand would undergo a conformational change and, presumably, be more rigid in the complex than in its free form.

That the monensin molecule undergoes conformational change during complexation is certain. In his ²³Na nmr study of reaction (46), Degani found that an activated complex, MonNa*, is formed, which then undergoes a conformational change to MonNa (172). Similarly, in reaction (47) the monensin molecule goes from the free acid form to the conformation of the sodium salt. Whether or not the ligand is more rigid in the complex is subject to question, however. The free acid, MonH, is a structured, cyclic molecule in solution (166), but little is known

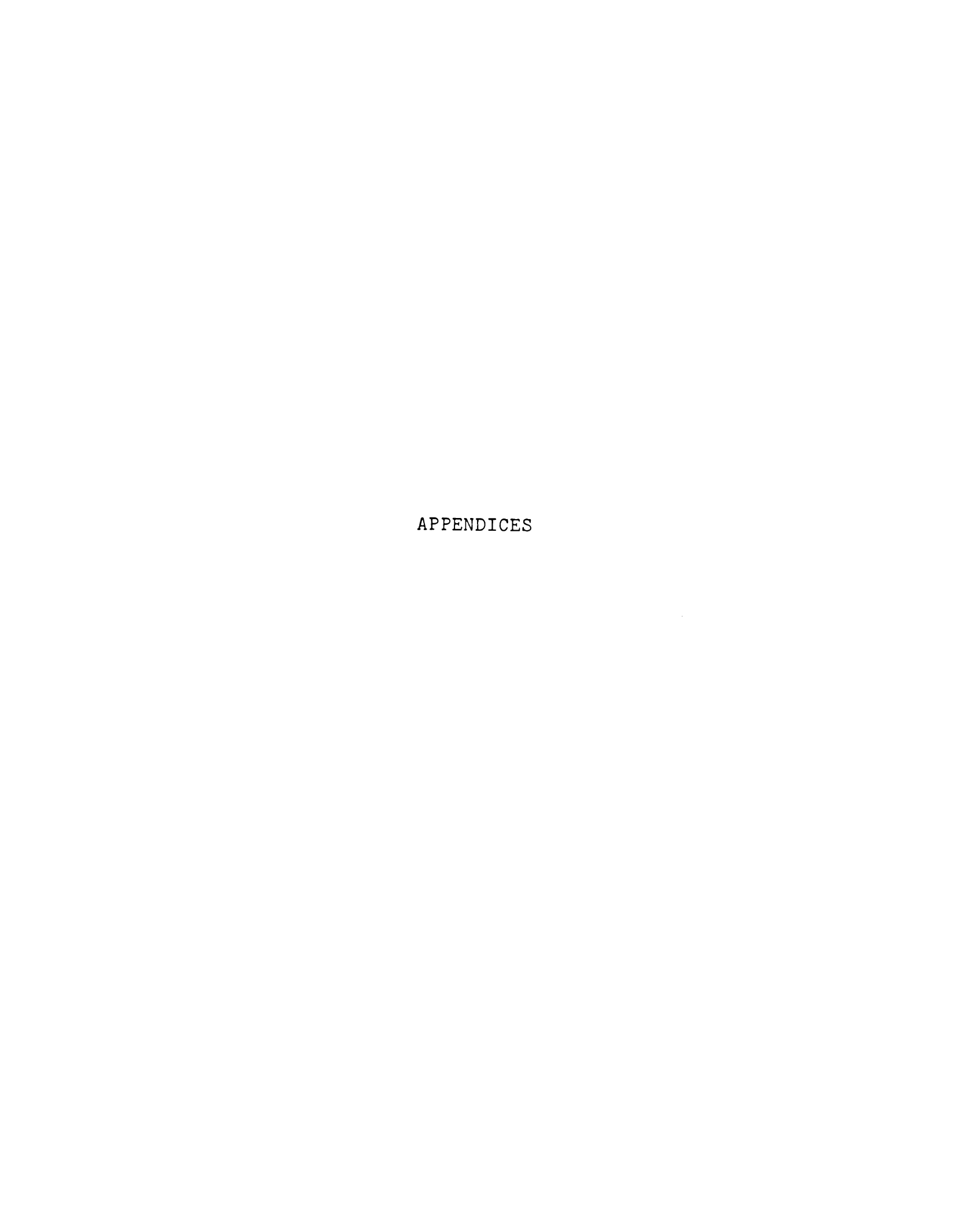
about the solution structure of the monensin anion, Mon.

The observed thermodynamic parameters for reaction (47) are in general agreement with the results from other reactions of alkali metal ions with uncharged ligands.

Kauffmann et al. showed that the alkali metal ion complexes with the cryptand C222 in water and in methanol were enthalpy stabilized and entropy destabilized (214). Similar results have been reported for the C222-Cs⁺ complex in methanol, acetone, propylene carbonate, and N,N-dimethylformamide (215) and for the 18-crown-6-Cs⁺ complex in pyridine (216).

5.3. CONCLUSIONS

The thermodynamic parameters ΔH° , ΔS° , and ΔG° have been obtained for the formation of MonH, MonNa, and MonHNa⁺ in methanol solutions. The observed trends have been interpreted in terms of the relative solvation of the reactants and products and in terms of the internal entropy of the ligand.



APPENDIX A

APPLICATION OF THE COMPUTER PROGRAM

KINFIT4 TO THE CALIBRATION OF

ION-SELECTIVE ELECTRODES

APPLICATION OF THE COMPUTER PROGRAM KINFIT4 TO THE CALI-BRATION OF ION-SELECTIVE ELECTRODES

A.l. Electrodes Sensitive to Metal Ions

A.1.1. Program Function

Interaction with the KINFIT4 program was through SUBROUTINE EQN, into which the user inserts a function containing unknowns which are to be calculated from experimental data. In the electrode calibration equation

$$E = E^{\circ} + m \log (C_{M} + R)$$
 (11)

the unknowns are m, E°', and R, and in the computer program these parameters are designated U(1), U(2), and U(3), respectively. The FORTRAN code used in fitting the calibration curves is listed in Section A.1.2.

Data input includes the usual control cards as well as calibration curve data. The first control card gives the number of data points, the maximum number of iterations to be performed, the number of constants to be read, and the convergence tolerance. A title card follows, after which comes the card containing the values for the constants (if any) and then the card containing initial estimates for the unknown parameters. The remaining cards are data input. In the electrode calibration case, the data are input as observed potential as a function of the

PLEASE NOTE:

Dissertation contains small and indistinct print. Filmed as received.

UNIVERSITY MICROFILMS.

logarithm of the metal ion concentration. Each data entry is followed by its estimated variance. A sample data listing is provided in Section A.1.3.

A.1.2. SUBROUTINE EQN

```
SUPPOUTINE EON
COMMON ROUNTITAPE.JTAPE.INT.LAP.XIVCQ.NODT.NOVAR.NOJNK.X.U.ITMAX.
INTX.TESTI.JAY.RESID.IAR.ESS.TIYP.XX.EXTYP.DXII.FOP.FD.FU.P.ZL.ID.E
ZIGVAL.XST.T.OTAL.MIJJJY.DY.V.DY.VECT.NCST.CONST.NDAT.JDAT.MOPI.LOPT.
COMMON/REDYJ/METH
COMMON/RE
```

A.1.3. Sample Data Listing

A.2. Electrodes Sensitive to Hydrogen Ions

A.2.1. Program Function

Interaction with the KINFIT4 program was through the SUBROUTINE EQN. The electrode calibration curves were fit to the equation

$$E = E^{\circ} + \frac{2.303RT}{nF} \log (C_{H^{+}} + R)$$
 (52)

and the unknowns E°' and R were designated U(1) and U(2), respectively. Since the calibrations were based on the results of acid-base titrations, six constants were defined as follows: CONST(1), the initial volume (ml) of acid solution; CONST(2), the initial molar acid concentration; CONST(3), the analytical molar base concentration; CONST(4), the reaction temperature in °C; CONST(5), the titrant temperature in °C; CONST(6), the value for $\frac{2.303\text{RT}}{\text{nF}}$ at the reaction temperature. The FORTRAN code used in fitting the calibration equation is listed in Section A.2.2.

Data input includes the control cards described in Section A.l.l as well as the calibration curve data. The latter are input as observed potential as a function of the volume of base added, and each data entry is followed by its estimated variance. A sample data listing is given in Section A.2.3.

A.2.2. SUBROUTINE EON

```
TAPE (1) APLED

TO TO SET TO S
 C
 ç
c
c
c
```

A.2.3. Sample Data Listing

```
Calia CURVE FOR CORNING GLASS ELECTRODE MCLO4 IN TRAP. 24.9 DEGREES. V-91.
25.0 0.0019584 0.0130 24.9 59.14 59.14

0.000 1.0E-06 363.30 4.0E-02 0.750 1.0E-06 361.55 4.0E-02 0.750 1.0E-06 357.10 4.0E-02 0.750 1.0E-06 357
```

APPENDIX B

APPLICATION OF THE COMPUTER PROGRAM
MINIQUAD76A TO THE DETERMINATION OF
EQUILIBRIUM CONSTANTS FROM
POTENTIOMETRIC DATA

APPLICATION OF THE COMPUTER PROGRAM MINIQUAD76A TO THE
DETERMINATION OF EQUILIBRIUM CONSTANTS FROM POTENTIOMETRIC
DATA

B.1. Program Function

The MINIQUAD76A program is a general routine for calculation of equilibrium constants from potentiometric data. Up to 20 equilibria involving five reactants can be considered, and a maximum of three electrodes can be used to determine the concentrations of free reactants.

Equilibrium constants are calculated for reactions of the type

$$aA + bB + cC + A_aB_bC_c$$
 (53)

with the formation constant

$$\kappa_{\mathbf{f}}^{ABC} = \frac{\left[A_{\mathbf{a}}^{B}{}_{\mathbf{b}}^{C}{}_{\mathbf{c}}\right]}{\left[A\right]^{\mathbf{a}}\left[B\right]^{\mathbf{b}}\left[C\right]^{\mathbf{c}}}$$
(54)

A reaction such as

$$MonH + M^{+} \stackrel{?}{\downarrow} MonHM^{+}$$
 (55)

with the formation constant

$$K_{\mathbf{f}}^{\text{MonHM}^{\dagger}} = \frac{[\text{MonHM}^{\dagger}]}{[\text{MonH}][\text{M}^{\dagger}]}$$
 (56)

written in the form of Equation (53) becomes

$$Mon^{-} + H^{+} + M^{+} \stackrel{+}{\leftarrow} MonHM^{+}$$
 (57)

$$K_{f}' = \frac{[MonHM^{+}]}{[Mon^{-}][H^{+}][M^{+}]}$$
 (58)

The formation constants $K_{\mathbf{f}}^{\text{MonHM}^+}$ and $K_{\mathbf{f}}^{\mathbf{i}}$ are related through the formation constant of MonH from its components (reaction (19))

$$K_{f}^{\prime} = K_{f}^{\text{MonHM}^{+}} \cdot K_{f}^{\text{MonH}}$$
 (59)

In the analysis of volumetric titration data the user specifies the number of formation constants to be used in the calculations. The formation constants can be either held constant or refined in the calculations. For each constant, the stoichiometry of the complex is entered. Further specifications which are needed include the initial solution volume and temperature, the initial number of millimoles of each reactant, and the titrant concentration and its temperature. Electrode calibration parameters are entered as the slope and intercept of the Nernstian calibration plots. Finally, titration data consist of the measured electrode potentials as a function of the volume of titrant added.

By using mass-balance equations for each reactant along with the experimentally determined free reactant concentration(s), the program minimizes the error in the

calculated formation constants over the entire titration data set.

In some cases a single titrant solution may contain more than one reactant, and care must be exercised to maintain the correct mass-balance and volume conditions. For example, if a titrant contains two reactants at concentrations C_1 and C_2 , and a volume V of titrant is added, the reactant concentrations should be entered into the program as $2C_1$ and $2C_2$, and the volume of titrant added as $\frac{1}{2}V$.

In acid-base titrations, one of the mass-balance equations describes the concentration of species involving dissociable hydrogen ions. Under these conditions the hydroxide ion is considered to be a "negative proton", and the total concentration, $C_{\rm H}$, of protons in a basic titrant would be $C_{\rm H}$ = - $C_{\rm OH}$.

A more detailed description of the program function and several suggestions for use of the program are given in reference (186).

The MINIQUAD76A program has been designed for the determination of formation constants from potentiometric titration data. It should be noted, however, that potentiometry is only used to measure the concentrations of free reactants. Thus, data from any technique which measures free reactant concentrations could be analyzed by this program, if some programming is done to provide

MINIQUAD 76A with those free reactant concentrations.

- B.2. Data Input Instructions for MINIQUAD76A.
 - B.2.1. 1 card /20A4/: descriptive title.
 - B.2.2. 1 card /815/: LARS, NK, N, MAXIT, IPRIN, NMBEO, NCO.ICOM.

LARS is an indicator for the data points to be considered in the refinement: with LARS=1 all the data points are used, with LARS=] alternate points, with LARS=3 every third point, etc. (last points on all titration curves are always used).

NK is the total number of formation constants.

N is the number of formation constants to be refined.

MAXIT is the maximum number of iteration cycles to be performed: with MAXIT=0 and according to the values of JPRIN and JP (see below) the residuals on mass balance equations and/or the species distribution are evaluated for the given formation constants and conditions.

IPRIN=0 is normal; IPRIN=1 monitors the progress of the refinement at each cycle; IPRIN=2 produces an additional listing of of the experimental data at each titration point.

NMBEO is the total number of reactants (mass balance equations) in the system under consideration.

NCO is the maximum number of unknown concentrations of free reactants; if NCO=0 the whole job is abandoned before refinement.

ICOM=0 is normal; with ICOM=1 data points are eliminated before the refinement if the corresponding block of the normal equation matrix is found to be not positive-definite.

B.2.3. 1 card /3F10.6,8X,I2/: TEMP,ADDTEMP,ALPHA, NOTAPE

TEMP is the reaction temperature in °C.

ADDTEMP is the titrant temperature in °C.

ALPHA is the coefficient of cubical expansion for the solvent used, ${}^{\circ}C^{-1}$.

NOTAPE=0 is normal; NOTAPE=1 reads values for EZERO and SLOPE (see below) from device TAPE3. This allows calibration curve data to be calculated and used in the same computer run.

B.2.4. NK cards /F10.6,715/ : BETA(I), JPOT(I), JQRO(J,I) (NMBEO values), KEY(I).

The formation constants are expressed in exponential notation

$$\beta_i = BETA(I) \cdot 10^{JPOT(I)}$$
.

JQRO(J,I) (J=1,NMBEO) are the NMBEO stoichiometric coefficients of the <u>i</u>th species with formation constant β_1 . The order of coefficients is arbitrary, except that those referring to reactants of which the free concentration is determined potentiometrically must come last. Such a choice implies that a progressive integer number (from 1 to NMBEO) is assigned to each reactant.

KEY(I) is the refinement key of the <u>i</u>th formation constant: with KEY=0 the formation constant is not refined and with KEY=1 the formation constant is refined.

B.2.5. The following set of cards for each titration curve:

NMBE is the number of reactants (mass balance equations) involved in the titration curve.

JNMB holds the integer numbers previously assigned to the NMBE reactants involved.

NC is the number of unknown free concentrations at each point of the titration curve; the number of concentrations experimentally determined (i.e., the number of electrodes) is NEMF=NMBE-NC.

JP contains integer numbers corresponding to selected reactants: in the subroutine STATS the formation percentages relative to these reactants will be calculated, depending on the value of JPRIN.

1 card /5AlO/ : REACT(I) (NMBE values)

REACT contains the names of the reactants, listed in the same order as JNMB.

l card /4I5/ : JEL(I) (NEMF values), JCOUL.

JEL holds the number of electrons transferred at each electrode. If the decimal cologarithm of concentration (e.g., pH) is to be read in, put JEL(I)=0.

JCOUL=0 is normal; JCOUL=1 if the total volume of the solution does not change during the titration (e.g., coulometric experiments).

TOTC contains the initial number of millimoles of reactants in solution; the order of reactants is the same as in JNMB.

EZERO(I) holds the standard potential of the <u>i</u>th electrode (mV); the value is ignored if JEL(I)=0.

ADDC contains the molar concentrations of titrant solutions (there is one for each reactant); the order of the reactants is the same as in JNMB.

VINIT is the initial volume of the solution (cm^3) , and should correspond to the volume expected at the temperature of the TITRANT.

1 card /8F10.6/ : SLOPE (NEMF values).

SLOPE contains the slopes of the calibration curves for the species measured, in units of mV per decade of concentration, the value is ignored if JEL(I)=0.

cards /I5,8F8.3/ one for each point of the titration curve: LUIGI, TITRE(I) (NMBE values), EMF(I) (NEMF values).

LUIGI=0 is normal, LUIGI=1 indicates the end of a titration curve, LUIGI<0 indicates the end of all titration curves, LUIGI=2 indicates that, for coulometric titration, current (mA) and fractional current efficiency are read instead of a data point.

TITRE contains the volumes of titrant solutions (cm^3) added in volumetric titrations or time of current passage (sec) in coulometric experiments.

EMF contains the potentials (mV) measured on each electrode with non-zero JEL value (otherwise the decimal cologarithms of concentration).

B.2.6. 1 card /I5/ : JPRIN.

JPRIN controls the amount and type of output produced by STATS:

JPRIN	Statistical Analysis	<u>Tables</u>	Graphs
0	no	no	no
1	yes	no	no
2	yes	yes	no
3	yes	no	yes
4	yes	yes	yes

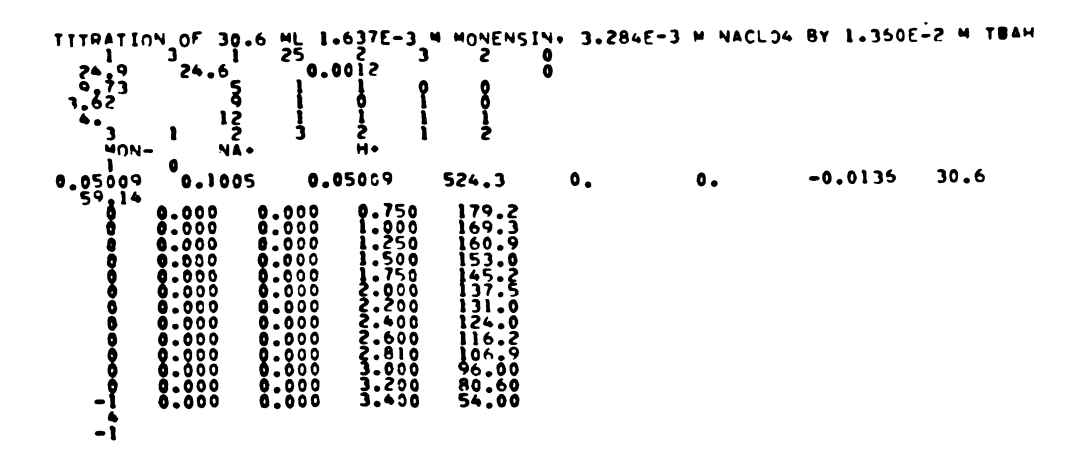
If JPRIN>1, the amount and type of tables and/or graphs is determined by the values contained in JP for each titration curve.

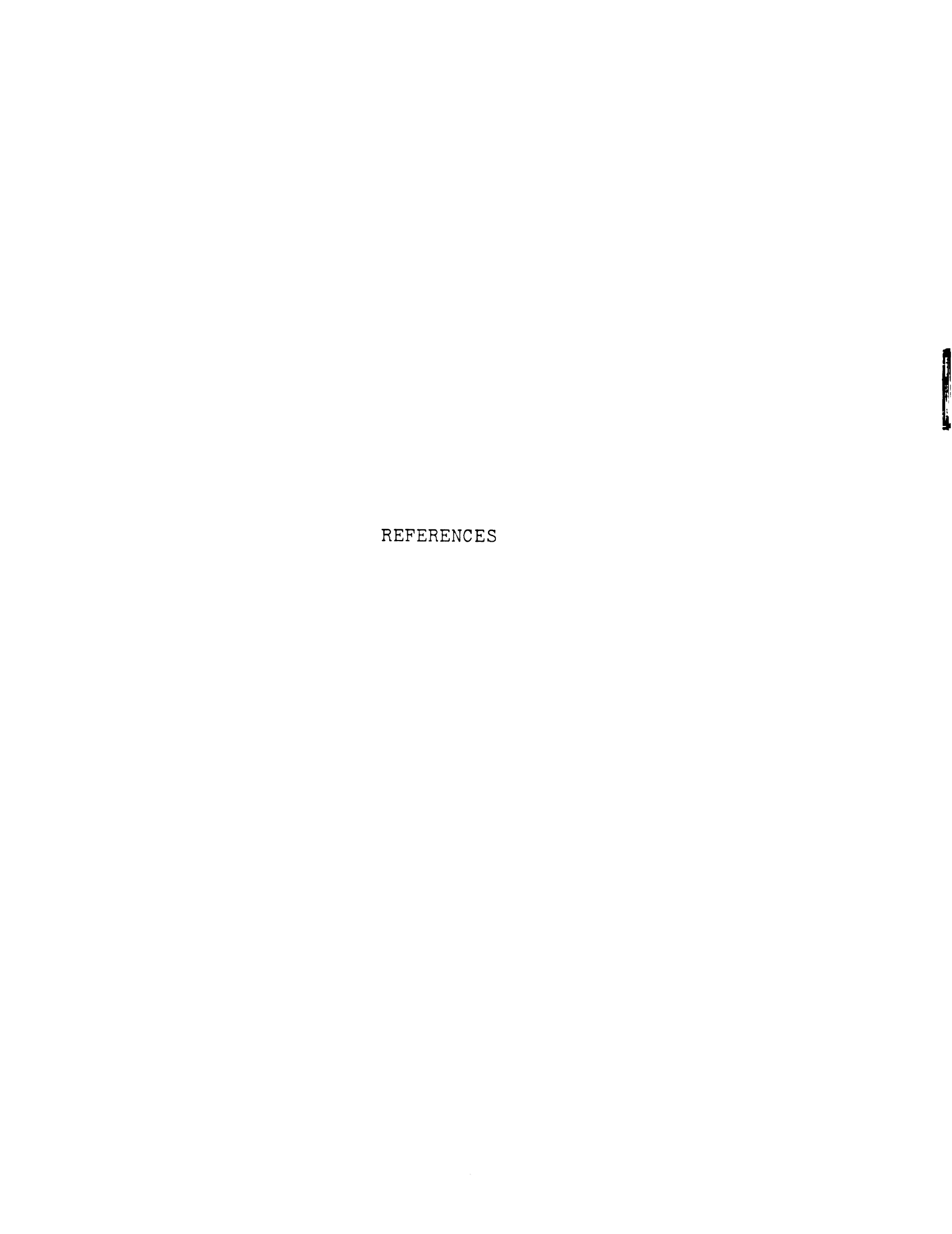
B.2.7. 1 card /I5/: NSET.

NSET=1 for another set of formation constants - items (i)-(iv), (vi) and (vii)

only -; NSET=0 for another complete set of data, NSET=-1 for the termination of the run.

B.3. Sample Data Listing





REFERENCES

- 1. A. Agtarap, J. W. Chamberlin, M. Pinkerton, and L. Steinrauf, J. Amer. Chem. Soc., 89, 5737 (1967).
- 2. M. E. Haney and M. M. Hoehn, Antimicrob. Ag. Chemother., 1967, 349 (1968).
- 3. W. M. Stark, N. G. Knox, and J. E. Westhead, Anti-microb. Ag. Chemother., 1967, 353 (1968).
- 4. R. H. L. Howe, U.S. Patent #4,007,115 (February 8, 1977), C. A. 86, 119263d.
- 5. A. Agtarap and J. W. Chamberlin, Antimicrob. Ag. Chemo-ther., 1967, 359 (1968).
- 6. W. K. Lutz, F. K. Winkler, and J. D. Dunitz, Helv. Chim. Acta., 54, 1103 (1971).
- 7. L. E. Day, J. W. Chamberlin, E. Z. Gordee, S. Chen, M. Gorman, R. L. Hamill, T. Ness, R. E. Weeks, and R. Stroshane, Antimicrob. Ag. Chemother., 4, 410 (1973).
- 8. D. R. Brannon and D. R. Horton, Ger. Offen. Patent #2,404,958 (August 22, 1974), C.A., 82, 41872x.
- 9. E. J. Corey, K. C. Nichlaou, and L. S. Melvin, Jr., J. Amer. Chem. Soc., 97, 653 (1975).
- J. W. Chamberlin, U.S. Patent #3,832,358 (August 27, 1974), C.A., 81, 135996x.
- 11. R. L. Harned, P. H. Hidy, C. J. Corum, and K. L. Jones, Antibiotics and Chemotherapy, 1, 594 (1951).
- 12. E. W. Czerwinski and L. K. Steinrauf, Biochem. Biophys. Res. Commun. 45, 1284 (1971).
- 13. J. W. Westley, R. H. Evans, Jr., T. Williams, and A. Stempel, J. Chem. Soc., Chem. Commun., 71 (1970).
- 14. H. Kimashi, N. Otake, and H. Yonehara, Tetrahedron Letters, 49, 4955 (1973).
- 15. T. J. Petchor and H.-P. Weber, J. Chem. Soc., Chem. Commun., 697 (1974).

- 16. P. Gachon, A. Kergomard, and H. Veschambre, J. Chem. Soc., Chem. Commun., 1421 (1970).
- 17. J. F. Blount and J. W. Westley, J. Chem. Soc., Chem. Commun., 533 (1975).
- 18. J. F. Blount, R. H. Evans, Jr., C.-H. Liu, T. Hermann, and J. W. Westley, J. Chem. Soc., Chem. Commun., 853 (1975).
- 19. N. Otake, M. Koenuma, H. Kimashi, S. Sato, and Y. Saito, J. Chem. Soc., Chem. Commun., 92 (1975).
- 20. C. Riche and C. Pascard-Billy, J. Chem. Soc., Chem. Commun., 951 (1975).
- 21. M. Alleaume, B. Busetta, C. Farges, P. Gachon, A. Kergomard, and T. Staron, J. Chem. Soc., Chem. Commun., 411 (1975).
- 22. N. Otake, H. Nakayama, H. Miyamae, S. Sato, and Y. Saito, J. Chem. Soc., Chem. Commun., 590 (1977).
- 23. N. D. Jones, M. O. Chaney, J. W. Chamberlin, R. L. Hamill, and S. Chen, J. Amer. Chem. Soc., <u>95</u>, 3399 (1973).
- 24. N. Otake, M. Koenuma, H. Miyamae, S. Sato, and Y. Saito, J. Chem. Soc., Perkin Trans. 2, 494 (1977).
- 25. D. H. Berg, R. L. Hamill, and M. M. Hoehn, U.S. Patent #7,506,920 (1975).
- 26. M. O. Chaney, P. V. Demarco, N. D. Jones, and J. L. Occolowitz, J. Amer. Chem. Soc., 96, 1932 (1974).
- 27. S. Estrada-O, B. Rightmire, and H. A. Lardy, Antimicrob. Ag. Chemother., 1967, 279 (1968).
- 28. S. Estrada-O and E. Calderon, Biochemistry, $\underline{9}$, 2092 (1970).
- 29. S. Estrada-O, C. DeCespedes, and E. Calderon, J. Bioenerg., 3, 361 (1972).
- 30. B. C. Pressman and D. H. Haynes, "The Molecular Basis of Membrane Function", Prentice-Hall, Englewood Cliffs, N.J., 1969, p. 221.
- 31. B. C. Pressman, Proc. Int. Congr. Pharmacol, 4th, 383 (1969).

- 32. H.-K. Wipf and W. Simon, Helv. Chim. Acta, <u>53</u>, 1732 (1970).
- 33. P. John and W. A. Hamilton, Eur. J. Biochem., <u>23</u>, 528 (1971).
- 34. G. Lysek and H. Von Witsch, Arch. Microbiol., 97, 227 (1974).
- 35. A. Thore, D. L. Keister, N. Shavit, and A. San Pietro, Biochemistry, 7, 3499 (1968).
- 36. M. Nishimura and B. C. Pressman, Biochemistry, 8, 1360 (1969).
- 37. M. R. Martinez Laranaga and A. Anadon Navarro, Arch. Farmacol. Toxicol, 1, 111 (1975).
- 38. M. A. Tarshis, A. G. Bekkuzin, and V. G. Ladygina, Arch. Microbiol., 109, 295 (1976).
- 39. H. Walkowiak, Life Sci., 15, 1353 (1974).
- 40. H. Walkowiak and G. Chambers, Life Sci., <u>16</u>, 297 (1975).
- 41. G. Kabell, P. Somani, R. Saini, B. Pressman, and N. de Guzman, Fed. Proc., Fed. Am. Soc. Exp. Biol., 36, 957 (1977).
- 42. A. L. Basset, J. R. Wiggins, D. E. Rodman, B. C. Pressman, and H. Gelband, Fed. Proc., Fed. Am. Soc. Exp. Biol., 36, 957 (1977).
- 43. P. Somani, B. C. Pressman, and N. T. de Guzman, Circulation, Suppl. II, 52, 242 (1975).
- 44. M. Shlafer, B. C. Pressman, P. Somani, and R. F. Palmer, Circulation, Suppl. II, <u>52</u>, 42 (1975).
- 45. M. B. Feinstein, E. G. Henderson, and R. I. Sha'afi, Biochim. Biophys. Acta., 468, 284 (1977).
- 46. R. Ashton and L. K. Steinrauf, J. Mol. Biol., <u>49</u>, 547 (1970).
- 47. H. W. Huang, J. Theor. Biol., 32, 351 (1971).
- 48. H. W. Huang, J. Theor. Biol., 32, 363 (1971).
- 49. E. L. Cussler, A. I. Ch. E. J., 17, 1300 (1971).

- 50. E. M. Choy, D. F. Evans, and E. L. Cussler, J. Amer. Chem. Soc., 96, 7085 (1974).
- 51. Anomymous, Chem. Eng. News, 52, 35 (1974).
- 52. E. L. Cussler and M. M. Breuer, A. I. Ch. E. J., <u>18</u>, 812 (1972).
- 53. R. G. Strout and C. A. Ouellette, Exp. Parasitol., 33, 477 (1973).
- 54. R. G. Wilson, Parasitology, <u>73</u>, 283 (1976).
- 55. R. F. Shumard and M. E. Callendar, Antimicrob. Ag. Chemother., 1967, 369 (1968).
- 56. J. Biely, Avian Diseases, 17, 362 (1973).
- 57. W. M. Reid, L. Kowalski, and J. Rice, Poult. Sci., 51, 139 (1972).
- 58. M. D. Ruff, W. M. Reid, and A. P. Rahn, Am. J. Vet. Res., <u>37</u>, 963 (1976).
- 59. S. Blagovic, A. Blajic, and B. Poljugan, Proc. World Vet. Congr., 20th, 3, 2416 (1975).
- 60. M. Splitek, B. Sandera, and R. Hauba, Agrochemia, 16, 288 (1976).
- 61. W. M. Reid, T. K. Hines, J. Johnson, and K. R. Stino, Poult. Sci., <u>55</u>, 1436 (1976).
- 62. R. E. Hurst, E. J. Day, and B. C. Dilworth, Poult. Sci., <u>53</u>, 434 (1974).
- 63. M. G. Murillo, L. S. Jensen, M. D. Ruff, and A. P. Rahn, Poult. Sci., <u>55</u>, 642 (1976).
- 64. R. M. Weppelman, G. Olson, D. A. Smith, T. Tamas, and A. Van Iderstine, Poult. Sci., <u>56</u>, 1550 (1977).
- 65. L. R. McDougald, Ger. Offen. Patent #2,712,048 (Sept. 29, 1977), C.A., <u>87</u>, 206533f.
- 66. B. L. Damron, R. H. Harms, A. S. Arafa, and D. M. Janky, Poult. Sci., <u>56</u>, 1487 (1977).
- 67. M. Mitrovic. E. Schidknecht, and C. Trainor, Poult. Sci., <u>56</u>, 979 (1977).

- 68. L. W. Luther, M. C. Thomas, W. D. Goatcher, M. R. Selwyn and J. J. Colaianne, Poult. Sci., <u>55</u>, 2058 (1976).
- 69. R. D. Wyatt and M. D. Ruff, Avian Diseases, <u>19</u>, 730 (1975).
- 70. M. D. Ruff and L. S. Jensen, Poult. Sci., <u>56</u>, 1956 (1977).
- 71. H. D. Chapman, Parasitology, <u>69</u>, 283 (1974).
- 72. H. D. Chapman, Vet. Parasitol., 2, 187 (1976).
- 73. W. M. Reid, J. Dick, J. Rice, and F. Stino, Poult. Sci., 56, 66 (1977).
- 74. T. K. Jeffers, Poult. Sci., 56, 1725 (1977).
- 75. Anonymous, Fed. Regist., August 14, 1973, 38(156), 21921.
- 76. Anonymous, Fed. Regist., October 17, 1974, 39(202), 37056-7.
- 77. Anonymous, Fed. Regist., December 18, 1974, 39(244), 43718-19.
- 78. Anonymous, Fed. Regist., August 29, 1975, 40(169), 39857-8.
- 79. Anonymous, Fed. Regist., January 8, 1976, 41(5), 1469-70.
- 80. Anonymous, Fed. Regist., January 13, 1976, 41(8), 1892-3.
- 81. Anonymous, Fed. Regist., December 16, 1975, 40(242), 58289-90.
- 82. B. F. Schlegel, D. I. Gard, R. P. Rathmacher, and D. K. Weymouth, Poult. Sci., 54, 1813 (1975).
- 83. M. Mohler, S. Klinger, G. Shemwell, D. E. Pratt, and W. J. Stadelman, Poult. Sci., <u>54</u>, 1697 (1975).
- 84. R. H. Harms, J. L. Fry, M. W. Moeller, and H. F. King, Poult. Sci., <u>55</u>, 2214 (1976).
- 85. D. J. Kingston, Aust. Vet. J., <u>53</u>, 251 (1977).
- 86. D. I. Gard, B. F. Schlegel, D. K. Weymouth, and R. P. Rathmacher, Poult. Sci., <u>54</u>, 1764 (1975).

- 87. W. I. Anderson, W. M. Reid, and L. R. McDougald, Avian Diseases, 20, 387 (1976).
- 88. L. R. McDougald, Poult. Sci., 55, 2442 (1976).
- 89. E. L. Potter, C. O. Cooley, A. P. Raun, L. F. Richardson, and R. P. Rathmacher, Proc., Annu. Meet.--Am. Soc. Anim. Sci., West. Sect., 25, 343 (1974).
- 90. H. Brown, L. H. Carroll, N. G. Elliston, H. P. Grueter, J. W. McAskill, R. D. Olson, and R. P. Rathmacher, Proc., Annu. Meet.—Am. Soc. Anim. Sci., West. Sect., 25, 300 (1974).
- 91. D. N. Mowat and J. G. Buchanan-Smith, Can. J. of Animal Sci., 56, 838 (1976).
- 92. O. O. Thomas and W. J. Langford, Proc., Annu. Meet--Am. Soc. Anim. Sci., West. Sect., 28, 210 (1977).
- 93. W. M. Oliver, J. Anim. Sci., 40, 190 (1975).
- 94. W. B. Anthony, V. L. Brown, and R. R. Harris, J. Anim. Sci., <u>40</u>, 190 (1975).
- 95. O. O. Thomas, Proc., Annu. Meet.—Am. Soc. Anim. Sci., West. Sect., 28, 216 (1977).
- 96. W. M. Oliver, J. Anim. Sci., 41, 999 (1975).
- 97. R. R. Harris, W. B. Anthony, J. A. Little, and V. L. Brown, Highlights Agric. Res., 23, 5 (1976).
- 98. E. L. Potter, C. O. Cooley, L. F. Richardson, A. P. Raun, and R. P. Rathmacher, J. Anim. Sci., 43, 665 (1976).
- 99. P. R. Utley, G. L. Newton, D. M. Wilson, and W. C. McCormick, J. Anim. Sci., 45, 154 (1977).
- 100. W. L. Mies and L. B. Sherrod, Proc., Annu. Meet.--Am. Soc. Anim. Sci., West. Sect., 28, 208 (1977).
- 101. L. DeMuth, H. W. Essig, L. J. Smithson, F. T. Withers, E. G. Morrison, and H. Chapman, Res. Rep.—Miss. Agric. For. Exp. Stn., 3, 4 (1977).
- 102. L. J. DeMuth, H. W. Essig, L. J. Smithson, E. G. Morrison, H. D. Chapman, and F. T. Withers, J. Anim. Sci., 42, 273 (1976).
- 103. W. M. Moseley, R. D. Randel, and M. M. McCartor, J. Anim. Sci., 42, 273 (1976).

- 104. J. Riley, L. Corah, and G. Fink, J. Anim. Sci., 42, 1368 (1976).
- 105. J. G. Linn, R. D. Goodrich, and J. C. Meiske, J. Anim.
 Sci., 42, 1368 (1976).
- 106. R. R. Harris, W. B. Anthony, V. L. Brown, and J. A. Little, J. Anim. Sci., 43, 265 (1976).
- 107. D. R. Gill, J. R. Martin, and R. Lake, J. Anim. Sci., 43, 363 (1976).
- 108. J. A. Boling, N. W. Bradley, and L. D. Campbell, J. Anim. Sci., 44, 867 (1977).
- 109. R. M. Dartt, J. A. Boling, and N. W. Bradley, J. Anim. Sci., 43, 318 (1976).
- 110. Y. Geay and C. Beranger, Ann. Zootech., 26, 59 (1977).
- 111. K. K. Bolsen, L. Corah, and J. G. Riley, J. Anim. Sci., 41, 392 (1975).
- 112. G. V. Davis and A. B. Erhart, J. Anim. Sci., 43, 1 (1976).
- 113. G. V. Davis and A. B. Erhart, J. Anim. Sci., <u>43</u>, 318 (1976).
- 114. R. W. Harvey, A. C. Linnerud and D. F. Tugman, J. Anim. Sci., <u>42</u>, 275 (1976).
- 115. D. A. Dinius and C. A. Baile, J. Anim. Sci., 45, 147 (1977).
- 116. O. O. Thomas, J. Anim. Sci., $\frac{42}{5}$, 1574 (1976).
- 117. P. R. Utley, G. L. Newton, and W. C. McCormick, J. Anim. Sci., <u>41</u>, 423 (1975).
- 118. P. R. Utley, G. L. Newton, R. J. Ritter, III, and W. C. McCormick, J. Anim. Sci., <u>42</u>, 754 (1976).
- 119. D. J. Hoffman, C. F. Speth, T. P. Ringkob, A. L. Lesperance, and J. A. McCormick, Proc., Annu. Meet.—Am. Soc. Anim. Sci., West. Sect., 28, 204 (1977).
- 120. J. A. Bogan, Med. Actual., 12, 246 (1976).
- 121. A. P. Raun, Fr. Demande #2,169,201 (October 12, 1973); C. A., 80, 69648m.

- 122. L. F. Richardson, A. P. Raun, E. L. Potter, C. O. Cooley, and R. P. Rathmacher, J. Anim. Sci., 43, 657 (1976).
- 123. P. Jagos, R. Dvork, and Z. Vrba, Veterinarstivi, 27, 342 (1977).
- 124. W. M. Beeson, T. W. Perry, and M. T. Mohler, Fed. Proc., Fed. Am. Soc. Exp. Biol., 35, 580 (1976).
- 125. M. M. McCartor, W. M. Moseley, and R. D. Randel, J. Anim. Sci., 42, 272 (1976).
- 126. E. C. Prigge and F. N. Owens, J. Dairy Sci., <u>59</u>, 21 (1976).
- 127. D. B. Beede and S. D. Farlin, J. Anim. Sci., <u>41</u>, 390 (1975).
- 128. E. C. Prigge and F. N. Owens, J. Anim. Sci., <u>42</u>, 258 (1976).
- 129. K. N. Von Glan and R. L. Vetter, J. Anim. Sci., <u>43</u>, 270 (1976).
- 130. A. P. Raun, C. O. Cooley, E. L. Potter, R. P. Rathmacher, and L. F. Richardson, J. Anim. Sci., 43, 670 (1976).
- 131. R. W. Van Maanen, J. H. Herbein, A. D. McGilliard, and J. W. Young, J. Dairy Sci., Suppl. 1, 60, 119 (1977).
- 132. R. P. Lemenager, F. N. Owens, and R. Totusek, J. Anim. Sci., <u>42</u>, 275 (1976).
- 133. R. Q. Van Hellen, D. K. Beede, R. E. Tucker, G. T. Schelling, N. Gay, and G. E. Mitchell, Jr., J. Anim. Sci., 43, 336 (1976).
- 134. J. H. Thornton, F. N. Owens, R. P. Lemenager, and R. Totusek, J. Anim. Sci., <u>43</u>, 336 (1976).
- 135. C. J. VanNevel and D. I. Demeyer, Appl. Environ. Microbiol., <u>34</u>, 251 (1977).
- 136. D. A. Dinius, M. E. Simpson, and P. B. Marsh, J. Anim. Sci., 42, 229 (1976).
- 137. D. A. Dinius and M. E. Simpson, J. Anim. Sci., <u>41</u>, 398 (1975).
- 138. M. E. Simpson, P. B. Marsh, and D. A. Dinius, J. Anim. Sci., 42, 1580 (1976).

- 139. H. A. Turner and R. J. Raleigh, Proc., Annu. Meet.--Am. Soc. Anim. Sci., West. Sect., 27, 320 (1976).
- 140. H. A. Turner, R. J. Raleigh, and D. C. Young, J. Anim. Sci., 44, 338 (1977).
- 141. W. C. Burrell, J. N. Wiltbank, W. N. Songster, and L. H. Carroll, Proc., Annu. Meet.—Am. Soc. Anim. Sci., West. Sect., 28, 195 (1977).
- 142. W. M. Moseley, M. M. McCartor, and R. D. Randel, J. Anim. Sci., <u>45</u>, 961 (1977).
- 143. E. L. Potter, A. P. Raun, C. O. Cooley, R. P. Rathmacher, and L. F. Richardson, J. Anim. Sci., 43, 678 (1976).
- 144. A. P. Raun, C. O. Cooley, R. P. Rathmacher, L. F. Richardson, and E. L. Potter, Proc., Annu. Meet.—Am. Soc. Anim. Sci., West. Sect., 25, 346 (1974).
- 145. H. P. Grueter, N. G. Elliston, J. W. McAskill, and E. L. Potter, Vet. Med./Small Anim. Clin., 71, 198 (1976).
- 146. T. W. Perry, W. M. Beeson, and M. T. Mohler, J. Anim. Sci., <u>42</u>, 761 (1976).
- 147. A. L. Donoho, R. J. Herberg, J. A. Manthey, and J. L. Occolowitz, Abstracts of Papers, #164 (Agricultural and Food Chemistry), 172nd ACS National Meeting, Aug. 29 (1976).
- 148. P. R. Fitzgerald and M. E. Mansfield, J. Protozool., 20, 121 (1973).
- 149. R. G. Leek. R. Fayer, and D. K. McLoughlin, Am. J. Vet. Res., 37, 339 (1976).
- 150. R. C. Bergstrom and L. R. Maki, Am. J. Vet. Res., <u>37</u>, 79 (1976).
- 151. R. C. Bergstrom and L. R. Maki, J. Am. Vet. Med. Assoc., 165, 288 (1974).
- 152. P. R. Fitzgerald, J. Protozool., 19, 286 (1972).
- 153. M. J. Gwyther and J. W. Dick, Poult. Sci., <u>55</u>, 1594 (1976).
- 154. R. E. Messersmith, U.S. Patent #4,027,034, 31 May 1977.

- 155. J. W. Stoker, Vet. Rec., <u>97</u>, 137 (1975).
- 156. T. Matsuoka, J. Am. Vet. Med. Assoc., 169, 1098 (1976).
- 157. H. Ohishi, T. Hayashi, K. Ando, T. Sagawa, S. Hirano, and K. Togashi, Japan. 74 11,048, 14 March 1974.
- 158. F. W. Kavanaugh and M. Willis, J. Assoc. Off. Anal. Chem., 55, 114 (1972).
- 159. H. L. Breunig, R. M. Kline, and H. Bikin, J. Assoc. Off. Anal. Chem., <u>55</u>, 718 (1972).
- 160. W. J. Begue and R. M. Kline, J. Chromatogr., <u>64</u>, 182 (1972).
- 161. T. Golab, S. J. Barton, and R. E. Scroggs, J. Assoc. Off. Anal. Chem., 56, 171 (1973).
- 162. D. C. Koufidis, Chem. Chron., 5, 239 (1976).
- 163. H. L. Breunig, R. E. Scroggs, L. V. Tonkinson and H. Bikin, J. Assoc. Off. Anal. Chem., 60, 179 (1977).
- 164. Anonymous, Analyst (London) 102, 206 (1977).
- 165. B. C. Pressman, Fed. Proc., Fed. Am. Soc. Exp. Biol., 27, 1283 (1968).
- 166. W. K. Lutz, H.-K. Wipf, and W. Simon, Helv. Chim. Acta, 53, 1741 (1970).
- 167. M. Pinkerton and L. K. Steinrauf, J. Mol. Biol., 48, 533 (1970).
- 168. L. K. Steinrauf, E. W. Czerwinski, and M. Pinkerton, Biochem. Biophys. Res. Commun., 45, 1279 (1971).
- 169. M. R. Truter, Structure and Bonding (Berlin) 16, 71 (1973).
- 170. J. W. Chamberlin and A. Agtarap, Org. Mass Spectrom., $\underline{3}$, 271 (1970).
- 171. D. H. Haynes, B. C. Pressman, and A. Kowalsky, Biochemistry, <u>10</u>, 852 (1971).
- 172. H. Degani, Biophys. Chem., 6, 345 (1977).
- 173. M. J. O. Anteunis, Bull. Soc. Chim. Belg., <u>86</u>, 367 (1977).

		:
		,

- 174. P. G. Gertenbach and A. I. Popov, J. Amer. Chem. Soc., 97, 4738 (1975).
- 175. B. C. Pressman, Fed. Proc., Fed. Am. Soc. Exp. Biol., 32, 1698 (1973).
- 176. P. U. Frueh, J. T. Clerc, and W. Simon, Helv. Chim. Acta., <u>54</u>, 1445 (1971).
- 177. W. K. Lutz, P. U. Frueh, and W. Simon, Helv. Chim. Acta, 54, 2767 (1971).
- 178. P. B. Chock, F. Eggers, M. Eigen, and R. Winkler, Biophys. Chem., <u>6</u>, 239 (1977).
- 179. G. Cornelius, W. Gärtner, and D. H. Haynes, Biochemistry, 13, 3052 (1974).
- 180. P. Gachon, G. Chaput, G. Jeminet, J. Juillard, and J.-P. Morel, J. Chem. Soc., Perkins II, 9, 907 (1975).
- 181. M. S. Greenberg, Ph.D. Thesis, Michigan State University, East Lansing, MI (1974).
- 182. H. K. Frensdorff, J. Amer. Chem. Soc., 93, 600 (1971).
- 183. J. G. Hoogerheide and P.-H. Heubel, "Constant Current Coulometer", (1977).
- 184. D. L. Ward, K.-T. Wei, J. G. Hoogerheide, and A. I. Popov, Acta Crystallogr., Sect. B, 34, 110 (1978).
- 185. J. L. Dye and V. A. Nicely, J. Chem. Educ., 48, 443 (1971).
- 186. A. Sabatini, A. Vacca, and P. Gans, Talanta, <u>21</u>, 53 (1974).
- 187. P. Gans, A. Sabatini, and A. Vacca, Inorg. Chim. Acta, 18, 237 (1976).
- 188. A. Vacca, personal communication.
- 189. J. J. Lingane, Chem. Rev., 29, 1 (1941).
- 190. A. Ringbom and L. Eriksson, Acta Chem. Scand., $\frac{7}{2}$, 1105 (1953).
- 191. L. Eriksson, Acta Chem. Scand., 7, 1146 (1953).
- 192. G. I. Goodfellow, D. Midgley, and H. M. Webber, Analyst (London) 101, 848 (1976).

- 193. D. Midgley, Anal. Chem., 49, 1211 (1977).
- 194. E. T. Roach, P. R. Handy, and A. I. Popov, Inorg. Nucl. Chem. Lett., 9, 359 (1973).
- 195. Y. M. Cahen, R. F. Beisel, and A. I. Popov, J. Inorg. Nucl. Chem. Suppl., 209 (1976).
- 196. J.-M. Lehn and A. I. Popov, "Physicochemical Studies of Crown and Cryptate Complexes", Chapter 9 in Chemistry of Macrocyclic Compounds, G. A. Melson, ed., Plenum, in press.
- 197. M. N. Hughes and W.-K. Man, Inorg. Chim. Acta, <u>20</u>, 237 (1976).
- 198. J.-M. Lehn, Struct. Bonding (Berlin), 16, 1 (1972).
- 199. J.-M. Lehn and J. P. Sauvage, J. Amer. Chem. Soc., 97, 6700 (1975).
- 200. G. A. Harlow, C. M. Noble, and G. E. A. Wyld, Anal. Chem., 28, 787 (1956).
- 201. R. H. Cundiff and P. C. Markunas, Anal. Chem., <u>28</u>, 792 (1956).
- 202. G. A. Harlow and D. B. Bruss, Anal. Chem., <u>30</u>, 1833 (1958).
- 203. L. W. Marple and J. S. Fritz, Anal. Chem., 34, 796 (1962).
- 204. G. A. Harlow, Anal. Chem., 34, 1482 (1962).
- 205. G. A. Harlow, Anal. Chem., <u>34</u>, 1487 (1962).
- 206. J. S. Fritz and F. E. Gainer, Talanta, 15, 939 (1968).
- 207. B. G. Cooksey, B. Metters, J. M. Ottaway, and D. W. Whymark, Talanta, 20, 371 (1973).
- 208. J. Juillard and M.-L. Dondon, Bull. Soc. Chim. Fr., 2535 (1963).
- 209. J. Juillard, Bull. Soc. Chim. Fr., 1727 (1966).
- 210. I. D. Tabagua, Tr. Sukhumsk. Gos. Ped. Inst., <u>15</u>, 119 (1962); C. A. 14373d (1964).
- 211. M. Kilpatrick, J. Amer. Chem. Soc., 75, 584 (1953).

- 212. A. L. Bacarella, E. Grunwald, and E. L. Purlee, J. Org. Chem., 20, 747 (1955).
- 213. C. S. Leung and E. Grunwald, J. Phys. Chem., 74, 696 (1970).
- 214. E. Kauffmann, J.-M. Lehn, and J.-P. Sauvage, Helv. Chim. Acta, 59, 1099 (1976).
- 215. E. Mei, J. L. Dye, and A. I. Popov, J. Amer. Chem. Soc., 99, 5308 (1977).
- 216. E. Mei, A. I. Popov, and J. L. Dye, J. Amer. Chem. Soc., 99, 6532 (1977).
- 217. P. J. F. Henderson, J. D. McGivan, and J. B. Chappell, Biochem. J., 111, 521 (1969).
- 218. J. G. Hoogerheide and A. I. Popov, J. Solution Chem., $\underline{7}$, 357 (1978).